From: Proteome Center Rostock, Medical Faculty and Natural Science Faculty, University of Rostock in collaboration with Steinbeis Center for Biopolymer Analysis and Biomedical Mass Spectrometry

Elucidation of molecular recognition structures of peptides and proteins to antibodies and DNA aptamers by biosensor- mass spectrometry combination

Dissertation

For the acquirement of the academic degree

Doktor der Medizinwissenschaften: "Dr. rer. hum."

Faculty of Medicine, University of Rostock

Submitted by

Loredana-Mirela Lupu, 09.01.1992

From Romania

Rostock 2022

https://doi.org/10.18453/rosdok_id00004458

Reviewers:

Evaluator 1: Prof. Markus Tiedge

Evaluator 2: Prof. Michael O. Glocker

Evaluator 3: Prof. Michael Przybylski

Month/Year of submission: Dec. 2022

Month/Year of examination: July 2023

Personal declaration

I hereby declare that the submitted thesis is based on the results from my original work and on work in collaboration with several colleagues as outlined below. The work has not been previously submitted to any academic institution for obtaining any other academic degree. The four publications included in the thesis are based on own research and on collaborative work.

In the publication “Antibody Epitope and Affinity Determination of the Myocardial Infarction Marker Myoglobin by SPR- Biosensor Mass Spectrometry” published in *Journal of the American Society for Mass Spectrometry* in 2021, parts of the experimental and theoretical work are original work. The original work is comprised of epitope analyses and SPR experiments.

In the publication “Antibody Epitope of human α-Galactosidase A revealed by affinity-mass spectrometry: A basis for reversing immunoreactivity in enzyme replacement therapy of Fabry’s Disease” published in *ChemMedChem* in 2018, parts of the experimental and theoretical work is original work. The original work is comprised of epitope analyses and SPR experiments.

In the publication “Molecular Epitope Determination of Aptamer Complexes of the Multi-domain Protein C-Met by Proteolytic Affinity- Mass Spectrometry” published in *ChemMedChem* in 2020, the entire experimental parts are original work.

The complete thesis includes own experiments on SPR biosensor analyses and epitope extraction/excision mass spectrometry experiments, and the testing and analysis of the developed PROTEX-SPR-MS instrumentation.

Loredana-Mirela Lupu

Acknowledgements

I am profoundly grateful to my mentor and PhD supervisor Prof. Dr. Michael Przybylski. Without his scientific advice, I could not have successfully performed my dissertation. Furthermore, I am thankful for the opportunities he provided and the support for many conference participations.

My supervisor, Prof. Dr. Michael Glocker gave me invaluable help with data analysis and biochemical evaluations. He is a true professor at heart, and I have learned professionally from him and on a personal level.

My research would not have been possible without the aid and support of all my colleagues and students at the Steinbeis Center for Biopolymer Analysis and Biomedical Mass Spectrometry, Russelsheim, Germany. Not only did they give me excellent advice, but they helped me grow as a person. They were my second family, and without them, I could not have overcome my fears and carried out my work.

I want to thank Dr. Zdeněk Kukačka, my first adviser in Germany and a good friend, and Yannick Baschung, my colleague both at the Steinbeis Center and the Proteome Center in Rostock, and a person who always supported me. Both gave me significant guidance for the projects and taught me to look at things from different perspectives.

Many thanks to Dr. Anna Tramarin, Hendrik Rusche, Dr. Francesca Rinaldi, Delia Mihoc and Stephan Rawer, from whom I learned what it is to be a scientist and how to be a friend and a good person. Also, thank you to all collaborators and colleagues for the outstanding scientific discussions. I want to acknowledge Pascal Wiegand and Biljana Brdar for everything they added to my work and personal life. Their advice and guidance were essential for my work. They became my colleagues and friends, and I could not have finished the work without their support.

Most important I am grateful to my family, my mother, Despina Lupu and my brother, Bogdan Alexa. They are my motivation, my drive, my strength and without them, I would never have arrived at this moment! Their sacrifice, love and guidance were more than anyone can ever ask for, and I will always be grateful for having such an incredible family. I also want to mention my chosen family, Karla Cara and Marvin Kohls! Their hugs, food and jokes made me laugh even when the experiments did not work as well as I needed!

The cumulative work in this thesis is the sum of all the personal contributions everyone in my life added, and I am thankful for each and every one of them.

Table of Content

1. INTRODUCTION

1.1. Molecular basis of protein-antibody and protein-nucleotide interactions

Immunoglobulins (antibodies) are essential among all proteins because of their function in the immune system. The first reference to the “Antikörper”, or antibody, was made in 1890 when Behring and Kitasato found an element in the blood that neutralized the diphtheria toxin [1,2]. The biological function of this “Antikörper” was to bind pathogens and their products to facilitate their removal [3]. The process of antibody formation, either membrane-bound or secreted, requires several steps: B cell maturation, cytokines produced by other lymphocytes and antigen-presenting cells, determining what class of immunoglobulin the B cell will produce [3,4]. The number of unique antibodies that a human body can produce is still unknown; however, a team led by Drs. Bryan Briney and Dennis R. Burton at Scripps Research, predicted that humans can produce an estimated one million unique antibodies (results were published in Nature, 2019) [5]. Human IgG class antibodies are Y-shaped proteins composed of a variable (FV region) and a constant region (FC region). The variable region has two identical light chains (LCs) of 25 kDa, and two identical heavy chains (HCs) of 50–70 kDa [6,7]. The HC and LC of the heterodimer are linked through disulfide bonds (Figure 1). In addition, both HCs and LCs contain complementarity determining regions (CDRs) that enable binding.

The interaction between two proteins (eg. antibody-protein interaction) is accomplished by overcoming the repulsion between the molecules. According to our current understanding, this is obtained by a mechanism in which the two interacting molecules are close enough so that the attraction is achieved by long-distance forces such as ionic and hydrophobic bonds [7]. These forces allow the molecules to move closer by overcoming the hydration energies and expelling the surrounding water molecules. In addition, van der Waals forces and ionic groups often prevail, forming the antibody-protein assembly. The strength of the interaction depends on how well the two puzzle pieces complement each other [8]. Moreover, the affinity is determined by the distribution of charges and hydrophobic groups. This type of interaction can be disrupted by high salt concentrations, different pH, detergents, and in some cases by competition with high concentrations of the epitope itself [9].

The F_V region from antibodies bind to proteins via contact with amino acid residues (AA) located in the CDRs. These amino acid sequences are termed paratope peptides. Their binding structure and mechanism depends on the location and shape of the antigen. For example, if the antigen is a small

peptide, it is more likely to fit in a small pocket made by the binding AAs of the antibody. In contrast, antigens such as a large protein generally bind to the antibody on its surface, involving several CDRs. Moreover, the 3D structure of the antibody surface can be concave, flat, undulating, or even convex [8-11] (Figure S1).

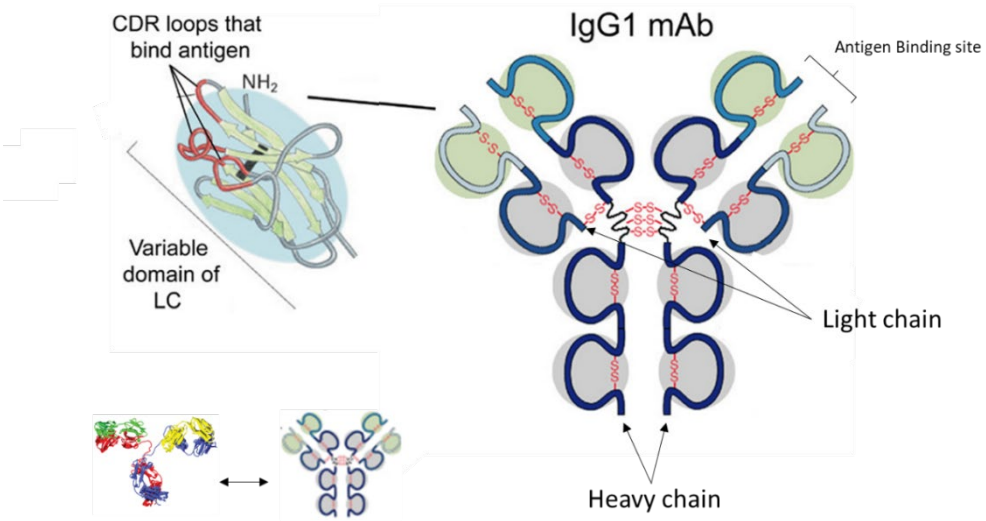

Figure 1: Schematic representation of an immunoglobulin G structure and the antigen binding site/ The antibody consists of two heavy chains bound together by disulfide bonds in the hinge region. Every Heavy chain consists of 3 constant and one variable region. Every Light chain consists of one variable region and one constant region.

Complementary to paratopes, the amino acid sequences (from the protein) involved in the interactions are denominated as epitopes. According to the Macmillan Dictionary of Immunology: an epitope or antigenic determinant is defined as “the portion of an antigen that makes contact with a particular antibody or T cell receptor” [12,13]. The epitope can be composed of any different surface peptide and an antibody can recognize a large variety of surfaces: a small linear peptide, multiple peptide sequences on the surface, peptides with post-translational modifications or just a large area of a protein surface [14,15]. Epitopes are classified as continuous, i.e. consecutive amino acids form a binding site, or discontinues when the amino acids necessary for binding are part of multiple different peptides. This classification is sometimes referred to as linear and non-linear, or consecutive and assembled epitopes [16]. However, the type of epitope identified can be difficult to assign. One such example is that the epitope consists of one long peptide chain that forms two different contact points in the structure [17].

For medical research, the immune system is often a main target, with IgG antibodies analysis having high priority. Antibody interactions have been shown to have specific characteristics. For example,

they demonstrate high specificity for their targets and confer effector functions such as receptor-ligand blocking, target cell cytotoxicity and receptor antagonism [18]. When antibodies (from a different host) are used for treatment, the immune system is often triggered, and the treatment is rendered futile [19,20]. To overcome this, alternative molecules can be used as substitutes. One possible alternative for antibodies are single stranded DNA or RNA aptamers.

Recently, DNA and RNA aptamers have emerged as a possible new class of immuno-therapeutics because of their ability to bind to specific targets (Figure 2). Aptamers can be described as molecules with many similar attributes to antibodies. One type of aptamers are single-stranded oligonucleotides, they have specific and strong interactions with other molecules [21 A nucleic acid aptamer can be either a DNA or RNA oligonucleotide with a base number typically between 15 and 70 [22]. An aptamer-protein interaction occurs via similar forces to that providing antibody- protein interaction as well as shape complementarity and base stacking [23]. Likewise, the 3D structure of aptamers is crucial for the complex formation with proteins [24]. In contrast to antibodies, which are produced in vivo, oligonucleotide aptamers are typically isolated by a selection procedure called “Systematic Evolution of Ligands by EXponential Enrichment” (SELEX). The oligonucleotides identified can be chemically synthesized [25].

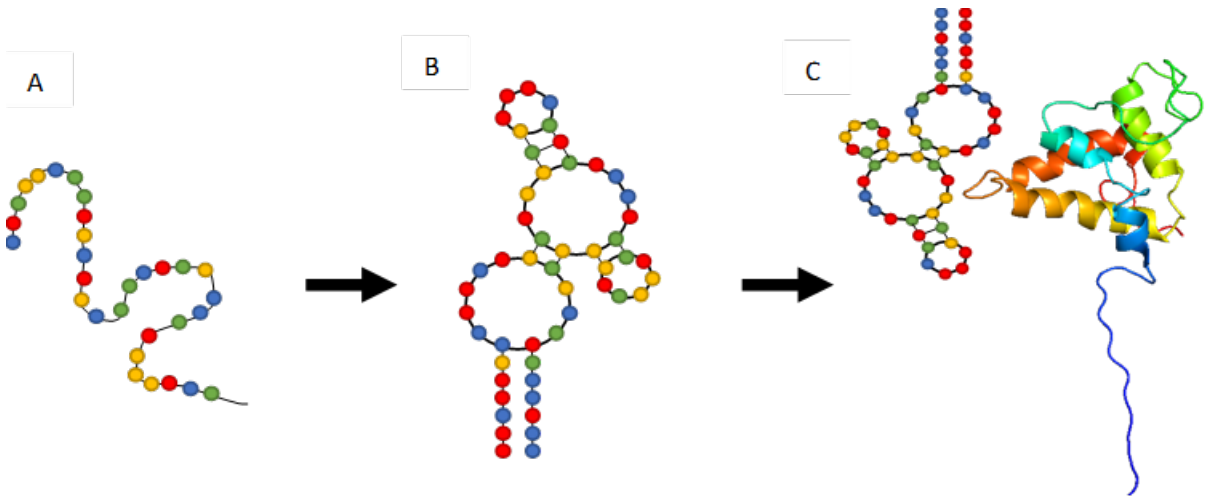

Figure 2: Schematic diagram of a DNA aptamer folding and binding to a protein target [26]. The aptamer sequence is shown with the four bases in different color. Adenine (A) is shown in blue, Thymine (T) in red, Guanine (G) in green and Cytosine (C) in yellow. 2A. A single stranded random linear DNA sequence. 2B. The same DNA aptamer folding to form a stable two-dimensional structure. 2C. Representation of the DNA aptamer interacting with a model of a target protein.

The SELEX method is a complete in vitro procedure comprising incubation of a random library of oligonucleotides with a selected target followed by washing steps to remove all non-binding nucleotides; and negative controls (incubation steps with alternate molecules). Aptamers typically

have a broad specificity and the selection is ending in an amplification of the obtained oligonucleotides [27,28]. Not only the production of antibodies and aptamers differs, the stability of the two molecules is different, as well as the production costs, the half-life in the human organism and many others. One strong argument in support of the aptamer alternative to antibodies is that the production and identification is completely chemically based, and needs no host organism(s). In contrast, antibodies need an animal host for their production. Therefore, aptamers appear to be a promising alternative, and their in-depth development is certainly needed [29-32].

Several aptamers and antibodies have become FDA approved therapeutics for several diseases (viral or bacterial infections, degenerative diseases, autoimmune diseases). One fundamental problem of aptamers (and also antibodies) is the selection of the specific target. For example, Pegaptanib (PEGylated aptamer) has been FDA approved in 2004 for the treatment of age-related macular degeneration [33,34]. Moreover, aptamers for Cancer, viral infections and different infectious diseases are being researched with potential for both treatment and early detection [35-43].

However, diseases are generally not based only on a single protein mutation, but rather on malfunction or poor regulation of an arrangement of proteins that cause a variety of symptoms. Because only a few interactions are well understood, i.e., not all peptides important in these interactions are known, the selection of the correct epitope for the desired results is rather challenging.

1.2 Analytical methods for biopolymer interaction analysis

1.2.1 Methods for identification of antibody epitopes

Bio-affinity interactions between molecules are mainly studied using analytical biochemistry. With the development of soft ionization mass spectrometry [44], scientists can analyze intact molecules and their interactions without disrupting the structures. The molecule of interest can gain a change from a neutral species, forming ions that are submitted to the mass analyzer. The mass spectrum generated from the mass over charge (m/z) measurement provides the molecular mass and several structural information of the molecules [45].

Initial protein structure analysis of an intact protein involved a partial or complete structure determination by capturing them in a crystal. X-ray Crystallography is a well-established method for structure determination of both single proteins and interacting proteins. This method has proven highly efficient for drug discovery [46], such as enzyme-based therapies [47] and novel protein structure identifications [48]. However, X-ray Crystallography has many limitations based on the protein type and structure. One example is that crystallization can become difficult due to the

conformational differences of the sample, and depends on the size and solubility of the target protein [49].

MS-based protein identification and characterization methods are often used for interaction studies. Using an MS system for analyzing an antigen-ligand interaction, one can obtain both epitope data, paratope structures and compare and assess the affinities [50-57]. Recently, new MS-based methods, such as Intact transition epitope mapping (ITEM), have been developed for both epitope mapping and affinity determination at native-like conditions in the MS alone [58,59]. With this approach, an epitope mass can be analyzed by separating a peptide-antibody complex from a sample mixture and dissociating the peptide in the MS instrument. However, both antibody and peptides need to be injected into the MS and depending on the limits of the instrument, large amounts of antibody may be required for epitope mapping (when comparing ITEM to epitope extraction, where the antibody affinity column can be reused). Moreover, significant development is still needed for affinity determinations and calculations of K_D dissociation constants.

Some widespread methods for epitope identification are based on chemical modifications such as hydrogen/deuterium exchange (HDX) (change of protein mass because of the exchange between amide hydrogens of the backbone and its surrounding solvent [60]), and fast photochemical oxidation of proteins (FPOP), (irreversible labelling of solvent-exposed amino acid side chains by hydroxyl radicals [61]). Among the several methods, Proteolytic Epitope Excision and Extraction mass spectrometry (PROTEX-MS) (Figure S2) has been established as a most successful and widely used method for epitope identification. The epitope extraction/excision methods are based on the native-like ligand-antigen interactions and are used to determine exact epitope peptides [53-62].

PROTEX-MS represents an in-solution analysis, therefore allowing the interaction of the affinity pair at native-like conditions. In epitope excision and extraction experiments, the ligand is immobilized and the analyte is allowed to bind. Epitope extraction mass spectrometry uses a proteolytic digestion mixture of the protein in order to determine the peptides binding to the antibody. Conversely, epitope excision mass spectrometry allows the affinity pair to form, thus providing shielding of the epitope peptides due to the interaction. Enzymatic digestion (typically using trypsin) is performed subsequently to the interaction and the protected peptides (i.e. the epitopes) are identified. For these experiments, typically 10 µg of ligand if immobilized on a column and 20 µg of intact protein (for epitope excision) or digested protein (for epitope extraction) are used for one column. These experiments are triplicated and at least one blank experiment is performed. Therefore, for an accurate epitope identification between a antibody-protein interaction is achieved with less than 50 µg of antibody and 100-200 µg of protein (if both epitope excision and extraction are made). Moreover, the enzymatic digestion can be made with different enzyme to protein ratios, from 1:10

to 1:100 (enzyme to protein). Consequently maximal 20 µg on enzyme is used for these experiments.

All these methods can be used for accurate epitope identification. However, two important aspects for biochemical analysis are sample consumption and reproducibility. While HDX, FPOP and crystallography are very accurate and can be reproduced, the sample consumption per experiment is between 0.1mg to 3 mg (including antibody consummation). On the other hand, the latter two types of epitope identification, ITEM and PROTEX-MS, are reproducible, accurate and require sample amounts between 0.1 ug and 100 ug, reducing the cost of an experiment at least 10 fold. All epitope identification methods are important and can complement and validate each other [63-65].

1.2.2 Biosensor technologies for affinity determination

Biosensors have emerged as a powerful method for biomolecular interaction analysis. A biosensor can provide rapid, real-time, accurate and reliable information about the analyte of interest. Ideally, a biosensor is a device capable of responding continuously, reversibly, and reliable about the affinity pair studied [66,67]. A typical instrument is based on an incident light source that allows a divergent or focused light to travel through a prism and reflect from a gold-coated chip's back surface. A detector then measures the reflected light. The energy from the photons hitting the metal surface at a specific angle, called resonance angle, is fully transferred to the electrons on the surface of the gold. In turn, the charged electrons start moving, thus creating plasmons. This can be visualized as a dark pattern in the detector when the rest of the light is reflected. Moreover, the exact resonance angle, the stability of the chip and immobilized molecules on the chip can be monitored using this shift in the resonance angle [68,69]. A surface plasmon resonance (SPR) biosensor offers interaction strength and provides real-time monitoring of biomolecular interactions for protein interaction.

The SPR biosensor method can be complementary to the information resulting from MS analysis because an SPR sensorgram reveals the affinity strength between two molecules (protein-protein, antibody-protein, aptamer-protein, etc.) as well as specificity, kinetic rates, concentration and equilibrium analysis (Figure S3) [70-72]. However, no chemical information from epitope and paratope a can be obtained by SPR.

1.2.3 SPR Biosensor- Mass spectrometry combination for epitope and affinity determination

Considering that many protein studies require information both on affinity and the binding chemical structure, a combination of mass spectrometry and biosensors will allow highly sensitive, specific and accurate analysis. To this aim, an affinity combination interface between the two different methods can make the two systems compatible and synergistic. By combining the two methods, one can determine the nature of interactions with precision.

A first combination of a biosensor with mass spectrometry was achieved using a surface acoustic wave (SAW) biosensor and electrospray- MS [51]. This combination provided proof of concept for an online system capable of determining both structural epitope information and affinity detection. However, one disadvantage was the lack of an efficient biosensor analysis and a suitable online connection for both ESI- and MALDI- MS. The SPR biosensor technology development has proven highly stable and reliable, and was selected as an alternative. For the SPR, a new system combining SPR and MS had to develop both the requirements for the MS analysis and the SPR because of different solvent requirements for sample preparation. Similar to epitope extraction, 5-10 µg of ligand is immobilized on a gold surface. However, depending on the affinity strength, the dilution series for K_D determinations can have significantly different concentrations. For a high affinity (K_D in the nM range) the concentrations of the sample range between 20nM to 200nM whereas for a low affinity (K_D in the µM/ mM) the sample consumption will increase leading to concentrations between 1 µM and 400 µM. For example, for a 17kDa protein, a dilution series from 20nM to 200 µM requires the samples from 100 ng to 1 mg.

This development enables both ESI (electrospray) and MALDI (Matrix-Assisted Laser Desorption/Ionization) MS for epitope identification. However, the functional principle of ESI- and MALDI-MS is different, and the two MS systems require different sample consideration. Initial combination of the MS with the SPR biosensor was carried out using ESI-MS. This type of MS is described best by looking at the injection (electrospray formation), the methods of separation analysis and the type of mass spectra obtained. For electrospray, a fine aerosol is formed by dispersing a liquid with the use of electricity [73,74]. This fluid contains the analyte of interest, and because the ionization involves extensive solvent evaporation, typically, an organic solvent is added to the buffer [75]. The solution is infused into the capillary at atmospheric pressure and maintained at a high electric potential. [76]. The final droplets become unstable (Rayleigh limit) and decrease more and more because the electrostatic repulsion is stronger than the surface tension of the droplets [77,78]. At this limit, the ESI droplets with a radius of a few nanometers are created and

detected by the MS [79,80]. The mass spectra obtained by an ESI-MS system is based on the nature of the sample, the charge of the sample and the concentration [81].

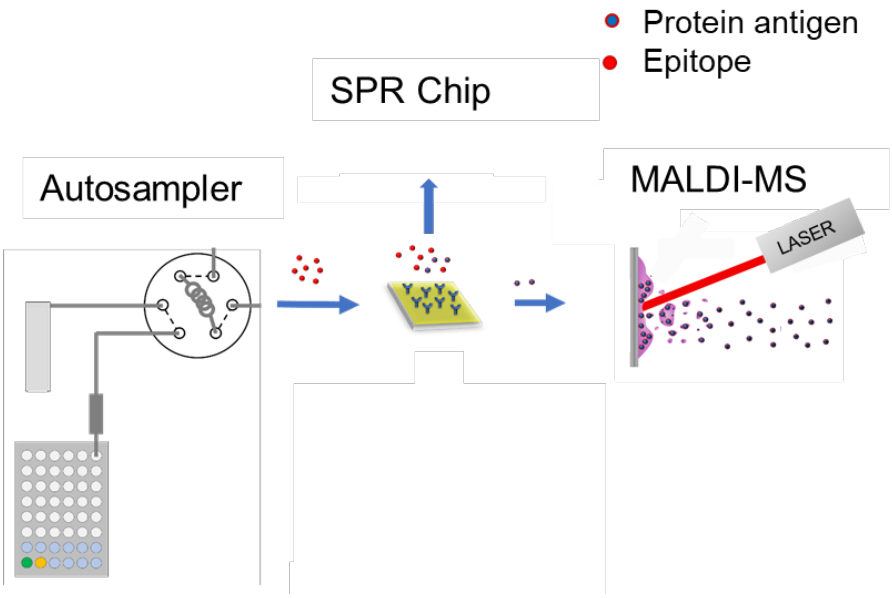

Figure 3: Schematic representation of SPR-Ms combination and pathway. The sample is injected from the automated autosampler to the SPR with the immobilized antibody. From the SPR chip affinity strength evaluation can be performed, while from the elution of the sample from the SPR chip and subsequent MS analysis, epitope identification can be made.

The combination of the two methods, SPR and ESI mass spectrometry has the principal advantage that the sample is injected in solution directly from the affinity interface to the ion source of the MS. Therefore, the interface system can be connected directly to the MS, and the proof of concept was made. The MS spectra obtained from the epitope extraction via the Protex-SPR-MS system shows the chromatogram of the entire experiment. The washing steps showing no peptides from the affiniy column and the elution fraction (obtained by slight acidification) of the epitope peptide after the elution buffer was injected.

In a further development the combination of mass spectrometry with biosensor was made to accommodate MALDI-MS instruments as well. For proteomics, MALDI-TOF has proven to be a powerful instrument for the direct identification and characterization of intact mass of proteins, peptides and digested samples. Moreover, combined with other separation methods and collision-induced dissociation (CID), it can give insights into AA modifications and/or specific mutations. The instrument can accurately measure the intact mass of a protein with the spectra showing only the singly, doubly and in some cases, triply charged proteins. MALDI-MS is one of the most utilized mass spectrometers, and by modifying the system, a new type of SPR-MS could be created [82].

Mechanically, a MALDI-MS instrument is made of: a sample target, where the molecule of interest is encapsulated in a crystal (chemical matrix); a laser to ensure the generation of the particle cloud with the ions of interest; time of flight tube and detector [83].

There are multiple ways to capture the molecules in the crystals. First, between 0,5µl-1µl of the matrix solution is pipetted onto the target plate: under the sample, when the matrix is left to dry followed by a mixture of sample matrix solution, on top of the sample, then the crystals can capture the molecules, or just by mixing the sample and the matrix and letting them dry. The mass analyzers can be a quadrupole, a tandem quadrupole, an ion trap or a time-of-flight, and variations and combinations of these methods for both ESI and MALDI MS [84].

Overall, both ESI- and MALDI-MS are sensitive tools for peptide and protein analysis. They can accurately identify epitope-paratope pairs with epitope excision and extraction protocols.

For all MS analysis, the sample will be prepared generally in an organic solvent at acidic pH, liquid injected into the MS in the case of ESI-MS and dried on a sample plate in the case of the MALDI-MS. It is beneficial for the affinity column, where the binding is made in salt-free buffers and elution with ionic solvents. However, incompatible with SPR, a method that requires high salt concentrations and short regeneration times.

Experiments using the SPR instrument are performed in native-like conditions to ensure the surface's stability and allow the binding measurements of the analyte to the ligand. PBS (phosphate-buffered saline) buffer is used for the binding event and a regeneration solution (Table 2) to remove the analyte and stabilize the surface. The buffer incompatibility obstacle (between an SPR and an MS) is overcome by constructing a solvent delivery system. This interface consists of an autosampler, two multiport valves, two syringe pumps and all the microfluidic cables required. To ensure reliability and reproducibility, the SPR-chip and the Sepharose affinity columns (for epitope excision/extraction MS) had the same antibody immobilized. In the case of the SPR, the antibody is immobilized from the system, only on one channel. Since the gold chip has two channels, the second one is used as a reference, resulting in the first experimental control of unspecific interaction. For the affinity experiments, the control is made by replacing the ligand column with the blank column and repeating the experiment. Both the control column and the experimental column are prepared outside the system and stored in the refrigerator at 4 degrees to ensure the antibody is stable for a longer time. Next, the sample (intact protein, peptide or peptide mixture) is injected into an affinity column. Within the instrument, all the washing steps are made and recorded by the MS and the elution fraction. Then, the same sample is injected into the SPR chip for K_D determination.

The concept of the PROTEX-MS was designed to provide all the samples requirements for both the SPR and MS. The automated system includes a sample rack, three six-port switching valves, two

pumps for sample delivery, washing, a buffer rack for all solvents, including waste and last but not least, the two detectors, SPR and MS. The ligand immobilized affinity column is prepared outside the system and connected to the fluidics. The analyte is injected from the autosampler over the SPR immobilized chip, and K_D determinations can be made. A two-port pump delivers PBS buffer to the SPR and facilitates the interaction. Following the SPR step, the sample is delivered to the affinity column connected to valve 2. A solvent dispenser makes sample washing and elution via pump 2. The MS spectra can be recorded at any point during the experiment. In Figure 4A the concept is presented as the sample being injected into the interface system and the results that can be read (K_D from the SPR and structural analysis from the MS). In Figure 4B one of the first constructions of the interface model. The housing of the instrument contains both the sample preparation level as well and sample delivery. On the upper level the pipetting robot can inject the sample (either intact protein or peptides) to the lower level, where the affinity column is situated. On the lower level all the steps for epitope extraction or excision can be made automatically via the switching valves and pump and it is delivered to the SPR and MS instruments for analysis. The steps the sample follows are described in detail in Figure S4. Form the pipetting robot the sample is delivered to the valve system where it can be transported for SPR analysis and epitope identification via MS. Currently, the PROTEX-SPR-MS interface model developed with SunChrome company is integrating an autosampler and an automated spotter for the MALDI analysis (Figure 5).

With the newly developed system that includes an SPR within an automated program, the experimental setup will become faster and require less sample amount. Instead of using the protein amounts in two separate experiments (two times the sample), the automatic system delivers the same sample (amount) to both the affinity column and the SPR. Therefore, even if the ligand amounts remain the same (since it will still be immobilized on both the SPR chip and affinity column media), the sample consumption is reduced to the amount the SPR requires for the K_D determination (20 nM to 200 µM if the affinity is low). The experiment combines all the necessary procedures for interaction analysis (intact protein- antibody/ -aptamer) and epitope determination and structural characterization of the protein. Moreover, any type of MS, ESI or MALDI can just be added to the instrument, making it more flexible for the user's need.

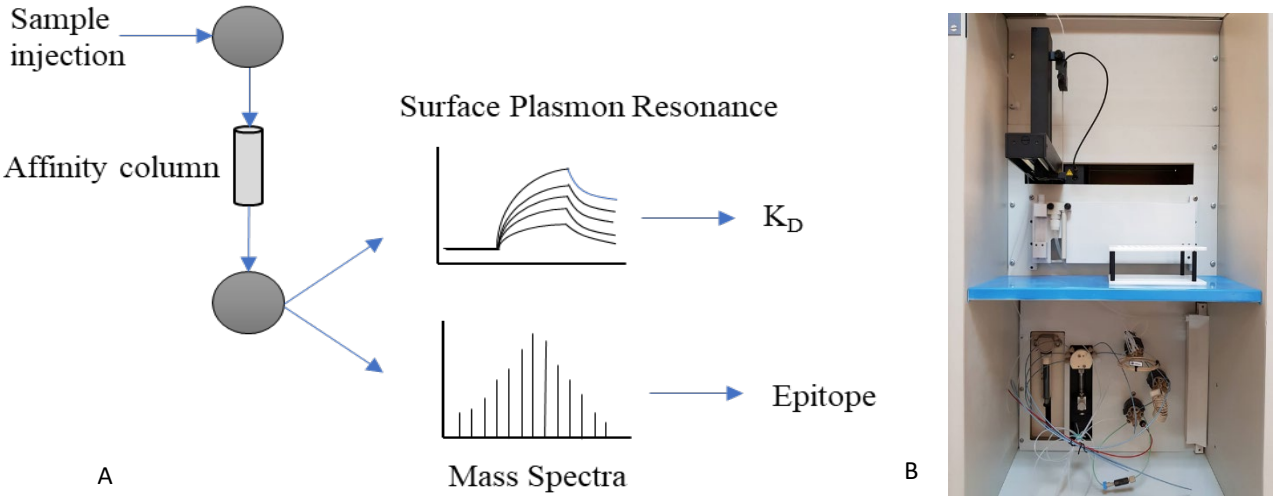

Figure 4: Schematic representation of the PROTEX-SPR-MS methodology and instrument design.4A. Sample path from the injection to an affinity column with final results after the online procedure- structural analysis (MS) and K_D determination (SPR). The proteins are injected to the interface part, where the affinity column is incorporated. The analysis of the dilution series from the interface goes on the SPR and the elution of the epitope from the SPR is injected to the MS. All the required sample buffer changes are made in the interface system. 4B. Design of the interface instrument. On the upper side the sample preparation and injection robot and on the lower level the interface containing the switching valves, affinity column and solvent switching pump.

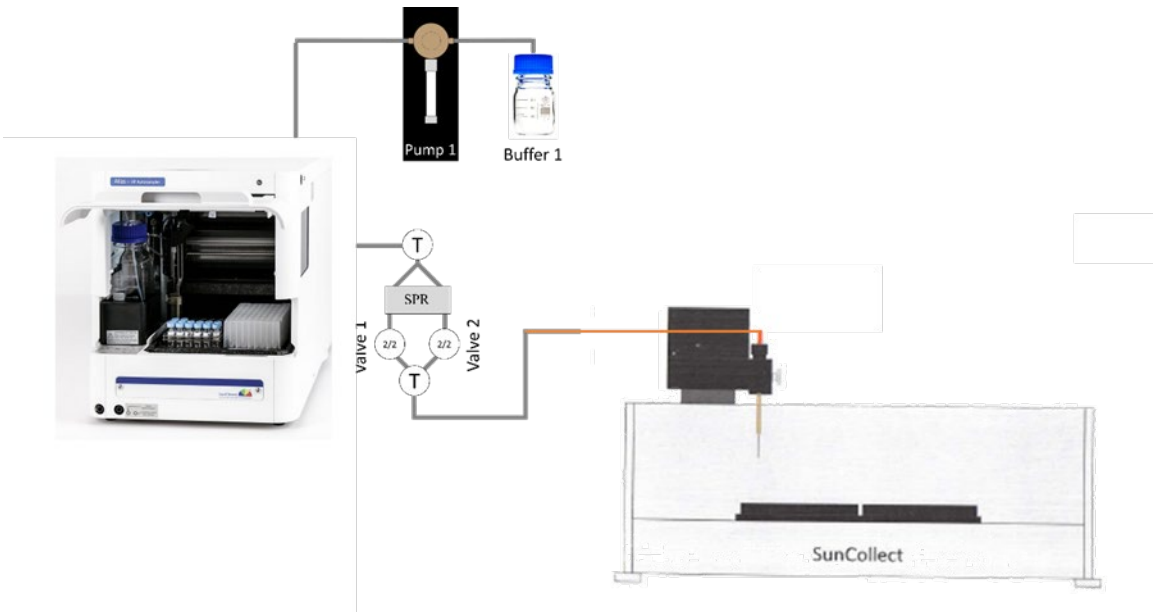

Figure 5: Scheme for PROTEX-SPR-MS. The automated autosampler delivers the sample to the interface with the buffer from the pump. The interface contains a SPR instrument for KD analysis and the sample is spotted with a MALDI plate spotter (SunCollect) for MALDI analysis.

2. OBJECTIVES OF THE DISSERTATION AND SELECTED APPLICATIONS

The development of a reliable molecular method for determination of molecule interactions is key in creating new biochemical targets for diagnosis and therapy. Molecular Excision/Extraction SPR-MS (PROTEX-SPR-MS) can be used to determine a new target for antibody production, for developing molecules towards immune response suppression or immune triggering, for better diagnosis possibilities, or even to identify and characterize new molecules. The presented work is comprised of two main objectives: (1) to develop an automated system for protein characterization by combining the potential application of both SPR and MS; (2) to apply it to currently unknown molecular interactions.

The work's success stems from all the affinity pairs studied and understood from a new perspective and from the developments that will follow from their analysis (Chapter 3.1 “Antibody Epitope and Affinity Determination of the Myocardial Infarction Marker Myoglobin by SPR- Biosensor Mass Spectrometry”; 3.2 “Antibody Epitope of human α-Galactosidase A revealed by affinity-mass spectrometry: A basis for reversing immunoreactivity in enzyme replacement therapy of Fabry’s Disease”; 3.3 “Molecular Epitope Determination of Aptamer Complexes of the Multi-domain Protein C-Met by Proteolytic Affinity- Mass Spectrometry”;).

PROTEX-SPR-MS method has been used to identify several epitopes with potential medical applications: an epitope peptide for antibody depletion by apheresis in Fabry’s disease was identified; and an epitope that could be used for early diagnosis of heart muscle injury was identified and characterized. Moreover, PROTEX-SPR-MS was used to study two different single stranded DNA aptamers interacting with a tumor biomarker protein. This analysis revealed that aptamers have very similar affinity and epitope binding to monoclonal antibodies, indicating they could be used for a variety of medical applications.

3. RESULTS

3.1. Antibody Epitope and Affinity Determination of the Myocardial Infarction Marker Myoglobin by SPR- Biosensor Mass Spectrometry

Mihoc D, Lupu L, Wiegand P, Kleinekofort W, Müller O, Völklein F, Glocker MO, Barka F, Barka G, Przybylski M
J. Am. Soc. Mass Spectrom,32,1,106-113,2021

“Myoglobin (MG) is a biomarker for heart muscle injury, making it a potential target protein for early detection of myocardial infarction. Elevated myoglobin levels alone have low specificity for acute myocardial infarction (AMI) but in combination with cardiac troponin T have been considered highly efficient diagnostic biomarkers. Myoglobin is a monomeric heme protein with a molecular weight of 17 kDa that is found in skeletal and cardiac tissue as an intracellular storage unit of oxygen. MG consists of eight α - helices connected by loops and a heme group responsible for oxygen-binding. Monoclonal antibodies are widely used analytical tools in biomedical research and have been employed for immunoanalytical detection of MG. However, the epitope(s) recognized by MG antibodies have been hitherto unknown. Precise molecular identification of the epitope(s) recognized by antibodies is of key importance for the development of MG as a diagnostic biomarker. The epitope of a monoclonal MG antibody was identified by proteolytic epitope extraction mass spectrometry in combination with surface plasmon resonance (SPR) biosensor analysis. The MG antibody was immobilized both on an affinity microcolumn and a gold SPR chip. The SPR kinetic analysis provided an affinity-binding constant KD of 270 nM for MG. Binding of a tryptic peptide mixture followed by elution of the epitope from the SPR-MS affinity interface by mild acidification provided a single-epitope peptide located at the C-terminus [146 − 153] [YKELGFQG] of MG. The specificity and affinity of the epitope were ascertained by synthesis and affinity-mass spectrometric characterization of the epitope peptide.”

3.2. Antibody Epitope of human α-Galactosidase A revealed by affinity-mass spectrometry: A basis for reversing immunoreactivity in enzyme replacement therapy of Fabry's Disease

Kukacka Z, Iurascu M, Lupu L, Rusche H, Murphy M, Altamore L, Borri F, Maeser S, Papini A M, Hennermann J, Przybylski M

Chem. Med. Chem,13,9,909-915,2018

"Alpha-galactosidase (αGal) is a lysosomal enzyme that hydrolyses the terminal alpha-galactosyl moiety from glycosphingolipids. Mutations in the encoding genes for αGal lead to defect or misfolded enzyme which results in substrate accumulation and subsequent organ dysfunction. The metabolic disease caused by deficiency of human alpha-galactosidase A is called Fabry Disease (FD) or Fabry-Anderson Disease, and belongs to a larger group known as lysosomal storage diseases. Effective treatment of FD has been developed by enzyme replacement therapy (ERT) that employs infusions of purified recombinant enzyme, in order to increase enzyme levels and reduce the amounts of accumulated substrate. However, immunoreactivity and IgG antibody formation are major, therapy-limiting, and eventually life-threatening complications of ERT. The present study focused on the epitope determination of human alpha-galactosidase A against its antibody formed. Here we report the identification of the epitope of human αGal (309-332) recognized by a human monoclonal anti-αGal antibody, using a combination of proteolytic excision of the immobilized immune complex and surface plasmon resonance (SPR)- biosensor-mass spectrometry. The epitope peptide, αGal (309-332) was synthesized by solid-phase peptide synthesis. Its affinity determination by SPR analysis provided high binding affinity to the antibody (KD - 39 x 10-9 M), which is nearly identical to that of the full length enzyme (KD - 16 x 10-9 M). The proteolytic excision-affinity mass spectrometry method is shown here to be an efficient tool for epitope identification of an immunogenic lysosomal enzyme. Since the full length alpha-galactosidase and the antibody epitope showed comparable binding affinities, this is providing a basis for reversing immunogenicity upon enzyme replacement therapy by (i), treatment of patients with epitope peptide to neutralizing antibodies, or (ii), removal ofantibodies by apheresis, and thus significantly improve the response to ERT. "

3.3. Molecular Epitope Determination of Aptamer Complexes of the Multi-domain Protein C-Met by Proteolytic Affinity- Mass Spectrometry

Lupu L, Wiegand P, Hüttmann N, Rawer S, Kleinekofort W, Shugureva I, Kichkailo A S, Tomilin F N, Lazarev A, Berezovski M V, Przybylski M

Chem. Med. Chem.,15,4,363-369,2020

“C-Met protein is a glycosylated receptor tyrosine kinase of the hepatocyte growth factor (HGF), composed of an alpha and a beta chain. Upon ligand binding, C-Met transmits intracellular signals by a unique multi-substrate docking site. C-Met can be aberrantly activated leading to tumorigenesis and other diseases and has been recognized as a biomarker in cancer diagnosis. C-Met aptamers have been recently considered a useful tool for detection of cancer biomarkers. Here we report a molecular interaction study of human C-Met expressed in kidney cells with two DNA aptamers of 60 and 64 bases (CLN0003 and CLN0004), obtained using the SELEX (Systematic Evolution of Ligands by Exponential Enrichment) procedure. Epitope peptides of aptamer- C-Met complexes were identified by proteolytic affinity- mass spectrometry in combination with SPR biosensor analysis (PROTEX-SPR-MS), using high-pressure proteolysis for efficient digestion. High affinities (KD, 80-510 nM) were determined for aptamer- C-Met complexes, with two-step binding suggested by kinetic analysis. A linear epitope, C-Met (381-393) was identified for CLN0004, while the CLN0003 aptamer revealed an assembled epitope comprised of two peptide sequences, C-Met (524-543) and C-Met (557-568). Structure modeling of C-Met- aptamers were consistent with the identified epitopes. Specificities and affinities were ascertained by SPR analysis of the synthetic epitope peptides. The high affinities of aptamers to C-Met, and the specific epitopes revealed render them of high interest for cellular diagnostic studies. “

4. DISCUSSION AND CONCLUSIONS

Epitope characterization has numerous applications in the field of medicine; understanding diseases, improved treatment and development of preventive medicine. In virology, epitope characterization proved key for determining neutralizing sequences for human immunodeficiency virus (HIV) [85] as well as for developing new vaccines for diseases such as influenza A infection, Japanese encephalitis, Yellow Fever and others [86-88]. Furthermore, epitope-based vaccines were developed against parasite infections, e.g. Theileria parasites, Schistosoma mansoni [89,90] as well as bacterial infections, e.g. Clostridioides difficile [91], of Mycobacterium tuberculosis [92]. Other sources show that epitope identification can help characterize immune reactions and food allergies [93-95] which would help with enhance diagnosis and treatment, improving life quality for millions of people. As for epitope related treatment, cancer, tuberculosis and Alzheimer's disease are among the prominent diseases showing the importance of epitope identification and characterization [94-100].

Within this work, the development of the SPR-MS combination, multiple epitope characterizations were achieved. Structural analysis and affinity determinations were achieved for a cancer related protein (C-Met), a mitochondrial infarction protein (myoglobin) and for an enzyme for Fabry's Disease. However, the initial idea of the combination between a biosensor and epitope identification mass spectrometry was tested by analysing the interaction between an antibody-protein pair related to Alzheimer's disease (AD).

As of 2020, 55 million people worldwide are estimated to be living with Dementia and by 2050 the number is expected to be as high as 139 million [100,102]. AD is a highly complex, not yet fully understood disease with many complex protein interactions and modifications. Among many hypotheses related to the onset and development of AD, two prominent theories are the most currently supported by the scientific community: the amyloid cascade hypothesis and the tau hypothesis [103,104]. According to the first, aggregated amyloid-beta (Aβ), protein accumulation is the main factor in AD onset and progression [105]. This protein has many receptors [106] and is involved in a variety of different processes in the brain [107]. The amino acid (AA) sequence length of Aβ protein can vary, from 38-43 AA; however, a biomarker for AD has been suggested to be the upregulation of the highly aggregation-prone Aβ42 [108]. It is thought that senile plaques develop from an increase of Aβ oligomers that aggregate and form plaques. They are considered a hallmark of AD, being one of the first indicators for AD seen on MRI scans. Therefore, more information on the aggregation process and how to suppress it could lead to an improved treatment [109]. In 2021 a monoclonal antibody (aducanumab) was approved for treatment of AD under the accelerated

approval pathway by the FDA, despite the Phase III clinical trial having been halted based on a futility analysis as well as clear indications the treatment was not efficient [110-113]. This antibody was shown in laboratory tests to reduce Aβ plaques (targeting Amyloid beta peptides), and was one of several antibodies studied for Aβ inhibition that exhibited different selectivity for soluble oligomers compared to plaques.

The SPR-MS procedure was tested using the 40 amino acid Aβ peptide (Figure 6) that contains four possible tryptic digestion sites. This specific peptide is highly researched and multiple antibodies were developed against it. The interaction between the antibody used for this work and Amyloid Beta was analyzed prior and the epitope (peptide 4-10) was already determined [114]. Moreover, the interaction strength of 22 nM was published as well [115]. With the existing information on this affinity pair the initial testing of the new PROTEX-SPR MS could be validated. This combination proved effective for epitope identification when applied on an anti-Aβ antibody – Aβ 1-16 affinity pair (with the epitope peptide being the 4-10 AA). The washing and elution steps were recorded in the chromatogram (Figure 6A). The experiment included all the steps of a typical epitope extraction procedure, an injection over the affinity column, a long washing after the injection until no peptides could be measured, and an elution step to identify the epitope. In comparison to previous experiments [116] in this system, all the washing and elution steps were made within 20 minutes. A typical epitope extraction (including the washing and elution steps) usually requires 1 hour. The time requirements can be reduced within the combination because of the constant monitoring via the MS of the washing steps. With this feature the washing steps can be adjusted as soon as all the supernatant is removed. Without the MS monitoring, the washing is preformed manually, without a constant flowrate and with a specific volume. This volume can be too less or too high and it adds to the time required for the experiment. Moreover, the flowrate could affect the interaction and the epitope peptide could be removed.

In this initial test, the chromatogram of the washing fractions detects no Aβ corresponding molecular ions present (the first MS spectra (data from chromatogram 1.2-17.6 minutes) Figure 6B). The elution fraction can be observed in the last section of the chromatogram (minutes 19.3-21.4). The respective MS spectra (Figure 6C) contains the $[M+2]^{+2}$, $[M+3]^{+3}$ and $[M+4]^{+4}$ ions of the Aβ 1-16 measured. Since there are differences in the automated combination and the manual one, the Aβ 1-16 peptide was delivered to the sample loop and injected to the affinity column with a low flow rate (5 µl/min), these conditions simulate the incubation time when compared with an offline system. The washing step was made with ammonium bicarbonate buffer 10mM at a continuous, constant flow rate of 5ul/ min.

Aβ 1-DAEFRHDSGYEVHHQKLVFFAEDVGSNKGAIIGLMVGGVV-40

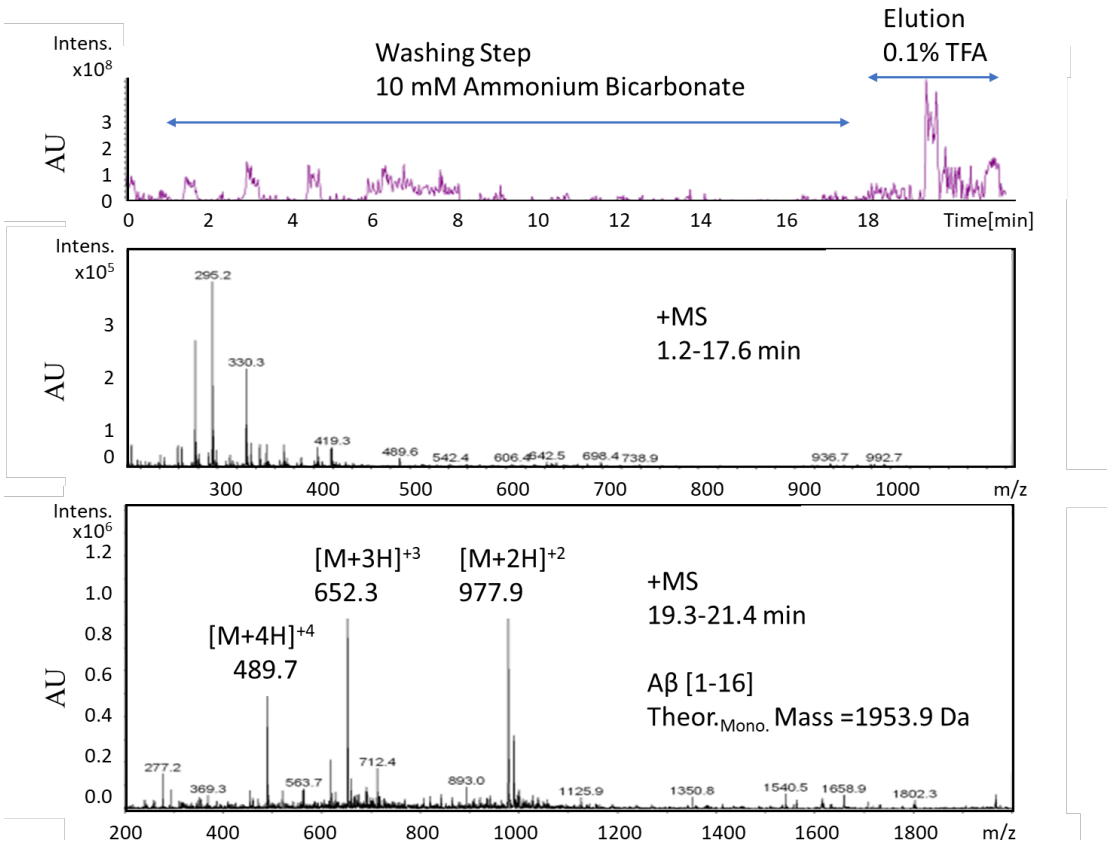

Figure 6: ESI-MS results of the online interface system used for the study of Aβ 1-16 peptide with a known Anti Aβ antibody. 6A The chromatogram presenting the 20 minutes experiment of the washing and elution steps (of the Aβ 1-16) from affinity column. Washing steps were made with ammonium-bicarbonate buffer and elution was performed with 0.1% TFA. 6B MS spectra containing the data of the chromatogram from minute 1.2 to minute 17.6 min and showing that no peptide where eluting from the column. 6C MS spectra containing the data of the chromatogram from minute 19.3 to minute 21.4 showing the elution step of the Aβ 1-16 peptide from the column with three ions of the peptide visible. Aβ 1-16 has the theoretical mass of 1953.9 Da and the ions measured in the ESI-MS elution fractions were the $[M+2]^{+2}$, $[M+3]^{+3}$ and $[M+4]^{+4}$. All Y axes have arbitrary units.

SPR-MS system introduces epitope identification and the K_D determination in one experiment. Therefore, the interaction strength between anti-Aβ antibody and Aβ 1-16 peptide was carried out on the SPR- biosensor system with the antibody immobilized on the gold chip (Figure 7). Kinetic analysis calculated the K_D in the nanomolar range, and the results were consistent with the known affinities of this pair.

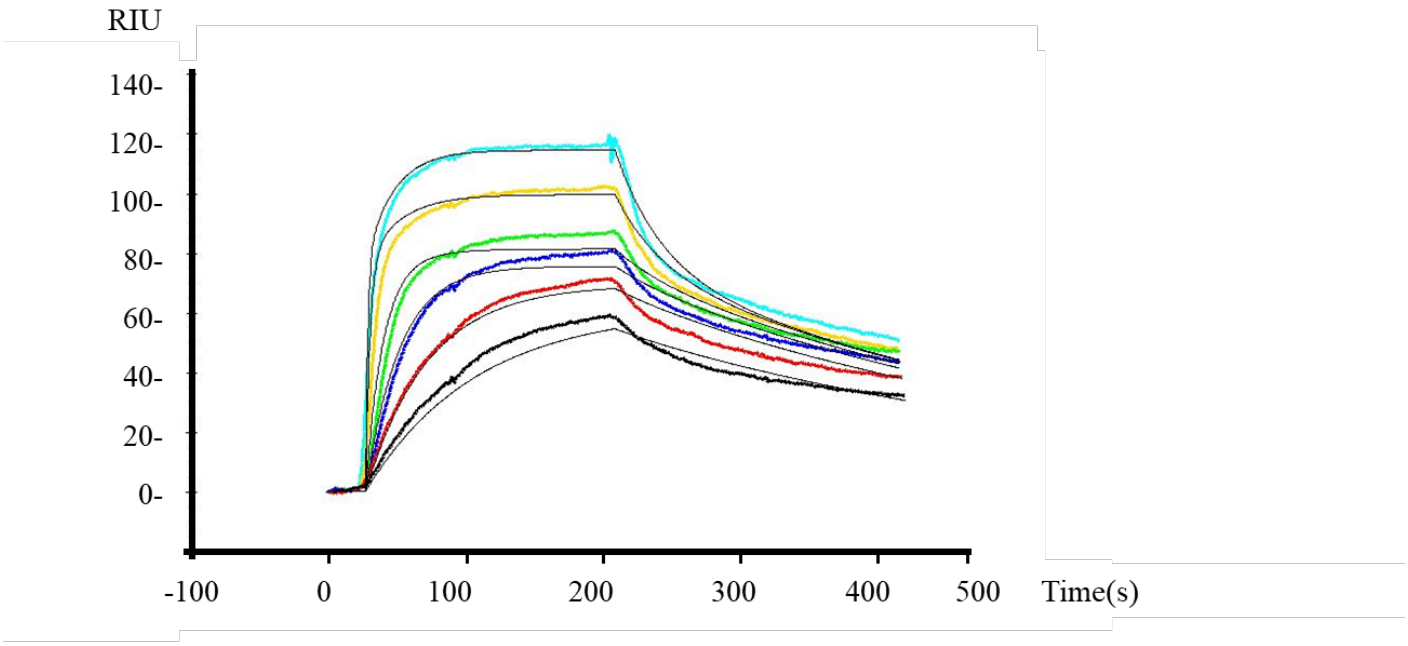

Figure 7: SPR kinetic evaluation of dilution series of intact Aβ 1-16 peptide interacting with immobilized monoclonal anti-Aβ antibody. Analysis made after reference and buffer subtraction via the TraceDrawer program [117]. K_D evaluation shows a strong binding affinity in the nano Molar range.

Based on the initial success of the SPR and MS for the anti-Aβ antibody – Aβ 1-16 affinity pair, other novel affinity pairs were studied. Three different types of molecular interactions were analyzed in this work; one was the study of antibody-protein interaction, another was antibody-enzyme and last was based on two aptamers interacting with one protein.

The second application on an antibody-protein pair demonstrated the reproducibility of the experimental procedure for the SPR-MS. Moreover, the antibody-myoglobin affinity pair could lead to the developments of an early diagnosis tool for Acute Myocardial Infarct. Analysis on horse heart myoglobin protein interacting with a monoclonal antibody demonstrated that both the epitope (peptide sequence 146 – 153 with the m/z of 941,4 Da) and affinity strength (270 nM) endorsed the automated procedure for an antibody-protein pair. Moreover, the novelty of these results supported the efficiency of the system for molecules with higher molecular mass.

Similar performance of the SPR-MS combination was determined with an antibody-enzyme affinity pair, more specific the analysis of the interaction between alpha-galactosidase A enzyme (used as a treatment in enzyme replacement therapy) and an antibody that the human immune system produces against the treatment. Fabry's disease is part of the metabolic diseases and is caused by an abnormal quantity of glycosphingolipids found in the lysosomes.

The main reason for de accumulation is cause by a deficiency of alpha-galactosidase A (glycoside hydrolase enzyme). Moreover, since this a genetic disease, the treatment is limited, summing up to enzyme replacement therapy or (more recent) gene therapy [118]. Since the treatment induces an immune response, the options for the patients are limited and can have grave consequences (some studies show that over 60% of patience develop antibodies) [119]. Therefore, an epitope peptide could be used as a blocker for the antibodies, improving the results of the treatment. The results of these analysis found that the αGal peptide with the 309-332 AA sequence was the one interacting with the antibody and determined that epitope peptide and the protein have very similar affinities. Moreover, epitope analysis on such diseases can lead to personalized medicine, since the immune system does not have universal characteristic that all patients share [120].

The effectiveness of the new combination was also demonstrated on a novel affinity pair, aptamer-protein. For the work on this affinity interaction the C-Met protein (tyrosine-protein kinase Met) - aptamer complex was characterized. C-Met is a highly complex protein involved a multiple-pathways. It has many important roles in development of cancer via the activation of key oncogenic pathways, sprouting of new blood vessels from pre-existing ones to supply a tumour with nutrients and scatter (cells dissociation due to metalloprotease production), which often leads to metastasis. In view of that fact, a large number of C-Met inhibitors have been developed (small molecules; antibodies) [121-124]. However, a newer technology for inhibitors has arisen, that could have benefits in this field. Aptamers as inhibitor molecules [125] are gaining interest as they are less likely to trigger an immune response, they are easy to produce (after the sequence is known) and less expensive. Based on this information, two different aptamers CLN0003 and CLN0004 were tested for their interaction with the C-Met protein. The two aptamers differ by size, structure and interaction strength and they were modified with a C16 amino group to facilitate their immobilization. Although previous work showed high affinity and inhibition to the protein, the epitope peptides for the two aptamers researched within this work were not previously described [126]. Since the two aptamers show high binding affinity and inhibition properties, the epitope identification help elucidate the binding mechanisms between the C-Met and its natural receptor. Moreover, the epitope data identified could lead to more efficient inhibitor molecules.

The PROTEX-SPR-MS system takes advantage of mass spectrometry structural characterization and of the SPR biosensor interaction analysis that can be applied for many affinity pairs [127,128]. The automated system consists of the sample delivery, incubation and sample analysis and it can be used both for qualitative and quantitative analysis. With more than one construction, numerous tests and redesign, the combination was made for the use of both ESI-MS or MALDI-MS and with any SPR system.

5. BIBLIOGRAPHY

1. Black CA. A brief history of the discovery of the immunoglobulins and the origin of the modern immunoglobulin nomenclature. Immunol Cell Biol. 1997, 75:65-8.
2. Schroeder HW Jr, Cavacini L. Structure and function of immunoglobulins. J Allergy Clin Immunol. 2010, 125: S41-52.
3. Joyce, C., Burton, D.R. & Briney, B. Comparisons of the antibody repertoires of a humanized rodent and humans by high throughput sequencing. Sci Rep. 2020, 10, 1120.
4. Pone EJ, Zhang J, Mai T, White CA, Li G, Sakakura JK, Patel PJ, Al-Qahtani A, Zan H, Xu Z, Casali P. BCR-signalling synergizes with TLR-signalling for induction of AID and immunoglobulin class-switching through the non-canonical NF-κB pathway. Nat Commun. 2012, 3, 3:767.
5. Briney B, Inderbitzin A, Joyce C, Burton DR. Commonality despite exceptional diversity in the baseline human antibody repertoire. Nature. 2019, 566(7744):393-397.
6. Stigter D, Dill KA. Charge effects on folded and unfolded proteins. Biochemistry. 1990, 29(5):1262-71.
7. Van Oss CJ. Hydrophobic, hydrophilic and other interactions in epitope-paratope binding. Mol Immunol. 1995, 32(3):199-211
8. Reverberi R, Reverberi L. Factors affecting the antigen-antibody reaction. Blood Transfus. 2007, 5(4):227-40.
9. Guseman AJ, Speer SL, Perez Goncalves GM, Pielak GJ. Surface Charge Modulates Protein-Protein Interactions in Physiologically Relevant Environments. Biochemistry. 2018, 57(11):1681-1684.
10. Chiu ML, Goulet DR, Teplyakov A, Gilliland GL. Antibody Structure and Function: The Basis for Engineering Therapeutics. Antibodies (Basel) 2019, 8(4):55.
11. Polonelli L, Pontón J, Elguezabal N, Moragues MD, Casoli C, Pilotti E, Ronzi P, Dobroff AS, Rodrigues EG, Juliano MA, Maffei DL, Magliani W, Conti S, Travassos LR. Antibody complementarity-determining regions (CDRs) can display differential antimicrobial, antiviral and antitumor activities. PLoS One. 2008, 3(6):e2371.
12. Janeway CA Jr, Travers P, Walport M, et al., Immunobiology: The Immune System in Health and Disease, 2001, 5th edition. New York: Garland Science.
13. Fred S. Rosen, Lisa A. Steiner, Emil R. Unanue, Macmillan Dictionary of Immunology, reprint 1989 University of California Macmillan, 2010.
14. Moise A, André S, Eggers F, Krzeminski M, Przybylski M, Gabius HJ, Toward bioinspired galectin mimetics: antigenidentification of ligand-contacting peptides by proteolytic-excision mass spectrometry, J. Am. Chem. Soc. 2011, 133: 14844-14847.
15. Opuni KFM, Al-Majdoub M, Yefremova Y, El-Kased RF, Koy C, Glocker MO. Mass spectrometric epitope mapping. Mass Spectrom Rev. 2018, 37:229-241.
16. Uversky VN, Van Regenmortel MHV. Mobility and disorder in antibody and antigen binding sites do not prevent immunochemical recognition. Crit Rev Biochem Mol Biol. 2021, 56(2):149-156.
17. Hager-Braun C, Tomer KB. Determination of protein-derived epitopes by mass spectrometry. Expert Rev Proteomics. 2005, 2(5):745-56.

18. van Schouwenburg PA, Rispens T, Wolbink GJ. Immunogenicity of anti-TNF biologic therapies for rheumatoid arthritis. Nat Rev Rheumatol. 2013, 9:164-72.

19. Vaisman-Mentesh A, Rosenstein S, Yavzori M, Dror Y, Fudim E, Ungar B, Kopylov U, Picard O, Kigel A, Ben-Horin S, Benhar I, Wine Y. Molecular Landscape of Anti-Drug Antibodies Reveals the Mechanism of the Immune Response Following Treatment With TNFα Antagonists. Front Immunol. 2019, 10:2921.

20. van Brummelen EM, Ros W, Wolbink G, Beijnen JH, Schellens JH. Antidrug Antibody Formation in Oncology: Clinical Relevance and Challenges. Oncologist. 2016, 21(10):1260-1268.

21. Keefe, A.D.; Pai, S.; Ellington, A. Aptamers as therapeutics. Nat. Rev. Drug Discov. 2010, 9, 537–550.

22. Hong, K.L.; Sooter, L.J. Single-Stranded DNA Aptamers against Pathogens and Toxins: Identification and Biosensing Applications. Biomed. Res. Int. 2015, 31.

23. Gelinas AD, Davies DR, Janjic N. Embracing proteins: structural themes in aptamer-protein complexes. Curr Opin Struct Biol. 2016, 36:122-32.

24. Barciszewski, J.; Clark, B.F.C. RNA Biochemistry and Biotechnology; Springer: Dordrecht, The Netherlands, 2012.

25. Tuerk, C.; Gold, L. Systematic evolution of ligands by exponential enrichment: RNA ligands to bacteriophage T4 DNA polymerase. Science 1990, *249*, 505–510.

26. Sun H, Zhu X, Lu PY, Rosato RR, Tan W, Zu Y. Oligonucleotide aptamers: new tools for targeted cancer therapy. Mol Ther Nucleic Acids. 2014, 3(8):e182.

27. Ellington, A.D.; Szostak, J.W. *In vitro* selection of RNA molecules that bind specific ligands. Nature 1990, *346*, 818–822.

28. Wang, Y.; Luo, Y.; Bing, T.; Chen, Z.; Lu, M.; Zhang, N.; Shangguan, D.; Gao, X. DNA aptamer evolved by cell-SELEX for recognition of prostate cancer. PLoS ONE 2014, 9, e100243.

29. Zhu Q, Liu G, Kai M. DNA Aptamers in the Diagnosis and Treatment of Human Diseases. Molecules. 2015, 20(12):20979-97.

30. Gold L. Oligonucleotides as research, diagnostic, and therapeutic agents. J Biol Chem. 1995, 270(23):13581-4.

31. Keefe AD, Pai S, Ellington A. Aptamers as therapeutics. Nat Rev Drug Discov. 2010, 9(7):537-50.

32. Ali MH, Elsherbiny ME, Emara M. Updates on Aptamer Research. Int J Mol Sci. 2019, 20(10):2511.

33. Gragoudas ES, Adamis AP, Cunningham ET Jr, Feinsod M, Guyer DR; VEGF Inhibition Study in Ocular Neovascularization Clinical Trial Group. Pegaptanib for neovascular age-related macular degeneration. N Engl J Med. 2004, 351(27):2805-16.

34. Chames P, Baty D. Bispecific antibodies for cancer therapy: the light at the end of the tunnel? MAbs. 2009, 1(6):539-47.

35. Soldevilla MM, Meraviglia-Crivelli de Caso D, Menon AP, Pastor F. Aptamer-iRNAs as Therapeutics for Cancer Treatment. Pharmaceuticals (Basel). 2018, 11(4):108.

36. Soldevilla MM, Villanueva H, Meraviglia-Crivelli D, Menon AP, Ruiz M, Cebollero J, Villalba M, Moreno B, Lozano T, Llopiz D, Pejenaute Á, Sarobe P, Pastor F. ICOS Costimulation at the Tumor Site in Combination with CTLA-4 Blockade Therapy Elicits Strong Tumor Immunity. Mol Ther. 2019, 27(11):1878-1891.

37. Tran PH, Xiang D, Nguyen TN, Tran TT, Chen Q, Yin W, Zhang Y, Kong L, Duan A, Chen K, Sun M, Li Y, Hou Y, Zhu Y, Ma Y, Jiang G, Duan W. Aptamer-guided extracellular vesicle theranostics in oncology. Theranostics. 2020, 10(9):3849-3866.

38. Xiang D, Shigdar S, Qiao G, Wang T, Kouzani AZ, Zhou SF, Kong L, Li Y, Pu C, Duan W. Nucleic acid aptamer-guided cancer therapeutics and diagnostics: the next generation of cancer medicine. Theranostics. 2015, 5(1):23-42.

39. Soule EE, Yu H, Olson L, Naqvi I, Kumar S, Krishnaswamy S, Sullenger BA. Generation of an anticoagulant aptamer that targets factor V/Va and disrupts the FVa-membrane interaction in normal and COVID-19 patient samples. Cell Chem Biol. 2022, 29(2):215-225.e5.

40. Kim TH, Lee SW. Aptamers for Anti-Viral Therapeutics and Diagnostics. Int J Mol Sci. 2021, 22(8):4168.

41. Shatunova EA, Korolev MA, Omelchenko VO, Kurochkina YD, Davydova AS, Venyaminova AG, Vorobyeva MA. Aptamers for Proteins Associated with Rheumatic Diseases: Progress, Challenges, and Prospects of Diagnostic and Therapeutic Applications. Biomedicines. 2020, 8(11):527.

42. Wan Q, Liu X, Zu Y. Oligonucleotide aptamers for pathogen detection and infectious disease control. Theranostics. 2021,11(18):9133-9161.

43. Chakraborty B, Das S, Gupta A, Xiong Y, T-V V, Kizer ME, Duan J, Chandrasekaran AR, Wang X. Aptamers for Viral Detection and Inhibition. ACS Infect Dis. 2022, 8(4):667-692

44. Dahl PF, Flash of the Cathode Rays: A History of J. J. Thomson's Electron, Bristol, U.K.: Institute of Physics, CRC Press.1997.

45. Hoffman ED, Stroobant V, Mass Spectrometry: Principles and Applications, 2nd ed., John Wiley and Sons, 2001.

46. Maveyraud L, Mourey L. Protein X-ray Crystallography and Drug Discovery. Molecules. 2020, 25(5):1030.

47. [38]Papageorgiou AC. X-Ray Crystallography in Structure-Function Characterization of Therapeutic Enzymes. Adv Exp Med Biol. 2019, 1148:81-103.

48. Zheng H, Handing KB, Zimmerman MD, Shabalin IG, Almo SC, Minor W. X-ray crystallography over the past decade for novel drug discovery - where are we heading next?. Expert Opin Drug Discov. 2015, 10(9):975-989.

49. Acharya KR, Lloyd MD. The advantages and limitations of protein crystal structures. Trends Pharmacol Sci. 2005, 26(1):10-4.

50. Przybylski M. Mass spectrometry. In: Gauglitz G, Moore DS, editors. Hand-book of spectroscopy. Weinheim, Germany: Wiley-VCH, 2014, pp. 357–405.

51. Dragusanu M, Petre BA, Slamnoiu S, Vlad C, Tu T, Przybylski M. Online bioaffinity-electrospray mass spectrometry for simultaneous detection, identification, and quantification of protein-ligand interactions. J Am Soc Mass Spectrom, 2010, 21:1643–1648.

52. Paraschiv G, Vincke C, Czaplewskac P, Manea M, Muyldermans S and Przybylski M Epitope structure and binding affinity of single chain llama anti-ß-amyloid antibodies revealed by proteolytic excision affinity-mass spectrometry. Mol. Recognition. 2013, 26: 1–9.

53. Perdivara I, Deterding LJ, Cozma C, Tomer KB, Przybylski M. Glycosylation profiles of epitope-specific anti-beta-amyloid antibodies revealed by liquid chromatography-mass spectrometry. Glycobiology 2009, 19: 958-970.

54. Macht M., A. Marquardt, S.O. Deininger, E. Damoc, M. Kohlmann, and M. Przybylski.Affinity-proteomics: Direct protein identification from biological material using mass spectrometric epitope mapping. Bioanal. Chem. 2004, 378: 1102-1111.

55. Manea M., Kalászi A., Mezo G., Horváti K., Bodor A., Horváth A., Farkas O., Perczel A., Przybylski M., Hudecz F. Antibody recognition and conformational flexibility of a plaque-specific beta-amyloid epitope modulated by non-native peptide flanking regions. Med. Chem. 2008, 51: 1150-1161.

56. Kaur U, Meng H, Lui F, Ma R, Ogburn RN, Johnson JHR, Fitzgerald MC, Jones LM. Proteome-Wide Structural Biology: An Emerging Field for the Structural Analysis of Proteins on the Proteomic Scale. J Proteome Res. 2018,17(11):3614-3627.

57. Yefremova Y, Opuni KFM, Danquah BD, Thiesen HJ, Glocker MO. Intact Transition Epitope Mapping (ITEM). J Am Soc Mass Spectrom. 2017, 28(8):1612-1622.

58. Danquah BD, Yefremova Y, Opuni KFM, Röwer C, Koy C, Glocker MO. Intact Transition Epitope Mapping - Thermodynamic Weak-force Order (ITEM - TWO). J Proteomics. 2020, 212:103572.

59. Danquah BD, Röwer C, Opuni KM, El-Kased R, Frommholz D, Illges H, Koy C, Glocker MO. Intact Transition Epitope Mapping - Targeted High-Energy Rupture of Extracted Epitopes (ITEM-THREE). Mol Cell Proteomics. 2019, 18(8):1543-1555.

60. Masson GR, Burke JE, Ahn NG, Anand GS, Borchers C, Brier S, Bou-Assaf GM, Engen JR, Englander SW, Faber J, Garlish R, Griffin PR, Gross ML, Guttman M, Hamuro Y, Heck AJR, Houde D, Iacob RE, Jørgensen TJD, Kaltashov IA, Klinman JP, Konermann L, Man P, Mayne L, Pascal BD, Reichmann D, Skehel M, Snijder J, Strutzenberg TS, Underbakke ES, Wagner C, Wales TE, Walters BT, Weis DD, Wilson DJ, Wintrode PL, Zhang Z, Zheng J, Schriemer DC, Rand KD. Recommendations for performing, interpreting and reporting hydrogen deuterium exchange mass spectrometry (HDX-MS) experiments. Nat Methods. 2019,16(7):595-602

61. Johnson DT, Di Stefano LH, Jones LM. Fast photochemical oxidation of proteins (FPOP): A powerful mass spectrometry-based structural proteomics tool. J Biol Chem. 2019, 294(32):11969-11979.

62. Bilkova Z., Stefanescu R., Cecal R., Korecka L., Ouzka S., Jezova J., Viovy J.L., Przybylski M., Epitope extraction technique using a proteolytic magnetic reactor combined with Fourier-transform ion cyclotron resonance mass spectrometry as a tool for the screening of potential vaccine lead peptides. J. Mass Spectrom.2005, 11: 489-495.

63. Suckau D, Köhl J, Karwath G, Schneider K, Casaretto M, Bitter-Suermann D, Przybylski M. Molecular epitope identification by limited proteolysis of an immobilized antigen-antibody complex and mass spectrometric peptide mapping. Proc Natl Acad Sci U S A. 1990, 87(24):9848-52.

64. Kukacka Z, Iurascu M, Lupu L, Rusche H, Murphy M, Altamore L, Borri F, Maeser S, Papini AM, Hennermann J, Przybylski M. Antibody Epitope of Human α-Galactosidase A Revealed by Affinity Mass Spectrometry: A Basis for Reversing Immunoreactivity in Enzyme Replacement Therapy of Fabry Disease. ChemMedChem. 2018,13(9):909-915.

65. Iuraşcu MI, Marroquin Belaunzanar O, Cozma C, Petrausch U, Renner C, Przybylski M. An HLA-B27 Homodimer Specific Antibody Recognizes a Discontinuous Mixed-Disulfide Epitope as Identified by Affinity-Mass Spectrometry. J Am Soc Mass Spectrom. 2016, 27(6):1105-12.

66. Homola, J. Surface Plasmon Resonance Sensors for Detection of Chemical and Biological Species. Chem.Rev., 2008, 108: 462-493.

67. Richard B. M. Schasfoort, Introduction to Surface Plasmon Resonance, Handbook of Surface Plasmon Resonance: Edition 2, 2017, 1-26.

68. Oman, Srecko F., Camões, M. Filomena, Powell, Kipton J., Rajagopalan, Raj and Spitzer, Petra. Guidelines for potentiometric measurements in suspensions Part A. The suspension effect (IUPAC Technical Report, Pure and Applied Chemistry, vol. 79, no. 1, 2007, pp. 67-79.

69. Li Y, Liu Z, Guo Q, Luo M. Long-term Fiber Photometry for Neuroscience Studies. Neurosci Bull. 2019, 35(3):425-433.

70. Piliarik M, Homola J. Surface plasmon resonance (SPR) sensors: approaching their limits? Opt Express. 2009, 17(19):16505-17.

71. Pol, E., R. Karlsson, H. Roos, et al. Biosensor-based characterization of serum antibodies during development of an anti-IgE immunotherapeutic against allergy and asthma. Journal of Molecular Recognition, 2007, 20: 22-31.

72. Šípová H, Homola J. Surface plasmon resonance sensing of nucleic acids: a review. Anal Chim Acta. 2013, 773:9-23.

73. Ho CS, Lam CW, Chan MH, Cheung RC, Law LK, Lit LC, Ng KF, Suen MW, Tai HL. Electrospray ionisation mass spectrometry: principles and clinical applications. Clin Biochem Rev. 2003, 24(1):3-12.

74. Wilm M. Principles of electrospray ionization. Mol Cell Proteomics. 2011; 10(7).

75. Covey TR, Thomson BA, Schneider BB. Atmospheric pressure ion sources. Mass Spectrom Rev. 2009, 28(6):870-97.

76. Li KY, Tu H, Ray AK. Charge limits on droplets during evaporation. Langmuir. 2005, 21(9):3786-94.

77. Kebarle P, Verkerk UH. Electrospray: from ions in solution to ions in the gas phase, what we know now. Mass Spectrom Rev. 2009, 28(6):898-917.

78. Fenn JB. Electrospray wings for molecular elephants (Nobel lecture). Angew Chem Int Ed Engl. 2003, 42(33):3871-94.

79. Kebarle P, Verkerk UH. Electrospray: from ions in solution to ions in the gas phase, what we know now. Mass Spectrom Rev. 2009, 28(6):898-917.

80. Nolting D, Malek R, Makarov A. Ion traps in modern mass spectrometry. Mass Spectrom Rev. 2019, 38(2):150-168

81. Przybylski, M, Glocker, MO, Electrospray Mass Spectrometry of Biomacromolecular Complexes with Noncovalent Interactions—New Analytical Perspectives for Supramolecular Chemistry and Molecular Recognition Processes. Angew. Chem. Int. Ed. Engl., 1996, 35: 806-826.

82. Vestal ML. Modern MALDI time-of-flight mass spectrometry. J Mass Spectrom. 2009; 44(3):303-17.

83. Karas M, Bachmann D, Hillenkamp F, Influence of the Wavelength in High-Irradiance Ultraviolet Laser Desorption Mass Spectrometry of Organic Molecules, Analytical Chemistry, 1985, vol. 57, no. 14, pp. 2935-39.

84. Ouedraogo R, Daumas A, Capo C, Mege JL, Textoris J. Whole-cell MALDI-TOF mass spectrometry is an accurate and rapid method to analyze different modes of macrophage activation. J Vis Exp. 2013; 26;(82):50926.

85. Datta R, Roy Chowdhury R, Manjunath K, Hanna LE, Varadarajan R. A facile method of mapping HIV-1 neutralizing epitopes using chemically masked cysteines and deep sequencing. Proc Natl Acad Sci U S A. 2020, 117(47):29584-29594.

86. Tarrahimofrad H, Rahimnahal S, Zamani J, Jahangirian E, Aminzadeh S. Designing a multi-epitope vaccine to provoke the robust immune response against influenza A H7N9. Sci Rep. 2021,11(1):24485.

87. Chakraborty S, Barman A, Deb B. Japanese encephalitis virus: A multi-epitope loaded peptide vaccine formulation using reverse vaccinology approach. Infect Genet Evol. 2020, 78:104106.

88. Stryhn A, Kongsgaard M, Rasmussen M, Harndahl MN, Østerbye T, Bassi MR, Thybo S, Gabriel M, Hansen MB, Nielsen M, Christensen JP, Randrup Thomsen A, Buus S. A Systematic, Unbiased Mapping of $CD8^+$ and $CD4^+$ T Cell Epitopes in Yellow Fever Vaccinees. Front Immunol. 202, 11:1836.

89. Kar PP, Srivastava A. Immuno-informatics Analysis to Identify Novel Vaccine Candidates and Design of a Multi-Epitope Based Vaccine Candidate Against *Theileria* parasites. Front Immunol. 2018, 9:2213

90. Sanches RCO, Tiwari S, Ferreira LCG, Oliveira FM, Lopes MD, Passos MJF, Maia EHB, Taranto AG, Kato R, Azevedo VAC, Lopes DO. Immunoinformatics Design of Multi-Epitope Peptide-Based Vaccine Against *Schistosoma mansoni* Using Transmembrane Proteins as a Target. Front Immunol. 2021, 12:621706.

91. Razim A, Pacyga K, Naporowski P, Martynowski D, Szuba A, Gamian A, Górska S. Identification of linear epitopes on the flagellar proteins of Clostridioides difficile. Sci Rep. 2021, 11(1):9940.

92. Liu J, Chen X, Wang J, Wu F, Zhang J, Dong J, Zhang H, Liu X, Hu N, Wu J, Zhang L, Cheng W, Zhang C, Zhang WJ. Prediction and identification of CD4+ T cell epitope for the protective antigens of Mycobacterium tuberculosis. Medicine (Baltimore). 2021, 100(6):e24619.

93. Pomés A, Mueller GA, Chruszcz M. Structural Aspects of the Allergen-Antibody Interaction. Front Immunol. 2020, 11:2067.

94. Deak PE, Vrabel MR, Kiziltepe T, Bilgicer B. Determination of Crucial Immunogenic Epitopes in Major Peanut Allergy Protein, Ara h2, via Novel Nanoallergen Platform. Sci Rep. 2017, 7(1):3981.

95. Suprun M, Getts R, Raghunathan R, Grishina G, Witmer M, Gimenez G, Sampson HA, Suárez-Fariñas M. Novel Bead-Based Epitope Assay is a sensitive and reliable tool for profiling epitope-specific antibody repertoire in food allergy. Sci Rep. 2019, 9(1):18425.

96. Sanami S, Azadegan-Dehkordi F, Rafieian-Kopaei M, Salehi M, Ghasemi-Dehnoo M, Mahooti M, Alizadeh M, Bagheri N. Design of a multi-epitope vaccine against cervical cancer using immunoinformatics approaches. Sci Rep. 2021, 11(1):12397.

97. Herrera LRM. Reverse Vaccinology Approach in Constructing a Multi-Epitope Vaccine Against Cancer-Testis Antigens Expressed in Non-Small Cell Lung Cancer. Asian Pac J Cancer Prev. 2021, 22(5):1495-1506.

98. Herrera LRM. Reverse Vaccinology Approach in Constructing a Multi-Epitope Vaccine Against Cancer-Testis Antigens Expressed in Non-Small Cell Lung Cancer. Asian Pac J Cancer Prev. 2021, 22(5):1495-1506.

99. Liu J, Chen X, Wang J, Wu F, Zhang J, Dong J, Zhang H, Liu X, Hu N, Wu J, Zhang L, Cheng W, Zhang C, Zhang WJ. Prediction and identification of CD4+ T cell epitope for the protective antigens of Mycobacterium tuberculosis. Medicine (Baltimore). 2021,100(6):e24619.

100. Barrera-Ocampo A, Lopera F. Amyloid-beta immunotherapy: the hope for Alzheimer disease? Colomb Med (Cali). 2016, 47(4):203-212.

101. Alzheimer's Association® 225 N. Michigan Ave. Chicago, IL 60601, 2021.

102. Sarah E. Tom, Rebecca A. Hubbard, Paul K. Crane, Sebastien J. Haneuse, James Bowen, Wayne C. McCormick, Susan McCurry, and Eric B. Larson, Characterization of Dementia and Alzheimer's Disease in an Older Population: Updated Incidence and Life Expectancy With and Without Dementia, American Journal of Public Health, 2015, 105, 408-413.

103. Bloom GS. Amyloid-β and tau: the trigger and bullet in Alzheimer disease pathogenesis. JAMA Neurol. 2014;71(4):505-8.

104. Prasad, AS. V. Physiological Basis of Memory Dysfunction in Alzheimer's Disease – An Overview. International Journal of Biochemistry Research & Review, 2020, 29(2), 9-24.

105. Smith LM. & Strittmatter SM. A mechanistic hypothesis for the impairment of synaptic plasticity by soluble Aβ oligomers from Alzheimer's brain, Cold Spring Harbor perspectives in medicine,2017, 7(5).

106. Jarosz-Griffiths HH, Noble E, Rushworth JV, Hooper NM. Amyloid-β Receptors: The Good, the Bad, and the Prion Protein. J Biol Chem. 2016, 291(7):3174-83.

107. Smith LM, Strittmatter SM. Binding Sites for Amyloid-β Oligomers and Synaptic Toxicity, Cold Spring Harbor perspectives in medicine,2017; 7(5).

108. Zhi Ruan, Dhruba Pathak, Srinidhi Venkatesan Kalavai, Asuka Yoshii-Kitahara, Satoshi Muraoka, Nemil Bhatt, Kayo Takamatsu-Yukawa, Jianqiao Hu, Yuzhi Wang, Samuel Hersh, Maria Ericsson, Santhi Gorantla, Howard E Gendelman, Rakez Kayed, Seiko Ikezu, Jennifer I Luebke, Tsuneya Ikezu, Alzheimer's disease brain-derived extracellular vesicles spread tau pathology in interneurons, Brain, 2021, Volume 144, 1:288–309.

109. Das A, Korn A, Carroll A, Carver JA, Maiti S. Application of the Double-Mutant Cycle Strategy to Protein Aggregation Reveals Transient Interactions in Amyloid-β Oligomers. J Phys Chem B.,2021, 125, 45, 12426–12435.

110. Sevigny, J., Chiao, P., Bussière, T. et al. The antibody aducanumab reduces Aβ plaques in Alzheimer's disease. Nature, 2021, 537, 50–56.

111. Dhillon S. Aducanumab: First Approval. Drugs. 2021, 81(12):1437-1443.

112. Mahase E. Three FDA advisory panel members resign over approval of Alzheimer's drug BMJ 2021;

113. Walsh S, Merrick R, Milne R, Brayne C. Aducanumab for Alzheimer's disease? BMJ. 2021, 374:n1682.

114. McLaurin J, Cecal R, Kierstead ME, Tian X, Phinney AL, Manea M, French JE, Lambermon MH, Darabie AA, Brown ME, Janus C, Chishti MA, Horne P, Westaway D, Fraser PE, Mount HT, Przybylski M, St George-Hyslop P. Therapeutically effective antibodies against amyloid-beta peptide target amyloid-beta residues 4-10 and inhibit cytotoxicity and fibrillogenesis. Nat Med. 2002, 8(11):1263-9.

115. Ștefănescu R, Lupu L, Manea M, Iacob RE, Przybylski M. Molecular characterization of the β-amyloid(4-10) epitope of plaque specific Aβ antibodies by affinity-mass spectrometry using alanine site mutation. J Pept Sci. 2018, 24(1).

116. Wiegand P, Lupu L, Hüttmann N, Wack J, Rawer S, Przybylski M, Schmitz K. Epitope Identification and Affinity Determination of an Inhibiting Human Antibody to Interleukin IL8 (CXCL8) by SPR- Biosensor-Mass Spectrometry Combination. J Am Soc Mass Spectrom. 2020, 31(1):109-116.

117. Tracedrawer 1.6.1 Ridgeview Instruments, 752 37 Uppsala, SWEDEN

118. Azevedo O, Gago MF, Miltenberger-Miltenyi G, Sousa N, Cunha D. Fabry Disease Therapy: State-of-the-Art and Current Challenges. Int J Mol Sci. 2020, 22(1):206.

119. de Vries JM, Kuperus E, Hoogeveen-Westerveld M, Kroos MA, Wens SC, Stok M, van der Beek NA, Kruijshaar ME, Rizopoulos D, van Doorn PA, van der Ploeg AT, Pijnappel WW. Pompe disease in adulthood: effects of antibody formation on enzyme replacement therapy. Genet Med. 2017, 19(1):90-97.

120. D. Scharnetzki, F. Stappers, M. Lenders, E. Brand Detailed epitope mapping of neutralizing anti-drug antibodies against recombinant α-galactosidase A in patients with Fabry disease Mol Genet Metabol, 2020, 131, pp. 229-234.

121. Tanimura K, Yamada T, Okada K, Nakai K, Horinaka M, Katayama Y, Morimoto K, Ogura Y, Takeda T, Shiotsu S, Ichikawa K, Watanabe S, Morimoto Y, Iwasaku M, Kaneko Y, Uchino J, Taniguchi H, Yoneda K, Matoba S, Sakai T, Uehara H, Yano S, Kusaba T, Katayama R, Takayama K. HER3 activation contributes toward the emergence of ALK inhibitor-tolerant cells in ALK-rearranged lung cancer with mesenchymal features. NPJ Precis Oncol. 2022, 6(1):5.

122. Wang C, Sharma N, Veleeparambil M, Kessler PM, Willard B, Sen GC. STING-Mediated Interferon Induction by Herpes Simplex Virus 1 Requires the Protein Tyrosine Kinase Syk. mBio. 2021,12(6): e0322821.

123. Tao X, Chen C, Chen Y, Zhang L, Hu J, Yu H, Liang M, Fu Q, Huang K. β_2-adrenergic receptor promotes liver regeneration partially through crosstalk with c-met. Cell Death Dis. 2022,13(6):571.

124. Shao W, Zhu W, Lin J, Luo M, Lin Z, Lu L, Jia H, Qin L, Lu M, Chen J. Liver X Receptor Agonism Sensitizes a Subset of Hepatocellular Carcinoma to Sorafenib by Dual-Inhibiting MET and EGFR. Neoplasia. 2020, 22(1):1-9.

125. Nimjee SM, White RR, Becker RC, Sullenger BA. Aptamers as Therapeutics. Annu Rev Pharmacol Toxicol. 2017, 57:61-79.

126. Piater B, Doerner A, Guenther R, Kolmar H, Hock B. Aptamers Binding to c-Met Inhibiting Tumor Cell Migration. PLoS One. 2015, 10(12): e0142412.

127. Rinaldi F, Lupu L, Rusche H, Kukačka Z, Tengattini S, Bernardini R, Piubelli L, Bavaro T, Maeser S, Pollegioni L, Calleri E, Przybylski M, Temporini C, Epitope and affinity determination of recombinant Mycobacterium tuberculosis Ag85B antigen towards anti-Ag85 antibodies using proteolytic affinity-mass spectrometry and biosensor analysis. Anal Bioanal Chem, 2019, 411:439-448.

128. Tramarin A, Naldi M, Degani G, Lupu L, Wiegand P, Mazzolari A, Altomare A, Aldini G, Popolo L, Vistoli G, Przybylski M, Bartolini M. Unveiling the Molecular Mechanisms Underpinning Biorecognition of Early-Glycated Human Serum Albumin and Receptor for Advanced Glycation End Products. Anal Bioanal Chem, 2020, 412(18):4245-4259.

6. SUPPLEMENTARY FIGURES

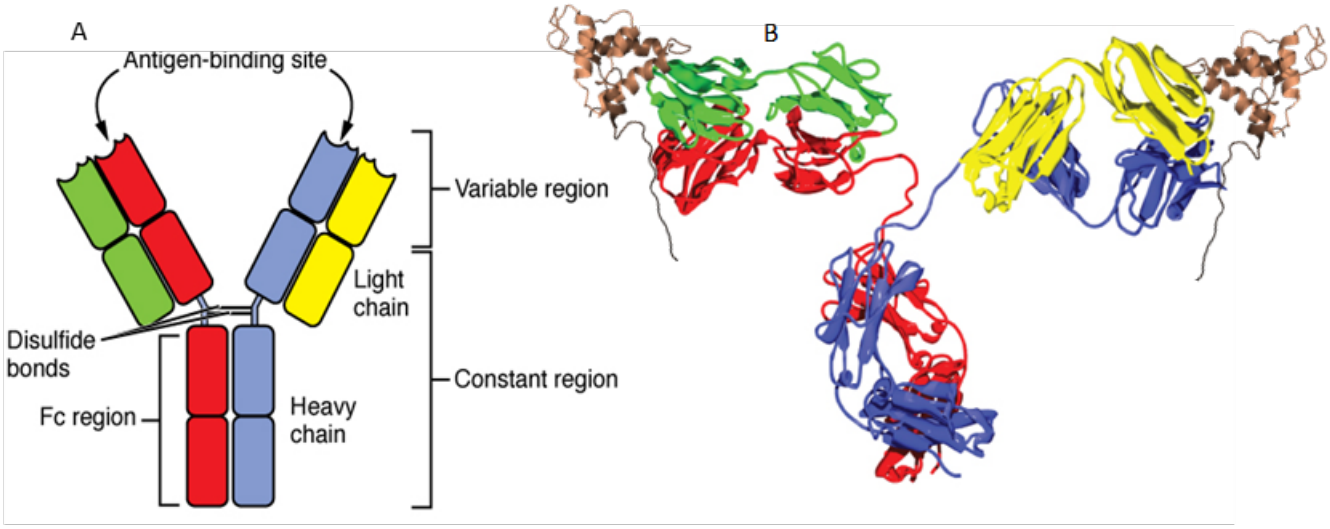

Figure S1: Schematic representation and molecular model of an IgG antibody structure. Figure 2A. Diagram representing the structure of an IgG antibody with the annotated regions. Red and blue highlight the heavy chain of the antibody, while yellow and green the light chain. Indicated in the figure are the two Cystein disulfide bridges that connect the variable region and the constant region and the antigen binding sites. Figure 2B. The molecular model of an antibody in the natural conformation with the same color code as before. In brown is a model of a protein illustrating an interaction between an antibody and a protein.

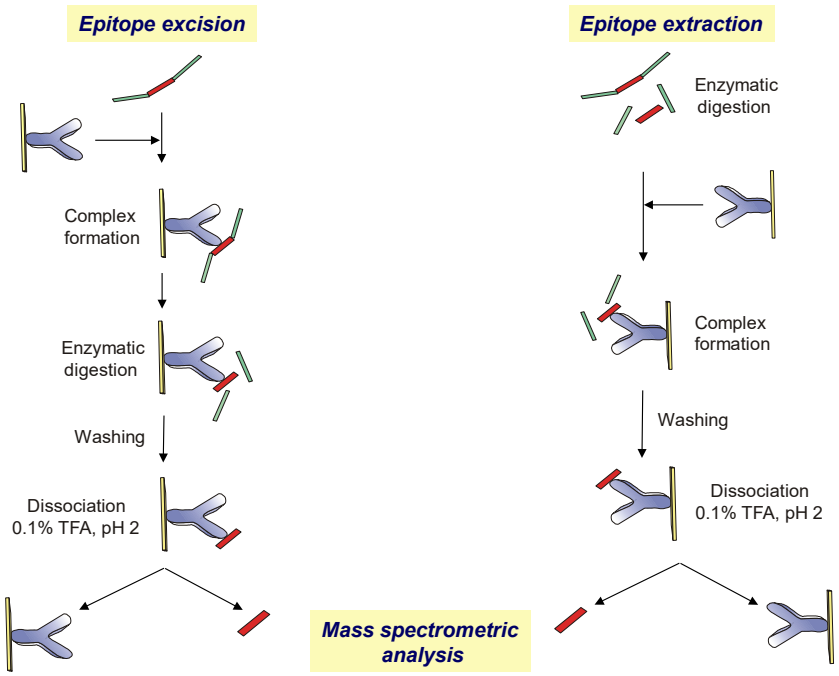

Figure S2: Schematic representation of proteolytic epitope extraction-MS (PROTEX-MS) and excision-MS for epitope identification. The protein of interest (antigen) is represented in blue with the highlighted epitope in green. 4A. Epitope extraction is based on the initial enzymatic digestion of the protein. (peptides represented in green with the blue bars). Following complete digestion, the peptides are incubated with the immobilized antibody, represented in red. An affinity complex is formed (epitope peptide- antibody complex) and all other peptides in the mixture are removed. Epitope determination is achieved by the elution of the bound peptide from the antibody [.4B. Epitope excision is based on the initial affinity complex formation (intact protein- antibody complex) followed by enzymatic digestion. Any possible cleavage sites present in the epitope are shielded by the interaction with the antibody and only the unbound peptides can be digested and removed from the mixture. Epitope determination is achieved by the elution of the bound peptide from the antibody .

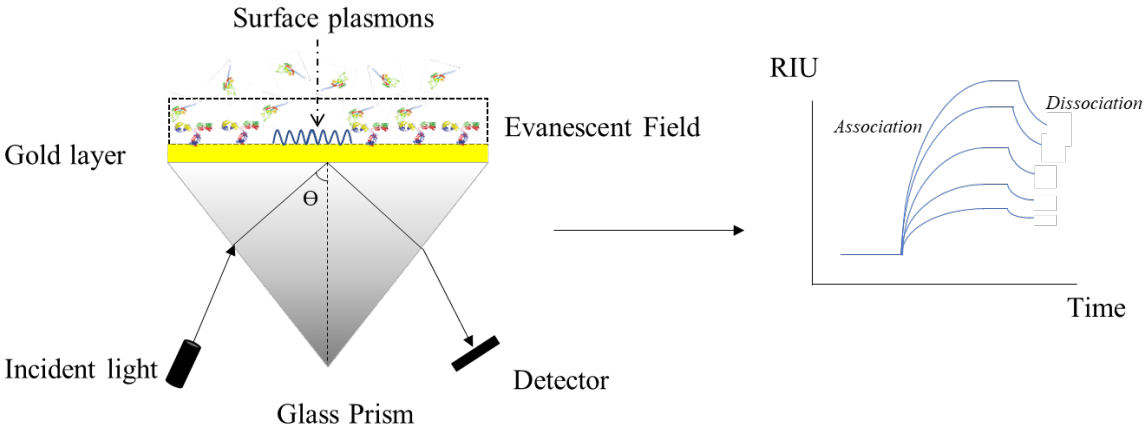

Supplementray

Figure S3: Biosensor pathway description. The gold surface of a SPR chip is represented in yellow and is placed above a glass prism. An incident light is directed through the prism to the back side of the chip and reflected to a detector at a specific angle (Θ). The evanescent filed is formed by the energy transfer between the photons and the electrons on the gold surface. Interaction events are transferred to a computer and the sensorgram is procced. Affinity strength is calculated by the analysis of a dilution series of the protein, each sample interacting separately with the antibody .

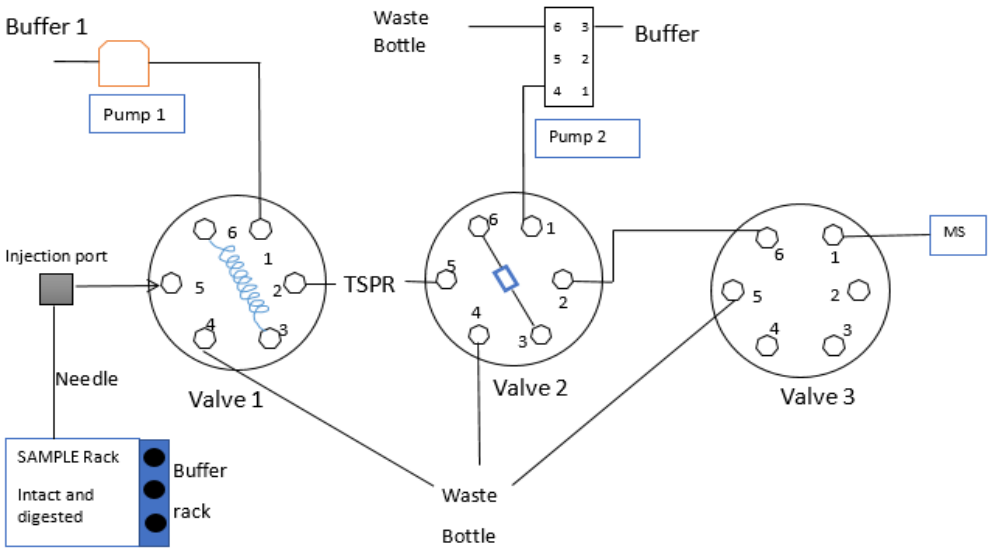

Figure S4: The interface mechanical design, containing 3 switching valves, 2 pumps, a sample holder, an injection port, a SPR and a MS; All instrument part are connected in one liquid flow, the sample beginning in the sample rack, transported from valve one to the SPR, then to the affinity column (depicted by the blue square in valve 2) and ending with the MS analysis of the intact protein and the epitope subsequently.

ACS Partner Journal

Journal of the American Society for Mass Spectrometry

pubs.acs.org/jasms

Research Article

Antibody Epitope and Affinity Determination of the Myocardial Infarction Marker Myoglobin by SPR-Biosensor Mass Spectrometry

Delia Mihoc, Loredana-Mirela Lupu, Pascal Wiegand, Wolfgang Kleinekofort, Oliver Müller, Friedemann Völklein, Michael O. Glocker, Frederik Barka, Günes Barka,* and Michael Przybylski*

Cite This: https://dx.doi.org/10.1021/jasms.0c00234

Read Online

ACCESS | Metrics & More | Article Recommendations | Supporting Information

ABSTRACT: Myoglobin (MG) is a biomarker for heart muscle injury, making it a potential target protein for early detection of myocardial infarction. Elevated myoglobin levels alone have low specificity for acute myocardial infarction (AMI) but in combination with cardiac troponin T have been considered highly efficient diagnostic biomarkers. Myoglobin is a monomeric heme protein with a molecular weight of 17 kDa that is found in skeletal and cardiac tissue as an intracellular storage unit of oxygen. MG consists of eight α-helices connected by loops and a heme group responsible for oxygen-binding. Monoclonal antibodies are widely used analytical tools in biomedical research and have been employed for immunoanalytical detection of MG. However, the epitope(s) recognized by MG antibodies have been hitherto unknown. Precise molecular identification of the epitope(s) recognized by antibodies is of key importance for the development of MG as a diagnostic biomarker. The epitope of a monoclonal MG antibody was identified by proteolytic epitope extraction mass spectrometry in combination with surface plasmon resonance (SPR) biosensor analysis. The MG antibody was immobilized both on an affinity microcolumn and a gold SPR chip. The SPR kinetic analysis provided an affinity-binding constant K_D of 270 nM for MG. Binding of a tryptic peptide mixture followed by elution of the epitope from the SPR-MS affinity interface by mild acidification provided a single-epitope peptide located at the C-terminus [146−153] [YKELGFQG] of MG. The specificity and affinity of the epitope were ascertained by synthesis and affinity-mass spectrometric characterization of the epitope peptide.

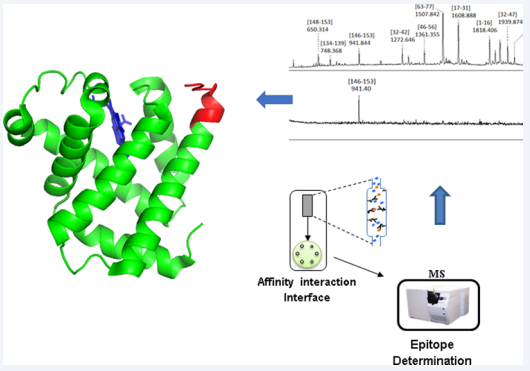

INTRODUCTION

The oxygen-binding protein myoglobin (MG) is one of the major proteins in skeletal and cardiac muscle. Myoglobin is a cytoplasmic heme protein consisting of a single polypeptide chain of 153 amino acids with a molecular weight of 17.8 kDa. Expressed solely in cardiac myocytes and oxidative skeletal muscle fibers (Figure 1),[1] myoglobin was named according to its functional and structural similarity to hemoglobin. However, unlike hemoglobin, MG reversibly binds oxygen and facilitates oxygen transport from red blood cells to mitochondria during periods of increased metabolic activity, with a single O_2-binding site and a hyperbolic saturation curve. Normal human myoglobin levels in blood range from 0 to 70 ng/mL. Myoglobin was the first protein for which a three-dimensional structure was determined.[2] Its structure has been extensively studied, with 75% of the main chain being folded in an α-helical conformation (Figure 1).

Myoglobin has recently gained increased interest due to its potential role as a biomarker for acute myocardial infarction (AMI), in comparison to previously characterized bio-markers.[3−5] Following cardiac muscle injury, both cardiac and skeletal serum levels of MG are dramatically increased and are also elevated in certain disorders caused by the release of myoglobin from damaged or necrotic muscle cells.[4,5] Due to its small molecular size, myoglobin is able to translocate into the vascular system without processing in the lymphatic system. Acute myocardial infarction (AMI) affects millions of people each year, and rapid, precise, and timely diagnosis is considered of key importance for therapeutic intervention, particularly within the first 6 h after AMI onset.[6] A principal tool for diagnosis of AMI is the development and application of monoclonal MG antibodies that can be employed as specific reagents in immunoassays for determination of MG in serum or plasma of AMI patients. Immunoassays have been employed for diagnosis and quantification of myocardial necrosis and infarction;[7−10] however, the binding epitope(s) of MG antibodies and their affinities have not been previously characterized. For the identification and affinity determination of biomolecular interaction epitopes, efficient methods have

Special Issue: Focus: Ionization Technologies Used in MS: Fundamentals and Applications

Received: June 17, 2020
Revised: July 28, 2020
Accepted: August 3, 2020
Published: August 3, 2020

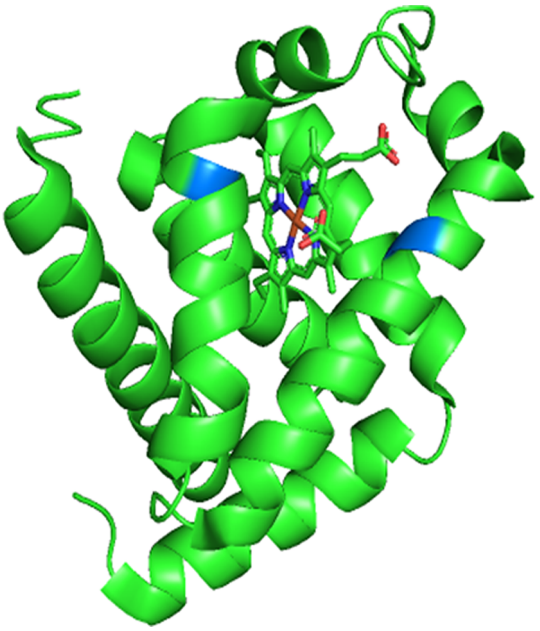

Figure 1. Structure of native human heme-myoglobin, ribbon presentation. Myoglobin consists of a backbone and heme-binding domain.[2] The backbone is composed of eight α-helices (blue) that wrap around a central pocket containing the heme group (red), capable of binding various ligands including oxygen, carbon monoxide, and nitric oxide.

been developed and employed in our laboratory using a combination of proteolytic excision and extraction electrospray (ESI) and MALDI mass spectrometry (MS) as well as surface plasmon resonance (SPR) biosensor analysis within an SPR-MS interface[11−17] (PROTEX-SPR-MS; Supporting Figure S1).

In this study, a monoclonal anti-MG antibody was immobilized on a self-assembled monolayer (SAM)-SPR affinity chip as well as on a Sepharose affinity microcolumn, and both were incubated with a proteolytic digestion mixture of MG. After nonbinding peptides were washed off, the fraction eluted by mild acidification was analyzed by mass spectrometry, and the presence of a single-epitope peptide was revealed. SPR determinations of the MG-antibody complex with intact myoglobin and the epitope peptide ascertained high, specific affinity. These results show that the anti-MG antibody-myoglobin epitope determination is an efficient diagnostic analysis for AMI.

■ EXPERIMENTAL SECTION

Materials and Samples. Myoglobin, native heme protein from equine heart (M1882), purity ≥ 90% (by SDS-PAGE), essentially salt-free, lyophilized powder was obtained from Sigma-Aldrich (Hamburg, Germany). Equine MG apoprotein, sequencing grade, was obtained from Sigma (München, Germany). The mouse monoclonal anti-MG antibody against apo-myoglobin was obtained from Santa Cruz Biotechnology (Heidelberg, Germany), with cross-reactivity for equine, human, and rat MG.[18] The vial contains 200 μg of IgG1 in 1.0 mL of PBS with <0.1% sodium azide. Other reagents and chemicals were of highest available purity from Sigma-Aldrich (München, Germany) and from Merck (Darmstadt, Germany).

Mass Spectrometric Characterization of Horse Heart Myoglobin. ESI-MS analysis of MG was performed on a Waters TripleQuad Ultima mass spectrometer by direct infusion in the positive ion mode. The ion source parameters employed were as follows: capillary voltage −4500 V, end plate offset −500 V, capillary exit voltage 278.5 V, nebulizer gas flow 12 psi, dry gas flow 9 L min^{-1}, and drying temperature 250 °C. Spectra were recorded in the full scan mode with a scan range of m/z 200−3000. The influence of different solvents on the ionization of MG was tested by preparation of 10 mM solutions of MG with the following solvents: 50% (v/v) acetonitrile, 50% (v/v) H_2O, and 0.1% (v/v) trifluoroacetic acid (TFA) and ammonium acetate buffer (10 mM ammonium acetate, pH 7.0) (Figure S2). Samples were introduced to the ESI source either by direct infusion with a syringe, operated with a pump system at a constant flow rate of 100 μL min^{-1}, or by infusion through the SPR-MS interface. Mass spectra were evaluated using the GPMAW 7.0 software,[19] which provides determination of molecular weights of proteins and peptides with known sequences, average or monoisotopic masses of multiply charged proteins or peptides, as well as masses of fragments.

Proteolytic Digestion. Prior to proteolytic digestion, the heme group of MG was removed in order to obtain a higher digestion yield and better sequence coverage. Removal of the heme group was performed by acidification with 0.1% TFA and passage through an Amicon Filter Ultra-15 (10 K). High pressure proteolytic digestion was performed with a Barocycler 2320EXT instrument (Pressure Biosciences; South Easton, USA) at a temperature of 37 °C and 25 kpsi pressure, using 120 cycles at 50 s/cycle pressure and 10 s off pressure, and a total digestion time of 120 min. A solution of 100 μg (1 mg/mL) of MG in 100 mM ammonium hydrogen carbonate was introduced in a PCT microtube and diluted with the same buffer to a 50 μg/μL final concentration. Keeping a protease-to-substrate ratio of 1:50, a solution of 1 μL of trypsin (0.5 mg/mL) from Sigma GmbH, München and Serva AG, Heidelberg, Germany was added to the protein. As a comparison, the same ratio of sample to enzyme was used for standard digestion (18 h, 37 °C). Tryptic digestion mixtures were characterized by MALDI-TOF-MS, using 2,5-dihydroxybenzoic acid (DHB) as a matrix.

Determination of digestion yields was performed by quantitative mass spectrometric determination of two specific peptide fragments within the digestion mixture. The abundance ratio was determined for the peptide fragment (146−153) (YKELGFQG) (m/z 941) to a synthetic reference peptide (FKELGFQG, m/z 925) spiked to aliquots of the digestion mixture at a concentration of 50 μL/min at 10, 20, 30, 60, and 90 min within the high pressure digestion. This evaluation in comparison to digestion at standard conditions showed that the high pressure proteolytic digestion proved to be most effective. The digestion yield was estimated to be >90% at 120 min, and no intact protein was detectable at this time by gel electrophoresis.

Antibody Immobilization. The antimyoglobin antibody was immobilized on a self-assembled monolayer (SAM) of the activated surface of an SPR chip, using amine coupling as previously described.[16,20] SAM chips were washed three times with alternating water and 70% aqueous ethanol and then immersed for 15 s in piranha solution (H_2SO_4/H_2O_2, 2:1). This step was repeated three times, and the final washing was performed with deionized water and 70% ethanol. The cleaned chip was incubated for 12 h at 20 °C with shaking in a solution of 16-mercaptohexadodecanoic acid in 99% chloroform (1

https://dx.doi.org/10.1021/jasms.0c00234
J. Am. Soc. Mass Spectrom. XXXX, XXX, XXX−XXX

mg/mL) and dried under N_2 for 24 h. All reactions were carried out in the microfluidic cell of the SPR biosensor with reagents injected via the autosampler.

The surface of the chip was first washed with 20 mL of PBST buffer (50 mM Na_2HPO_4, 150 mM NaCl, 0.05% (v/v) Tween-20, pH 7.5). Subsequently, activation of the carboxyl groups of the SAM was obtained by injection of 250 μL of a freshly prepared aqueous solution of 0.2 M EDC and 0.1 M NHS over the SAM chip at a constant flow rate of 25 μL min^{-1}. Coupling of the antibody was carried out with PBST buffer at pH 5.2. A solution of 25 μg of the monoclonal antibody in 10 mM sodium acetate buffer was injected over the chip surface at a flow rate of 25 μL min^{-1}. Unreacted NHS-esters were blocked by injection of 250 μL of ethanolamine solution (1 M, pH 8.5).

SPR-Biosensor Analysis. Affinity determinations of myoglobin and the anti-MG antibody were performed by SPR with the SPR-MS interface, using a dual-channel SR7500DC biosensor (Ametek- Reichert, Buffalo, USA). Determination of affinity-binding constants was performed by real-time analysis with activated gold chips as described above. Binding experiments were carried out at 25 °C with PBST buffer (50 mM Na_2HPO_4, 150 mM NaCl, 0.05% (v/v) Tween, pH 7.5). A 57 mM MG solution was freshly prepared and injected via the autosampler over the chip surface at a constant flow rate of 25 μL min^{-1}. Association and dissociation kinetics were evaluated using Trace Drawer software (Ridgeview Instruments AB, Vange, Sweden).[21] K_D values were calculated from association and dissociation rate constants (k_a and k_d) determined from duplicate affinity measurements at each concentration.

SPR-MS Interface for Epitope Analysis (Figure S1). For validation of the analytical accuracy of the SPR-MS interface, a comparison of (i), direct analysis of MG by direct ESI-MS, and (ii), analysis through the SPR-MS interface, was carried out. The instrumental combination of SPR with ESI-MS comprises valves that enable affinity isolation, mass spectrometric identification, and quantification of affinity-bound ligands from a protein-ligand complex immobilized on the gold chip. The SPR-MS interface provides sample concentration and in situ desalting for direct MS analysis of the ligand eluate.[14,20] Both ESI-ion trap and triple quad-MS systems can be coupled to the SPR-MS interface. Applications of the SPR-MS combination were previously described in studies of a mixed-disulfide antibody epitope of the rheumatoid target protein, HLA-B27, and the epitope identification of chaperone complexes of lysosomal enzymes.[14,17,22]

Epitope Identification by Proteolytic Epitope Extraction-MS Using an Affinity Column. The anti-MG antibody was immobilized on CNBr-activated Sepharose 4B (GE Healthcare Europe, Freiburg, Germany), by suspending the Sepharose (15.1 mg) in 0.3 mL of 1 mM HCl and incubating for 15 min at 20 °C with stirring. Subsequently, the suspension was extensively washed to remove the HCl using 10 mL of coupling solution (0.2 M $NaHCO_3$, 0.5 M NaCl, pH 8.3), which was then discarded. The Sepharose was then resuspended in 500 μL of coupling solution and incubated for 3 h with 10 μg of antibody at 25 °C with vigorous shaking. The matrix was then washed extensively with 10 mL of washing buffer (0.2 M NaOAc, 0.5 M NaCl, pH 4) and 10 mL of blocking solution (0.1 M ethanolamine, 0.5 M NaCl, pH 8.0) for 3 h to remove unreacted cyanogenic. The column matrix was equilibrated by washing with 10 mL of Milli-Q water and used directly for the next step. After preparation, the affinity column was tested with intact MG and the tryptic digestion mixture.

A solution of 20 μg of the tryptic digestion mixture was incubated in the affinity column for 2 h. Subsequently, the first drop (30−40 μL) was collected, and the matrix was washed with 10 mL of deionized water, of which the last elution drop (30−40 μL) was collected. The eluates were analyzed by MALDI-MS, which showed unbound peptides in the first elution drop, and no peptide signal in the final elution. Subsequently, elution from the antibody was performed with 300 μL of 0.1% TFA (500 μL final volume) followed by washing with 10 mL of water and a 1 mL aliquot collected for MS analysis. After concentration of the elution and last washing fraction to 20 μL, the elution fraction was analyzed by MALDI-MS. The final washing was also analyzed for control of the background prior to reuse of the affinity column.

For longer storage, the column was kept in deionized water at 0 °C. Several microcolumns were prepared in the same format.

Synthesis of Epitope Peptides. The epitope peptide (YKELGFQG) and modified epitope peptide sequences were synthesized by solid-phase peptide synthesis (SPPS) on an ABI 433A peptide synthesizer, using a preloaded PS-PBH-Arg-(PMC)-Fmoc resin (Rapp Polymere, Tuebingen, Germany). The following chemicals used in SPPS were obtained from Applied Biosystems (Darmstadt, Germany): *N*,*N*-dimethylformamide (DMF), *N*-methyl-2-pyrrolidone (NMP), dichloromethane (DCM), 2-(1-*H*-benzotriazol-1-yl)-1,1,3,3-tetramethyluronium-hexafluorophosphate (HTBU), methyl *tert*-butyl ether (MTBE), diisopropylethylamine (DIPEA), and TFA. Fmoc-amino acid derivatives were purchased from Nova-Biochem (Darmstadt, Germany), piperidine was purchased from Acros Organics (Fisher Scientific), and tri-isopropylsilane (TIS) was purchased from Alfa Caesar (Landau, Germany). Deprotection of the peptides from the resin was carried out by the addition of 5 mL of 95% TFA and 2.5% TIS to the resin for 3 h at 20 °C. Peptides were then precipitated by addition of the reaction mixture to 20 mL of MTBE, centrifugation, and subsequent decanting. The final purification was performed by HPLC on a semipreparative C18 column, and the homogeneity of peptides was confirmed by MALDI-MS.

RESULTS AND DISCUSSION

Affinity Characterization of Myoglobin by SPR Analysis. The binding affinities for the interaction of MG with the monoclonal antibody against equine apo-myoglobin were determined by SPR analysis. Immobilization of the antibody on the SPR chip surface and injection of a dilution series of the MG heme protein and apoprotein was carried out via the autosampler of the SPRMS interface, individually, as described in the Experimental Section. Binding constants were determined by subtraction of unspecific interactions using the reference channel of the dual-channel SPR detector. The binding association curve for the MG hemeprotein complex is shown in Figure 2. Kinetic evaluation using the Trace Drawer program[21] provided a dissociation constant K_D of 270 ± 14 nM. A comparable binding constant was determined for the MG-apoprotein (350 ± 13.5 nM), thus confirming the high affinity of the protein to the antibody, independent of the native helical structure.

Structural Characterization of Myoglobin by Mass Spectrometric Peptide Mapping. Prior to proteolytic

https://dx.doi.org/10.1021/jasms.0c00234
J. Am. Soc. Mass Spectrom. XXXX, XXX, XXX−XXX

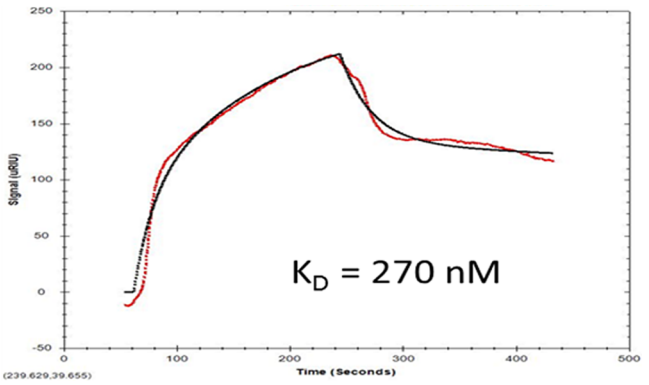

Figure 2. SPR analysis of the affinity interaction between intact native myoglobin and the mouse monoclonal anti-MG antibody (A6, Santa Cruz, Heidelberg, Germany). Following antibody immobilization, the K_D value obtained by direct SPR was comparable to that obtained by analysis in the SPRMS interface (K_D = 270 nM).

digestion, native equine heme-myoglobin was subjected to removal of the heme group under mild acidic conditions as described in the Experimental Section. ESI-MS analysis of the holoprotein (pH 7) and the apoprotein (pH 3) provided a characteristic most abundant $[M + 8H]^{8+}$ ion for the intact heme protein and the multiply charged ion distribution together with the dissociated heme ion for the apoprotein (Figure 3). Likewise, MALDI-MS provided an accurate characterization of the denatured apoprotein (Figure S2) as a basis for the determination of proteolytic fragments. Using the SPR-MS affinity interface, the apo-MG showed a sharp TIC elution signal at approximately 5 min and the multiply protonated molecular ions by ESI-MS, thus confirming the specific affinity-binding to the antibody microcolumn (Figure S3).

Apo-MG was digested with trypsin both at standard conditions at ambient pressure and at high pressure using a high pressure digestion instrument (Barocycler-2320EXT, Pressure Biosciences, Boston, USA). Digestion of MG with trypsin was performed at 37 °C for 18 h and at 30 kpsi for 120 min. Both proteolytic conditions provided complete sequence coverage for MG, albeit with significant differences of digestion yields. High pressure digestion provided a digestion yield >90% as estimated by monitoring the abundance ratio of the C-terminal peptide [146−153] (YKELGFQG) to a synthetic reference peptide (FKELGFQG). In contrast, digestion yields of 70−80% were estimated for ambient pressure digestion, and several miscleaved peptide fragments were observed. Corresponding MALDI-MS peptide mapping analyses at ambient pressure and at high pressure digestion are compared in Figure 4, and the identified tryptic peptides summarized in Table 1. At the high pressure digestion, all tryptic peptide fragments were identified within the MG sequence; in addition, several peptides were found resulting from cleavage at repeat lysine residues (Table 1 and Figure S4).

In contrast, in the tryptic digest mixture at ambient pressure, additional larger tryptic peptide fragments were found that resulted from miscleavages, such as peptides [78−96], [119−147], and [97−133]. In summary, the mass spectrometric peptide mapping provided the characterization of tryptic fragments over the complete sequence of myoglobin and thus were found suitable for unequivocal identification of antibody epitopes by proteolytic epitope extraction-MS.

Identification of the Antibody Epitope of Myoglobin. Identification of the epitope of MG to the monoclonal anti-MG antibody was obtained by proteolytic epitope extraction-MS using the SPR-MS interface in two modes: (i) with the Sepharose-immobilized antibody bound in an affinity microcolumn and (ii) binding of the MG tryptic mixture to the SPR chip containing the immobilized antibody and subsequent elution (Experimental Section). The epitope identification from the affinity microcolumn is shown in Figure 5. Following incubation of a 20 μg aliquot of the tryptic digestion mixture, unbound peptides were washed away, the corresponding supernatant peptides were verified by mass spectrometry, and the final washing fraction did not show any residual peptides (Figure 5a,b). Subsequent elution with 0.1% TFA (pH 3) provided a single peptide (Figure 5c), which was identified as the C-terminal epitope peptide sequence [146−153] (YKELGFQG). This peptide [146−153] was also found in the supernatant fraction (Figure 5a), which is readily explained

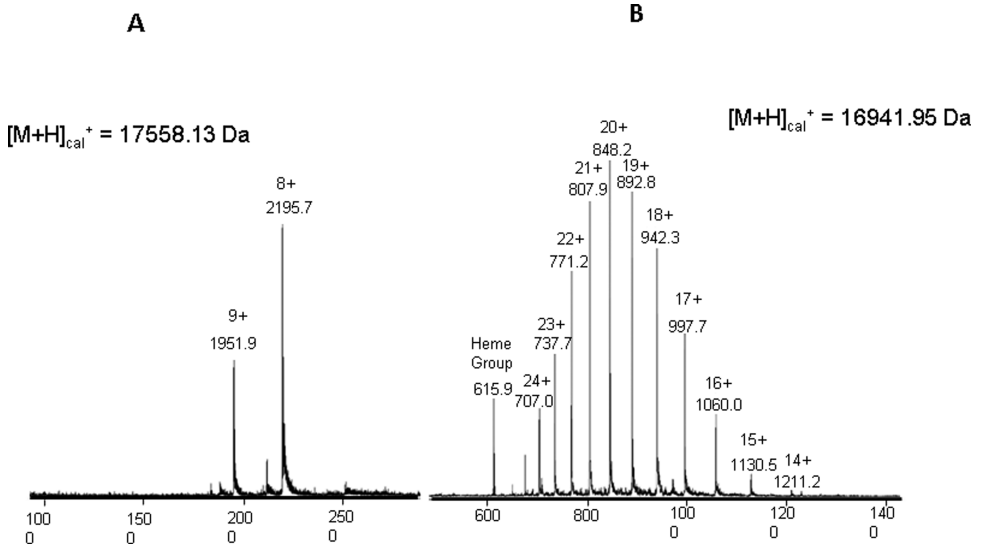

Figure 3. ESI-MS of (A) equine heme-myoglobin under native conditions (pH 7) (molecular mass, 17 557 Da); (B) myoglobin, apoprotein at acidic conditions (pH 2) (molecular mass, 16 941 Da).

https://dx.doi.org/10.1021/jasms.0c00234
J. Am. Soc. Mass Spectrom. XXXX, XXX, XXX−XXX

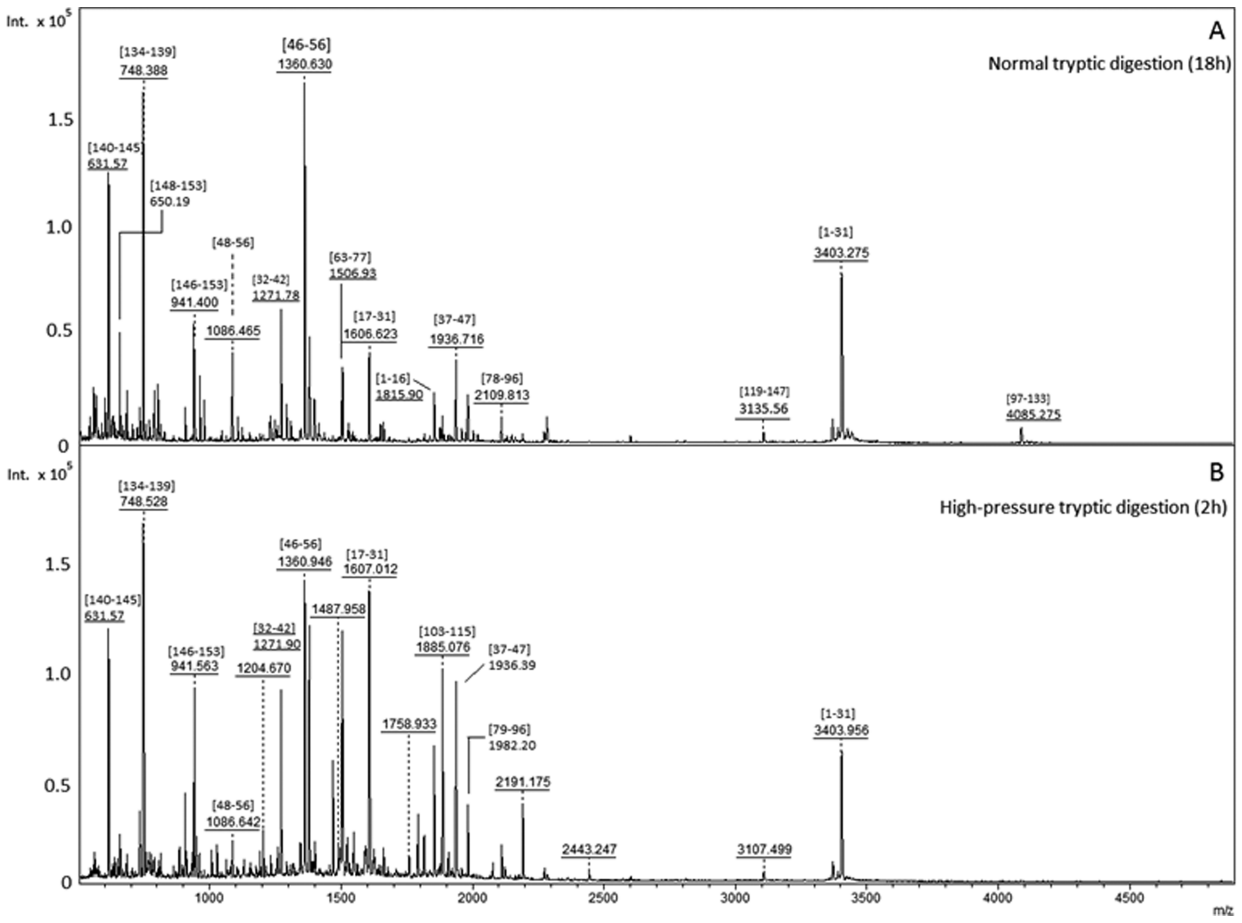

Figure 4. Proteolytic peptide mapping of MG (A) upon digestion at atmospheric pressure (37 °C, 12 h); (B) high pressure digestion using the Barocycler 2320EXT (37 °C, 90 min, 25 kpsi). Both digestions provided a sequence coverage > 92%.

Table 1. Tryptic Peptide Fragments of MG Identified by MALDI-MS Peptide Mapping upon High Pressure Digestion[a]

no.	*m/z*	AA sequence	sequence no.
1	1815.9024	GLSDGEWQQVLNVWGK.v	[1−16]
2	3403.7393	GLSDGEWQQVLNVWGKVEADIAGHGQEVLIR.l[4]	[11−31]
3	1606.8547	k.VEADIAGHGQEVLIR.l	[17−31]
4	1271.6630	r.LFTGHPETLEK.f	[32−42]
5	1661.8533	r.LFTGHPETLEKFDK.f[5]	[32−45]
6	1937.0167	r.LFTGHPETLEKFDKFK.h[6]	[32−47]
7	684.3715	k.FDKFK.h[1]	[43−47]
8	1086.5612	k.HLKTEAEMK.a	[48−56]
9	1857.9739	k.HLKTEAEMKASEDLKK.h[7]	[48−63]
10	3217.7977	k.HLKTEAEMKASEDLKKHGTVVLTALGGILK.k	[48−77]
11	790.4305	k.ASEDLKK.h	[57−63]
12	1378.8417	k.HGTVVLTALGGILK.k	[64−77]
13	1506.9366	k.HGTVVLTALGGILKK.k	[64−78]
14	2110.1516	k.KKGHHEAELKPLAQSHATK.h	[78−96]
15	1853.9617	k.GHHEAELKPLAQSHATK.h	[80−96]
16	735.4876	k.HKIPIK.y[2]	[97−102]
17	1885.0218	k.YLEFISDAIIHVLHSK.h	[103−118]
18	1502.6693	k.HPGDFGADAQGAMTK.a	[119−133]
19	748.4352	k.ALELFR.n	[134−139]
20	1360.7583	k.ALELFRNDIAAK.y	[134−145]
21	941.4727	k.YKELGFQG.[3]	[146−153]

[a]See Experimental Section.

by the nonstoichiometric ratio of the MG digest-to-antibody containing a molar excess of the MG digestion mixture. The background from the final washing following the elution was also analyzed and did not show remaining peptides (Figure

https://dx.doi.org/10.1021/jasms.0c00234
J. Am. Soc. Mass Spectrom. XXXX, XXX, XXX−XXX

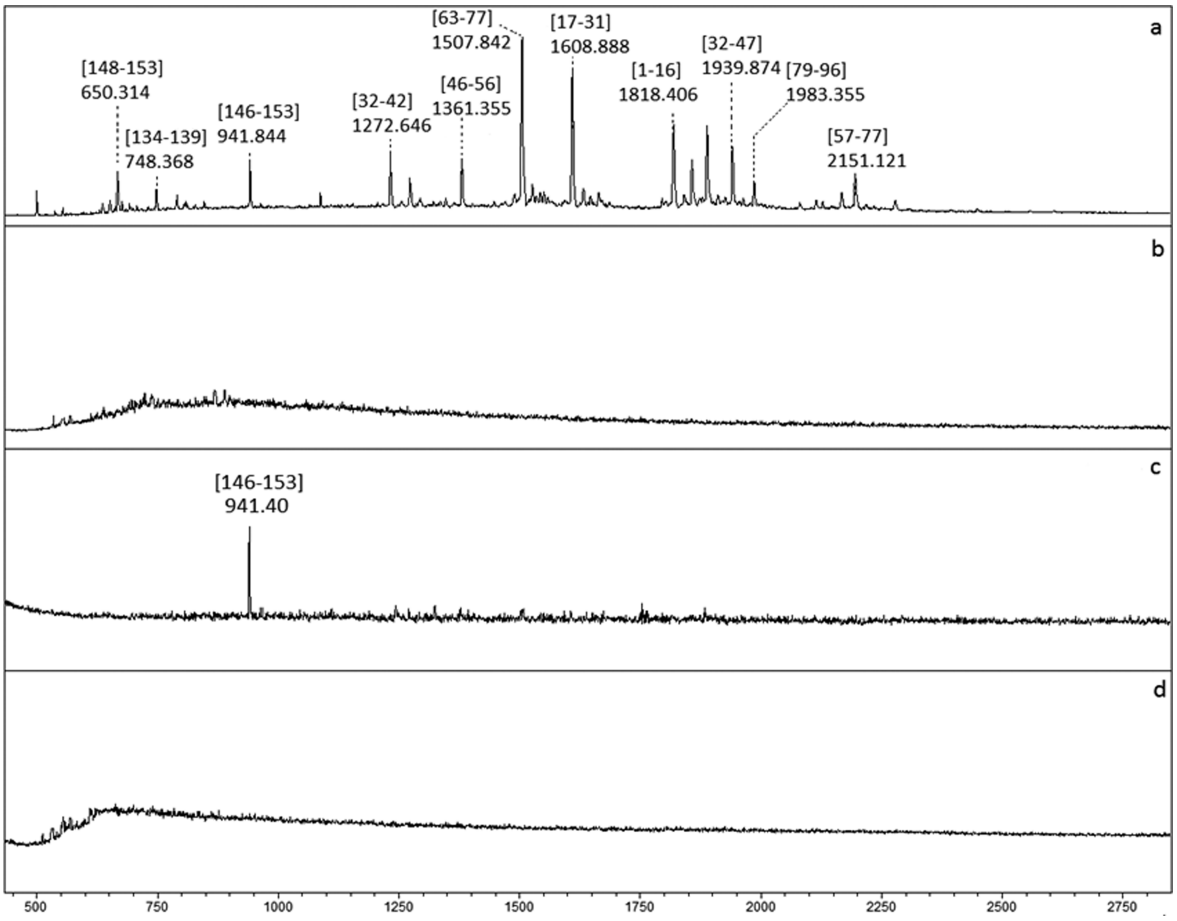

Figure 5. Identification of the apo-MG epitope by proteolytic extraction and MALDI- MS from the SPR-MS interface containing the immobilized anti-MG antibody. (a) Supernatant peptides from the antibody affinity column; (b) background spectrum before elution; (c) identification of epitope peptide, [146−153] (m/z 941.4), upon elution with 0.1% TFA; (d) background spectrum of last washing fraction after elution.

5d). In contrast to trypsin digestion, an epitope extraction-MS experiment using α-chymotrypsin as a protease did not provide a detectable epitope, due to the cleavage of MG at Y146 and F151 that cleaves the C-terminal epitope peptide sequence (data not shown).

Epitope analysis by SPR-MS upon binding and elution of the tryptic digestion mixture from the SPR chip containing the immobilized antibody provided the identical epitope peptide, [146−153] (Figure S5). The specificity of the epitope was ascertained by synthesis and affinity-MS characterization of the C-terminal peptide. In an affinity-MS experiment of a mixture of the C-terminal peptide (146−153) and the chymotryptic peptide (147−150), only the epitope peptide was retained, while the peptide (147−150) was found in the flowthrough.

CONCLUSIONS

In this study, the molecular epitope structure and affinity of equine heme-myoglobin and apo-myoglobin to a monoclonal antibody were determined using proteolytic epitope extraction mass spectrometry in combination with surface plasmon resonance (SPR) biosensor analysis. The sequence of the identified C-terminal epitope peptide is highlighted in Figure 6 in the structure of myoglobin. The epitope is shown to comprise the C-terminal sequence at the end of the final eighth α-helical loop of MG. The identified epitope, YKELGFQG, comprises the uncleaved residue lysine-146, suggesting the importance of the N-terminal sequence of the epitope for affinity-binding. The detailed affinity determination of the C-terminal epitope by SPR is carried out at present.

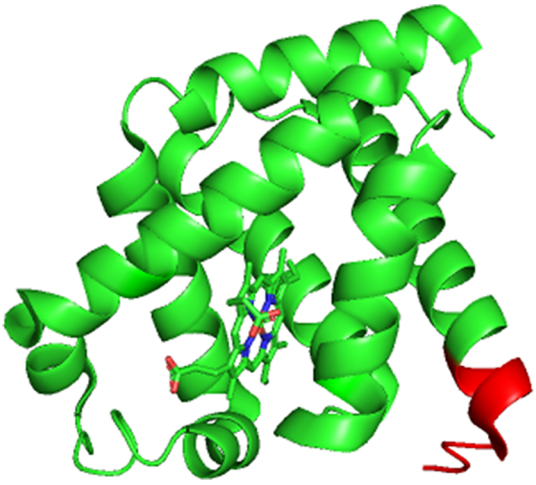

Figure 6. Structure of myoglobin with the C-terminal epitope peptide [146−153] highlighted in red.

The C-terminal epitope sequence is also in agreement with the binding affinity of the antibody to the denatured MG apoprotein. Moreover, the epitope is consistent with the cross-reactivity of the antibody for equine myoglobin with human MG and several other myoglobin proteins, described in

https://dx.doi.org/10.1021/jasms.0c00234
J. Am. Soc. Mass Spectrom. XXXX, XXX, XXX−XXX

previous publications.[6,18] These results confirm the efficiency of the molecular epitope characterization by proteolytic affinity-MS and the use of MG as a suitable model system in the development of the SPR-MS combination.

■ ASSOCIATED CONTENT

Supporting Information

The Supporting Information is available free of charge at https://pubs.acs.org/doi/10.1021/jasms.0c00234.

Figure S1: Schematic representation of the SPR-MS interface. (1) Autosampler/sample injector. (2) Interface containing microaffinity column or microchip with immobilized antibody. (3) SPR and SPR chip. SPR analysis and affinity-binding of immobilized antibody are performed at the interface and operation of the multiport valves. (4,5) Multiport valves for sample transfer and desalting/buffer change are located before affinity column and after elution before transfer to ESI-MS or SPR chip. (6) ESI-MS insertion port. Figure S2: MALDI-MS of (A) apo-myoglobin, (B) ESI-MS of apo-MG (pH 2; for details, see Experimental Section). Average molecular mass determined by MALDI-MS: 16 952.6 Da; monoisotopic mass determined by ESI-MS: 16 942.5 Da. Figure S3: Total ion chromatogram (A) and ESI-MS (B) of apomyoglobin upon affinity separation and elution in the SPR-MS interface. The TIC showed a sharp elution signal around 5.3 min. The multiply protonated molecular ions provide a molecular mass of 16.942 Da. Figure S4: Amino acid sequences of (A) horse heart myoglobin (PDB 1WLA), (B) human heart myoglobin (PDB 3RGK). Lysine and arginine residues are highlighted in red. Single mutation sites in human myoglobin are highlighted in blue. Figure S5: Identification of the apo-MG epitope [146−153] (m/z 941.4) by proteolytic extraction-ESI-MS upon elution from the SPR chip containing the immobilized anti-MG antibody (PDF)

■ AUTHOR INFORMATION

Corresponding Authors

Michael Przybylski − *Steinbeis Transfer Centre for Biopolymer Analysis and Biomedical Mass Spectrometry (STZ), 65428 Rüsselsheim am Main, Germany;* orcid.org/0000-0002-2611-5389; Phone: +49 (6142) 8345511; Email: Michael.Przybylski@stw.de; Fax: +49 (6142) 8345514

Günes Barka − *Sunchrom GmbH, 61381 Friedrichsdorf, Germany*; Phone: +49 (6172) 953350; Email: gbarka@sunchrom.de

Authors

Delia Mihoc − *Steinbeis Transfer Centre for Biopolymer Analysis and Biomedical Mass Spectrometry (STZ), 65428 Rüsselsheim am Main, Germany*

Loredana-Mirela Lupu − *Steinbeis Transfer Centre for Biopolymer Analysis and Biomedical Mass Spectrometry (STZ), 65428 Rüsselsheim am Main, Germany*

Pascal Wiegand − *Steinbeis Transfer Centre for Biopolymer Analysis and Biomedical Mass Spectrometry (STZ), 65428 Rüsselsheim am Main, Germany*

Wolfgang Kleinekofort − *Steinbeis Transfer Centre for Biopolymer Analysis and Biomedical Mass Spectrometry (STZ), 65428 Rüsselsheim am Main, Germany; Institute for Microtechnologies (IMTECH), Rhein Main University, 65428 Rüsselsheim am Main, Germany*

Oliver Müller − *Institute for Microtechnologies (IMTECH), Rhein Main University, 65428 Rüsselsheim am Main, Germany*

Friedemann Völklein − *Institute for Microtechnologies (IMTECH), Rhein Main University, 65428 Rüsselsheim am Main, Germany*

Michael O. Glocker − *Department of Immunology, Proteome Centre, Medical University Rostock, 18055 Rostock, Germany;* orcid.org/0000-0001-9190-482X

Frederik Barka − *Sunchrom GmbH, 61381 Friedrichsdorf, Germany*

Complete contact information is available at: https://pubs.acs.org/10.1021/jasms.0c00234

Notes

The authors declare no competing financial interest.

■ ACKNOWLEDGMENTS

This work has been supported by the State Ministery of Research Hessen, Wiesbaden, within the LOEWE-III programme (Hessen-Agentur, project No. HA-696-19/06). We gratefully acknowledge the expert assistance of Stephan Rawer in the synthesis of the myoglobin peptides. We are grateful to Dr. Kerstin Troidl and Dr. Christian Troidl, Clinical Cardiology Centre/Kerckhoff-Klinik, Bad Nauheim, Germany, for valuable discussion on cardiac biomarkers. We also thank Dr. Alexander Lazarev, Pressure Biosciences, Boston, USA, for support and valuable advice on high pressure proteolytic digestion.

■ REFERENCES

(1) Copeland, D. M.; Soares, A. S.; West, A. H.; Richter-Addo, G. B. Crystal structures of the nitrite and nitric oxide complexes of horse heart myoglobin. *J. Inorg. Biochem.* **2006**, *100*, 1413−1425.

(2) Kendrew, J. C.; Bodo, G.; Dintzis, H. M.; Parrish, R. G.; Wyckoff, H.; Phillips, D. C. A three dimensional model of the myoglobin molecule obtained by x-ray analysis. *Nature* **1958**, *181*, 662−666.

(3) Weber, M.; Rau, M.; Madlener, K.; Elsaesser, A.; Bankovic, D.; Mitrovic, V.; Hamm, C. Diagnostic utility of new immunoassays for the cardiac markers cTnI, myoglobin and CK-MB mass. *Clin. Biochem.* **2005**, *38* (11), 1027−30.

(4) Pickering, J. W.; Than, M. P.; Cullen, L.; Aldous, S.; Avest, E. T.; Body, R.; et al. Rapid Rule-out of Acute Myocardial Infarction With a Single High-Sensitivity Cardiac Troponin T Measurement Below the Limit of Detection: A Collaborative Meta-analysis. *Ann. Int. Med.* **2017**, *166* (10), 715−724.

(5) Weir, R. A.; McMurray, J. J.; Velazquez, E. J. Epidemiology of heart failure and left ventricular systolic dysfunction after acute myocardia infarction: prevalence, clinical characteristics and prognostic importance. *Am. J. Cardiol.* **2006**, *97* (10), 13−25.

(6) Mozaffarian, D.; Benjamin, E. J.; Go, A. S.; Arnett, D. K.; Blaha, M. J.; Cushman, M.; et al. Heart disease and stroke statistics–2015 update: a report from the American Heart Association. *Circulation* **2015**, *131* (4), e29−e322.

(7) Macht, M.; Fiedler, W.; Kürzinger, K.; Przybylski, M. Mass Spectrometric Mapping of Protein Epitope Structures of Myocardial Infarct Markers Myoglobin and Troponin T. *Biochemistry* **1996**, *35* (2), 15633−15639.

(8) YAO, Z.-J.; CHAN, M.-C.; KAO, M. C.C.; CHUNG, M. C.M. Linear epitopes of sperm whale myoglobin identified by polyclonal antibody screening of random peptide library. *Int. J. Pept. Protein Res.* **1996**, *48* (5), 477−485.

(9) Dutra, R. F.; Mendes, R. K.; Lins da Silva, V.; Kubota, L. T. Surface plasmon resonance immunosensor for human cardiac troponin T based on self-assembled monolayer. *J. Pharm. Biomed. Anal.* **2007**, *43*, 1744−1750.
(10) Kramer, S. D; Wohrle, J.; Rath, C.; Roth, G. An Online Tool for the Real-Time Kinetic Analysis of Binding Events. *Bioinf. Biol. Insights* **2019**, *13* (11), 1−10.
(11) Petre, B.-A.; Ulrich, M.; Stumbaum, M.; Bernevic, B.; Moise, A.; Döring, G.; Przybylski, M. When is Mass Spectrometry Combined with Affinity Approaches Essential? A Case Study of Tyrosine Nitration in Proteins. *J. Am. Soc. Mass Spectrom.* **2012**, *23* (11), 1831−1840.
(12) McLaurin, J.; Cecal, R.; Kierstead, M. E.; Tian, X.; Phinney, A. L.; Manea, M.; French, J. E.; Lambermon, M. H.; Darabie, A. A.; Brown, M. E.; Janus, C.; Chishti, M. A.; Horne, P.; Westaway, D.; Fraser, P. E.; Mount, H. T.; Przybylski, M.; St George-Hyslop, P. Therapeutically effective antibodies against amyloid-beta peptide target amyloid-beta residues 4−10 and inhibit cytotoxicity and fibrillogenesis. *Nat. Med.* **2002**, *8* (11), 1263−1269.
(13) Stefanescu, R.; Iacob, R. E.; Damoc, E. N.; Marquardt, A.; Amstalden, E.; Manea, M.; Perdivara, I.; Maftei, M.; Paraschiv, G.; Przybylski, M. Mass spectrometric approaches for elucidation of antigenantibody recognition structures in molecular immunology. *Eur. J. Mass Spectrom.* **2007**, *13* (1), 69−75.
(14) Iurascu, M. I.; Marroquin Belaunzanar, O.; Cozma, C.; Petrausch, U.; Renner, C.; Przybylski, M. An HLA-B27 Homodimer Specific Antibody Recognizes a Discontinuous Mixed-Disulfide Epitope as Identified by Affinity-Mass Spectrometry. *J. Am. Soc. Mass Spectrom.* **2016**, *27* (6), 1105−1112.
(15) Juszczyk, P.; Paraschiv, G.; Szymanska, A.; Kolodziejczyk, A. S.; Rodziewicz-Motowidlo, S.; Grzonka, Z.; Przybylski, M. Binding epitopes and interaction structure of the neuroprotective protease inhibitor cystatin C with beta-amyloid revealed by proteolytic excision mass spectrometry and molecular docking simulation. *J. Med. Chem.* **2009**, *52* (8), 2420−2428.
(16) Kukacka, Z.; Iurascu, M.; Lupu, L.; Rusche, H.; Murphy, M.; Altamore, L.; Borri, F.; Maeser, S.; Papini, A. M.; Hennermann, J.; Przybylski, M. Antibody Epitope of Human alpha-Galactosidase A Revealed by Affinity Mass Spectrometry: A Basis for Reversing Immunoreactivity in Enzyme Replacement Therapy of Fabry Disease. *ChemMedChem* **2018**, *13* (9), 909−915.
(17) Moise, A.; Maeser, S.; Rawer, S.; Eggers, F.; Murphy, M.; Bornheim, J.; Przybylski, M. Substrate and Substrate-Mimetic Chaperone Binding Sites in Human alpha-Galactosidase A Revealed by Affinity-Mass Spectrometry. *J. Am. Soc. Mass Spectrom.* **2016**, *27* (6), 1071−1078.
(18) Atassi, M. Z.; Tarlowski, D. P.; Paull, J. H. Immunochemistry of sperm whale myoglobin, vll. Correlation of immunochemical cross-reaction of eight myoglobins with structural similarity and its dependence on conformation. *Biochim. Biophys. Acta, Protein Struct.* **1970**, *221*, 623−640.
(19) Peri, S.; Steen, H.; Pandey, A. GPMAW–a software tool for analyzing proteins and peptides. *Trends Biochem. Sci.* **2001**, *26* (11), 687−689.
(20) Wiegand, P.; Lupu, L.; Hüttmann, N.; Wack, J.; Rawer, S.; Przybylski, M.; Schmitz, K. Epitope Identification and Affinity Determination of an Inhibiting Human Antibody to Interleukin IL8 (CXCL8) by SPR- Biosensor − Mass Spectrometry Combination. *J. Am. Soc. Mass Spectrom.* **2020**, *31*, 109.
(21) *Trace Drawer*, V. 1.7.1; Ridgeview Instruments AB: Vänge, Sweden.
(22) Rinaldi, F.; Lupu, L.; Rusche, H.; Kukačka, Z.; Tengattini, S.; Bernardini, R.; Piubelli, L.; Bavaro, T.; Maeser, S.; Pollegioni, L.; Calleri, E.; Przybylski, M.; Temporini, C. Epitope and affinity determination of recombinant Mycobacterium tuberculosis Ag85B antigen towards anti-Ag85 antibodies using proteolytic affinity-mass spectrometry and biosensor analysis. *Anal. Bioanal. Chem.* **2019**, *411*, 439−448.

https://dx.doi.org/10.1021/jasms.0c00234
J. Am. Soc. Mass Spectrom. XXXX, XXX, XXX−XXX

Supporting Information

Antibody Epitope and Affinity Determination of the Myocardial Infarct Marker Myoglobin by SPR- Biosensor Mass Spectrometry

Delia Mihoc[1], Loredana-Mirela Lupu[1], Pascal Wiegand[1], Wolfgang Kleinekofort[1,2], Oliver Müller[2], Friedemann Völklein[2], Michael O. Glocker[3], Frederik Barka[4], Günes Barka[4*], Michael Przybylski[1*]

[1*]Steinbeis Transfer Centre for Biopolymer Analysis and Biomedical Mass Spectrometry (STZ), Marktstrasse. 29, 65428, Rüsselsheim am Main, Germany

[2] Rhein Main University, Institute for Microtechnologies (IMTECH), 65428 Rüsselsheim am Main, Germany

[3]Medical University Rostock, Department of Immunology, Proteome Centre, Schillingallee 69, 18055 Rostock, Germany

[4*]Sunchrom GmbH, Industriestr. 27, 61381 Friedrichsdorf, Germany

Correspondence author:

Prof. Dr. Michael Przybylski
Steinbeis Centre for Biopolymer Analysis and Biomedical Mass Spectrometry
Marktstraße 29, 6542 Rüsselsheim am Main, Germany
Phone: +49 (6142) 8345511; Fax: +49 (6142) 8345514
Email: Michael.Przybylski@stw.de

Supporting Figures

Figure S1

Schematic representation of the SPR-MS interface. [1], autosampler / sample injector; [2], interface containing micro-affinity column or microchip with immobilized antibody. [3], SPR & SPR chip. SPR analysis and affinity binding of immobilized antibody are performed at the interface and operation of the multiport valves. [4, 5], Multiport valves for sample transfer and desalting/buffer change are located before the affinity column and following the elution for transfer of the eluate to the ESI-MS ion source or the SPR chip. [6], ESI-MS Insertion port.

Figure S2

MALDI-MS of (A), apo- myoglobin; (B), ESI-MS of apo- MG (pH 2; for details, s. Experimental Section). Determination of average molecular mass by MALDI-MS: 16.952,6 Da; monoisotopic mass determination by ESI-MS: 16.942,5 Da.

Figure S3

Total ion affinity chromatogram (A) and ESI-MS (B) of apo-myoglobin affinity separation prior to elution in the SPR-MS interface. The TIC yields a sharp elution signal around 5.3 min. The multiply protonated molecular ions provide a molecular mass determination of 16.942 Da.

Figure S4

Amino acid sequences of (A) horse heart myoglobin (PDB- 1WLA); (B), human heart myoglobin (PDB 3RGK). Lysine and Arginine residues are highlighted in red. Single mutation sites in human myoglobin are highlighted in blue.

Figure S5

Identification of the apo-MG epitope [146 – 153] (m/z 941,4) by proteolytic extraction- ESI-MS upon elution from the SPR chip containing the immobilized anti-MG antibody. S. Experimental section for details.

Figure S1

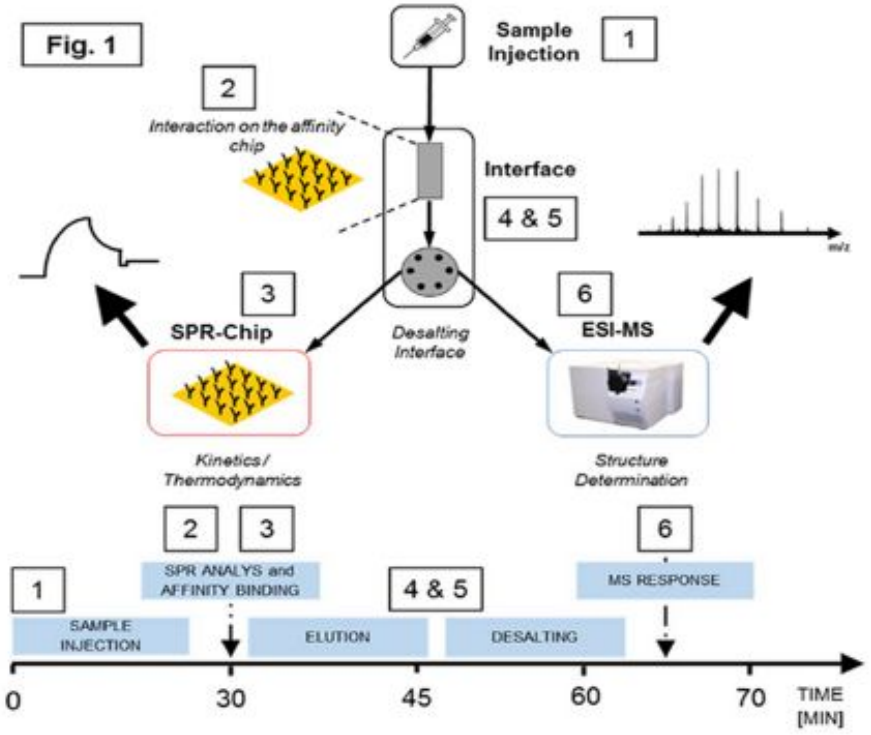
Fig. 1
Sample Injection
1
2
Interaction on the affinity chip
Interface
4 & 5
m/z
3
SPR-Chip
Desalting Interface
6
ESI-MS
Kinetics / Thermodynamics
Structure Determination
2
3
6
1
SPR ANALYS and AFFINITY BINDING
4 & 5
MS RESPONSE
SAMPLE INJECTION
ELUTION
DESALTING
0
30
45
60
70
TIME [MIN]

Figure S2

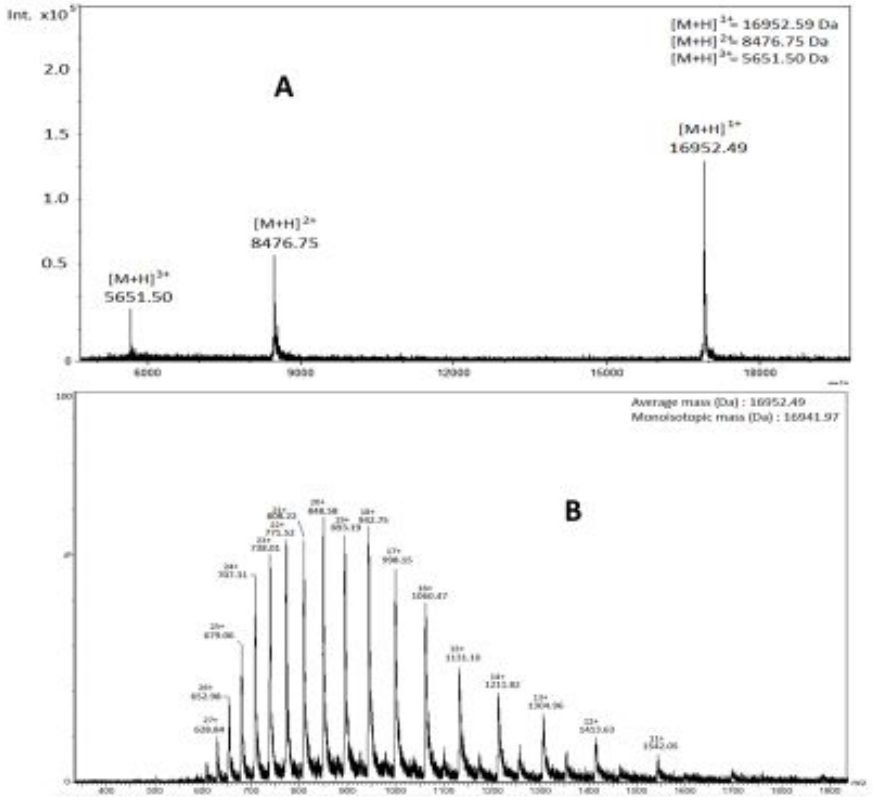
Int. x10^5
2.0
1.5
1.0
0.5
0
A
[M+H]3+= 16952.59 Da
[M+H]2+= 8476.75 Da
[M+H]3+= 5651.50 Da
[M+H]1+
16952.49
[M+H]2+
8476.75
[M+H]3+
5651.50
6000
9000
12000
15000
18000
Average mass (Da) : 16952.49
Monoisotopic mass (Da) : 16941.97
B

Figure S3

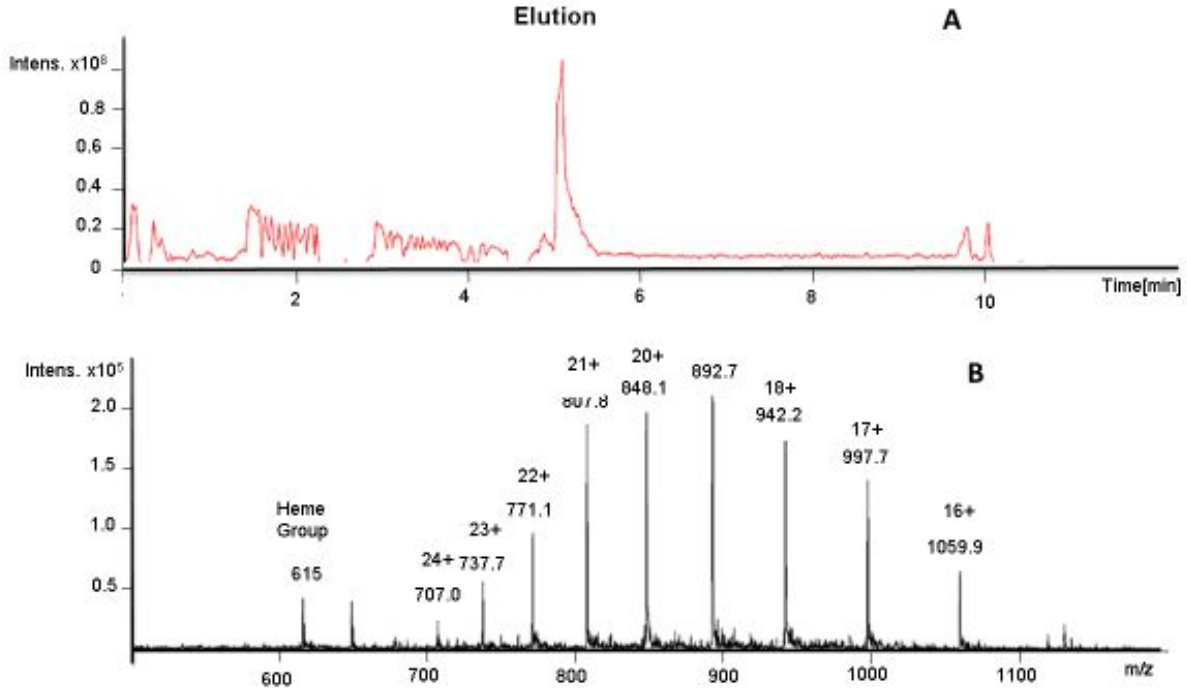
Elution
A
Intens. x10⁸
0.8
0.6
0.4
0.2
0
2
4
6
8
10
Time[min]
Intens. x10⁵
2.0
1.5
1.0
0.5
B
Heme
Group
615
707.0
24+
737.7
23+
771.1
22+
807.8
21+
848.1
20+
892.7
18+
942.2
17+
997.7
16+
1059.9
600
700
800
900
1000
1100
m/z

Figure S4

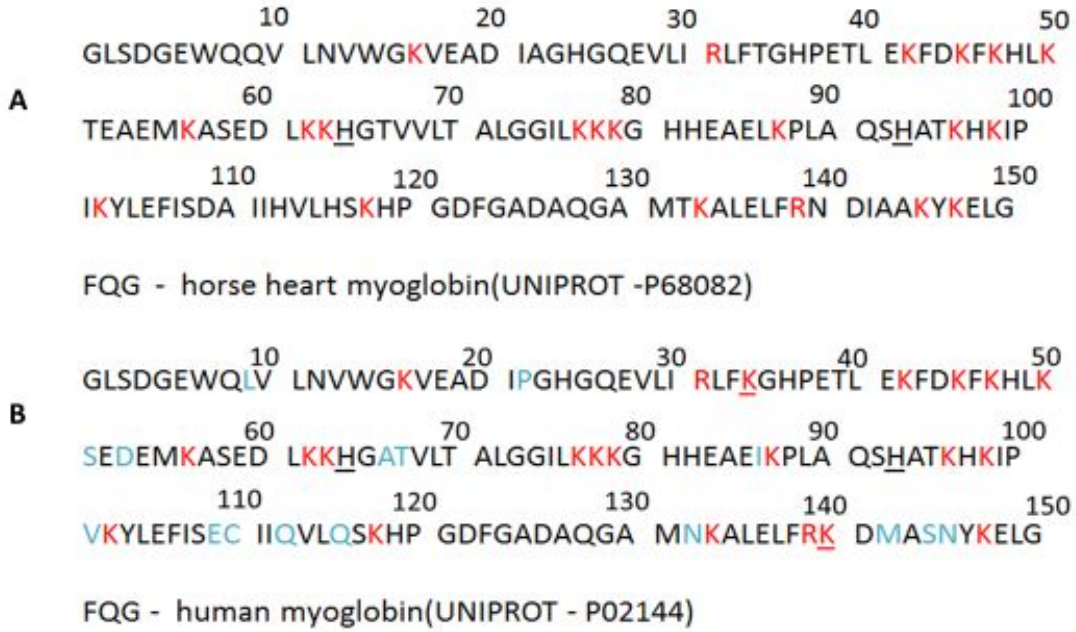
A
10 20 30 40 50
GLSDGEWQQV LNVWGKVEAD IAGHGQEVLI RLFTGHPETL EKFDKFKHLK
60 70 80 90 100
TEAEMKASED LKKHGTVVLT ALGGILKKKG HHEAELKPLA QSHATKHKIP
110 120 130 140 150
IKYLEFISDA IIHVLHSKHP GDFGADAQGA MTKALELFRN DIAAKYKELG
FQG - horse heart myoglobin(UNIPROT -P68082)
B
10 20 30 40 50
GLSDGEWQLV LNVWGKVEAD IPGHGQEVLI RLFKGHPETL EKFDKFKHLK
60 70 80 90 100
SEDEMKASED LKKHGATVLT ALGGILKKKG HHEAEIKPLA QSHATKHKIP
110 120 130 140 150
VKYLEFISEC IIQVLQSKHP GDFGADAQGA MNKALELFRK DMASNYKELG
FQG - human myoglobin(UNIPROT - P02144)

Figure S5

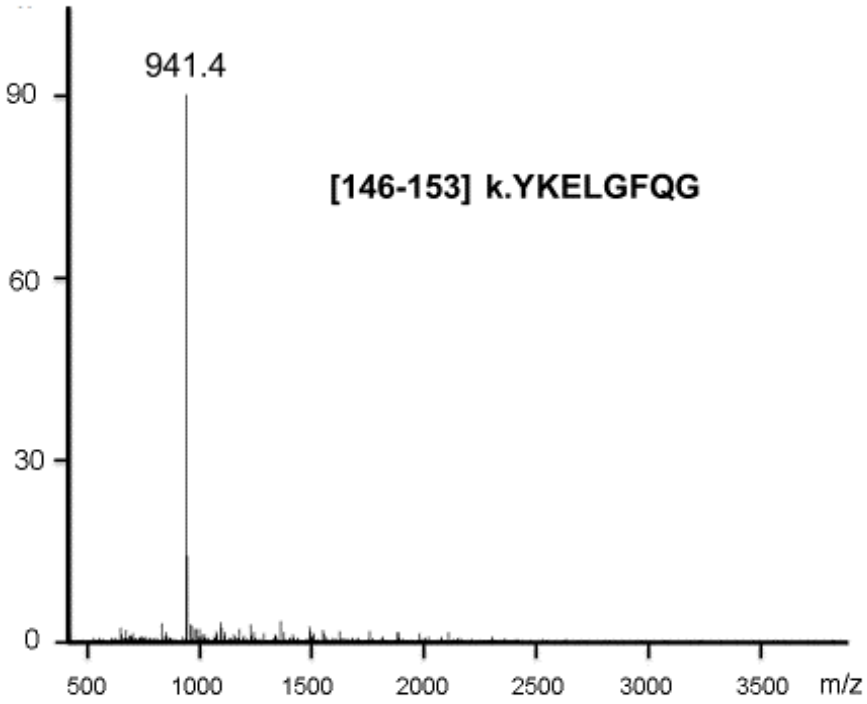
941.4
[146-153] k.YKELGFQG
90
60
30
0
500
1000
1500
2000
2500
3000
3500
m/z

ChemPubSoc Europe

DOI: 10.1002/cmdc.201800094

CHEMMEDCHEM Full Papers

Antibody Epitope of Human α-Galactosidase A Revealed by Affinity Mass Spectrometry: A Basis for Reversing Immunoreactivity in Enzyme Replacement Therapy of Fabry Disease

Zdenek Kukacka,[a, b] Marius Iurascu,[a, b] Loredana Lupu,[a, b] Hendrik Rusche,[a, b] Mary Murphy,[c] Lorenzo Altamore,[d, e, f] Fabio Borri,[d, e, f] Stefan Maeser,[a, b] Anna Maria Papini,[d, e, f] Julia Hennermann,[g] and Michael Przybylski*[a, b]

α-Galactosidase (αGal) is a lysosomal enzyme that hydrolyses the terminal α-galactosyl moiety from glycosphingolipids. Mutations in the encoding genes for αGal lead to defective or misfolded enzyme, which results in substrate accumulation and subsequent organ dysfunction. The metabolic disease caused by a deficiency of human α-galactosidase A is known as Fabry disease or Fabry–Anderson disease, and it belongs to a larger group known as lysosomal storage diseases. An effective treatment for Fabry disease has been developed by enzyme replacement therapy (ERT), which involves infusions of purified recombinant enzyme in order to increase enzyme levels and decrease the amounts of accumulated substrate. However, immunoreactivity and IgG antibody formation are major, therapy-limiting, and eventually life-threatening complications of ERT. The present study focused on the epitope determination of human α-galactosidase A against its antibody formed. Here we report the identification of the epitope of human αGal(309–332) recognized by a human monoclonal anti-αGal antibody, using a combination of proteolytic excision of the immobilized immune complex and surface plasmon resonance biosensing mass spectrometry. The epitope peptide, αGal(309–332), was synthesized by solid-phase peptide synthesis. Determination of its affinity by surface plasmon resonance analysis revealed a high binding affinity for the antibody ($K_D = 39 \times 10^{-9}$ M), which is nearly identical to that of the full-length enzyme ($K_D = 16 \times 10^{-9}$ M). The proteolytic excision affinity mass spectrometry method is shown here to be an efficient tool for epitope identification of an immunogenic lysosomal enzyme. Because the full-length αGal and the antibody epitope showed similar binding affinities, this provides a basis for reversing immunogenicity upon ERT by: 1) treatment of patients with the epitope peptide to neutralize antibodies, or 2) removal of antibodies by apheresis, and thus significantly improving the response to ERT.

[a] Dr. Z. Kukacka, Dr. M. Iurascu, L. Lupu, H. Rusche, Dr. S. Maeser, Prof. Dr. M. Przybylski
Steinbeis Centre for Biopolymer Analysis and Biomedical Mass Spectrometry, 65428 Rüsselsheim am Main (Germany)
E-mail: michael.przybylski@stw.de

[b] Dr. Z. Kukacka, Dr. M. Iurascu, L. Lupu, H. Rusche, Dr. S. Maeser, Prof. Dr. M. Przybylski
Department of Chemistry, University of Konstanz, 78457 Konstanz (Germany)

[c] Dr. M. Murphy
Ametek Reichert Technologies, Depew, NY 14043 (USA)

[d] L. Altamore, F. Borri, Prof. Dr. A. M. Papini
French–Italian Interdepartmental Laboratory of Peptide and Protein Chemistry and Biology, Università degli Studi di Firenze, 50019 Sesto Fiorentino (Italy)

[e] L. Altamore, F. Borri, Prof. Dr. A. M. Papini
Dipartimento di Chimica "Ugo Schiff", Università degli Studi di Firenze, Via della Lastruccia 13, 50019 Sesto Fiorentino (Italy)

[f] L. Altamore, F. Borri, Prof. Dr. A. M. Papini
PeptLab@UCP and Laboratory of Chemical Biology EA4505, Université Paris-Seine, 5 Mail Gay-Lussac, 95031 Cergy-Pontoise (France)

[g] Prof. Dr. J. Hennermann
Department of Pediatrics, Villa Metabolica, Universitätsmedizin Mainz, 55130 Mainz (Germany)

Supporting information and the ORCID identification number(s) for the author(s) of this article can be found under: https://doi.org/10.1002/cmdc.201800094.

Introduction

α-Galactosidase (αGal) is a lysosomal enzyme that hydrolyses the terminal α-galactosyl moiety from glycosphingolipids. Mutations in the gene encoding αGal or biochemical changes lead to the complete loss of the enzyme or its misfolding into an inactive form, resulting in accumulation of globotriaosylceramide (GL-3) substrate and related glycosphingolipids in lysosomes (Figure 1). This leads to increased substrate levels in the blood and in several organs including brain, and finally to organ dysfunction and diminished survival, especially due to stroke and renal disease.[1–3] The pathophysiology caused by αGal deficiency is termed Fabry disease (FD) or Fabry–Anderson disease, and belongs to a group of approximately 60–70 lysosomal storage diseases (LSDs). FD is an X-linked inherited disease, thus mainly males are affected, although females can also develop FD symptoms and require treatment.[3,4] Enzyme replacement therapies (ERTs) have been successfully developed for several LSDs, such as Gaucher's disease, Pompe disease, and FD.[1–4] FD therapy is performed through intravenous infusion with purified recombinant enzyme in order to increase enzyme levels in lysosomes and decrease accumulated substrate.[2,3] Currently, two recombinant enzymes are clinically

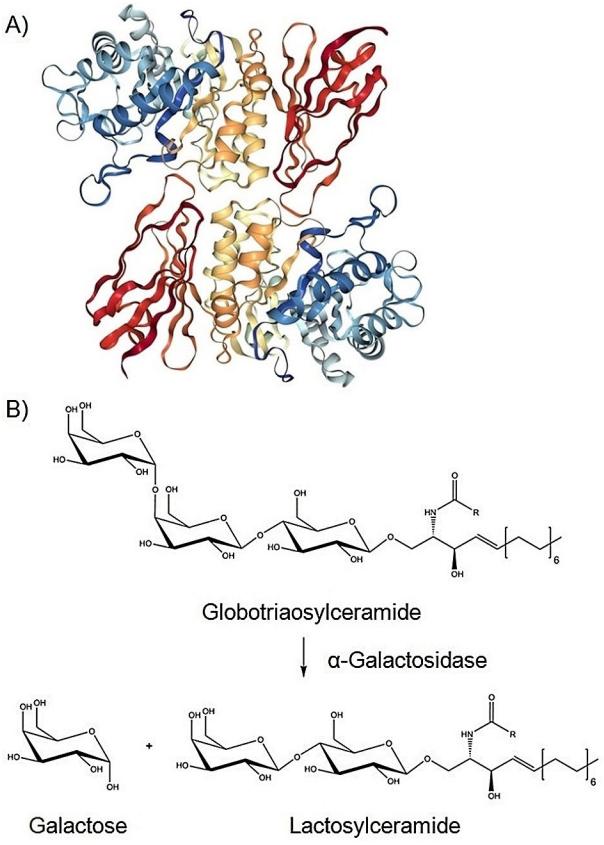

Figure 1. A) Structure of human α-galactosidase (PDB ID: 1R47); modified from Ref. [28]. B) Human αGal-catalyzed reaction of globotriaosylceramide (GL-3) to lactosylceramide and galactose.

used at different dosages: agalsidase-α and agalsidase-β.[1,4] Most males with FD are negative for cross-reacting immunological material (CRIM) due to frameshift or missense mutations. Therefore, exposure to infused αGal-A is expected to result in antibody formation.

Although effective for a number of LSDs, substantial problems and limitations are caused by the raising of antibodies upon ERT. ERT can trigger the formation of specific IgE antibodies, which may be associated with allergic reactions ranging from mild symptoms to anaphylactic shock.[5–9] Moreover, ERT can result in the production of neutralizing IgG antibodies that bind to the infused enzymes and might impair or even diminish the clinical effectiveness of ERT.[6] The emergence of neutralizing anti-αGal-A antibodies in FD patients treated with agalsidase-α or agalsidase-β has been reported in several studies.[3] In contrast to female patients, who did not develop detectable amounts of antibodies following ERT, a substantial proportion of male patients after six months of treatment showed high titers of IgG antibodies that cross-react in vitro with the recombinant enzyme and neutralized rh-αGal-A activity in up to 95% of patients. During infusion with rh-αGal-A, circulating enzyme–antibody complexes were formed, whereas all IgG-negative patients showed a significant decrease in urinary globotriaosylceramide substrates. Thus, in vivo neutralizing antibodies are frequently encountered in male FD patients and cross-reactivity of antibodies suggests that switching from one to the other recombinant enzyme is unlikely to prevent the immune response.[2,4] At present there is little understanding of the mechanisms of adverse immune reactions upon ERT, and almost no knowledge on the corresponding antibodies formed. Immunomodulating or immunosuppressive therapies are presently applied to decrease allergic reactions.[6,7] Immunomodulation has been reported in patients with Pompe disease and Gaucher's disease, with variable success, and temporary depletion of B cells (anti-CD20) has been mostly used.[8–10] However, only bone marrow transplantation in patients with mucopolysaccharidosis type I (another type of LSD) resulted in a decrease in antibody formation.[1,2] Thus, the development of alternative treatments by identification of antibody-specific epitopes and application of peptide epitopes capable of blocking antibodies represents a relevant clinical goal.

A variety of methods, including mass spectrometry (MS)-based approaches, have been developed for the identification of antibody-specific epitopes and for providing structural information about antigen–antibody complexes. These methods also include X-ray crystallography and NMR spectroscopy, immunoanalytical characterization of antigen–antibody interactions, and the design and synthesis of peptide–epitope mimotopes.[11–14] Proteolytic excision–extraction mass spectrometry (PROTEX-MS), hydrogen–deuterium exchange mass spectrometry (HDX-MS) of peptide backbone hydrogen atoms, and fast-photochemical oxidation of proteins are the major techniques for MS-based elucidation of antibody epitopes, but these tools alone do not provide quantitative affinity data.[15–18] We have recently developed an online surface plasmon resonance (SPR) biosensing technique combined with MS, which enables simultaneous affinity isolation, structure identification and affinity quantification of epitopes from an immobilized antibody–ligand complex, using an integrated, automated interface for sample concentration and in situ desalting for MS analysis.[19] The PROTEX-MS method, using either proteolytic epitope excision of intact immune complexes or epitope extraction from a defined peptide fragment mixture presented to the immobilized antibody, has been successfully applied to the identification of both linear and discontinuous epitopes of a wide range of protein antigens.[20–25] In general, the PROTEX-MS method is based on 1) the high stability of antibodies toward protease digestion, and 2) the proteolytic shielding of the epitope–paratope interaction structure.[15]

Here we report the structure identification and synthesis of the epitope of αGal and characterization of its affinity for a human monoclonal antibody that was shown to bind with high (nanomolar) affinity. A single 24-amino-acid peptide sequence was identified by proteolytic excision with trypsin, that contained two shielded, uncleaved lysine residues. The synthetic peptide epitope αGal(309–332) showed high, nanomolar affinity for the antibody, similar to that of the full-length enzyme, whereas partial sequences of the epitope showed substantially lower affinities. Therefore, this epitope peptide appears to be promising for the development of new approaches for antibody depletion upon ERT, such as by apheresis.

Results and Discussion

Primary structure characterization of human α-galactosidase

The primary structure of the recombinant human αGal was characterized by 1) MALDI-MS analysis of the intact enzyme, and 2) MALDI-TOF-MS and ESI–ion trap MS analysis of tryptic digestion mixtures (Table S1 in the Supporting Information). Identification using the MASCOT database revealed that the MALDI-MS analysis provided nearly all expected peptides except for small repetitive sequences such as the RK dipeptide fragment (392–393) with 95% sequence coverage, whereas ESI-MS analysis of the tryptic peptides yielded a 98% sequence coverage (Figure 2 and Table S1). Notably, the tryptic peptides (302–308), (309–314), and (315–326) were all found in the free enzyme (Table S1), but were not detected upon binding to the antibody, in which case lysine residues K314 and K326 were found uncleaved in the epitope peptide, as described below.

In the analysis of the tryptic digested peptide mixture, the three glycosylated peptide fragments comprising the N-glycosylation sites N139, N192, and N408 were also detected, albeit with low abundances. The MALDI-MS and ESI-MS peptide mapping in solution was fully achieved by in-gel digestion of the full-length protein band; however, the peptide recoveries were found to be lower than by digestion in solution.

Identification of the α-galactosidase epitope to the αGal antibody

To identify the epitope of αGal, both proteolytic epitope excision and extraction MS were employed using an affinity column with Sepharose-immobilized monoclonal anti-α-galactosidase antibody and trypsin digestion, as described in the Experimental Section. In an epitope extraction experiment, αGal was digested with trypsin in solution. The resulting peptide fragment mixture was subjected to interaction with the Sepharose-immobilized antibody, and first analyzed as a supernatant (Figure 3A). The ESI-MS analysis of the supernatant fraction revealed the identical tryptic peptide fragments and sequence coverage as for the free αGal sequence; nearly all peptides were identified except the short dipeptide sequence RK (392–393). The sequence coverage of the protein in the supernatant fraction was 96%.

The ESI-MS analysis of the fraction eluted from the antibody revealed a single tryptic epitope peptide, αGal(309–332), with a monoisotopic molecular mass of *m/z* 2696.5 Da, which showed protonated 3+, 4+ and 5+ charged ions as the most abundant (Figure 3B). In the epitope peptide, the lysine residues K314 and K326 were not cleaved by trypsin, thus confirming that these residues are shielded by antibody binding. The epitope was unequivocally identified by the molecular mass determination of the eluted peptide by MALDI-MS (*m/z* 2698.2 $[M+H]^+$), and by tryptic cleavage of the epitope peptide, which yielded fragments (309–314), (315–326), and (327–332) (data not shown). The peptide epitope (309–332) is highlighted in the tertiary structure of the αGal homodimer in Figure 4B, which suggests a defined conformational arrangement in the protein structure; however structural details of the epitope upon antibody binding were not obtained.

Synthesis and characterization of peptide epitopes

The complete 24-amino-acid peptide epitope αGal(309–332) was synthesized by solid-phase peptide synthesis (SPPS) with the Fmoc/*tert*-butyl strategy using a microwave-assisted synthesizer, which provided convenient conditions to obtain the crude peptide in high yield with high purity. In addition, the shorter partial peptides comprising the epitope—αGal(309–314), αGal(315–326), and αGal(327–332)—were prepared by standard SPPS conditions using a semiautomatic peptide synthesizer, as described in the Experimental Section. With the use of the microwave synthesizer, two deprotection steps were used: 1) the first for 15 s, 155 W at 75 °C; 2) the second for 30 s, 30 W at 90 °C (Table S2).

Following cleavage of the peptides from the resin and deprotection with TFA/H_2O/TIS solution, the crude products were precipitated with diethyl ether, lyophilized, and the final products purified using solid-phase extraction. The purity of all peptides was examined by ESI-MS and found to exceed 95%. The epitope peptides were also identified by MALDI-MS, which in all cases showed abundant protonated molecular ions $[M+H]^+$ consistent with the correct sequences (Table S2).

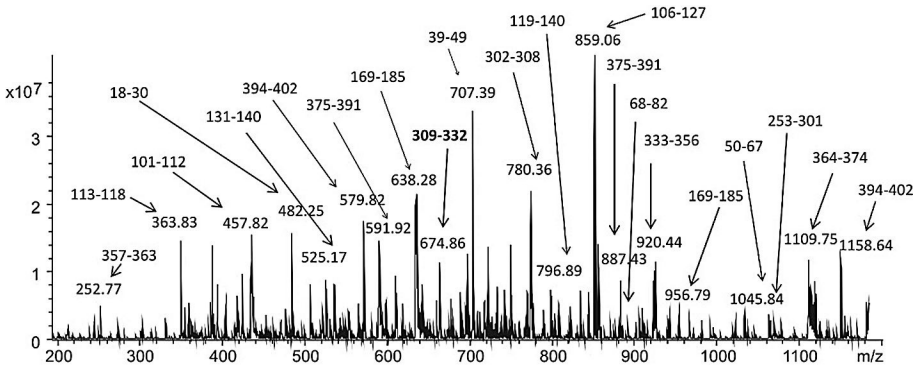

Figure 2. ESI-MS analysis of the tryptic peptide digestion mixture of human αGal. Partial peptide sequences are assigned to the singly and multiply protonated ions, as indicated.

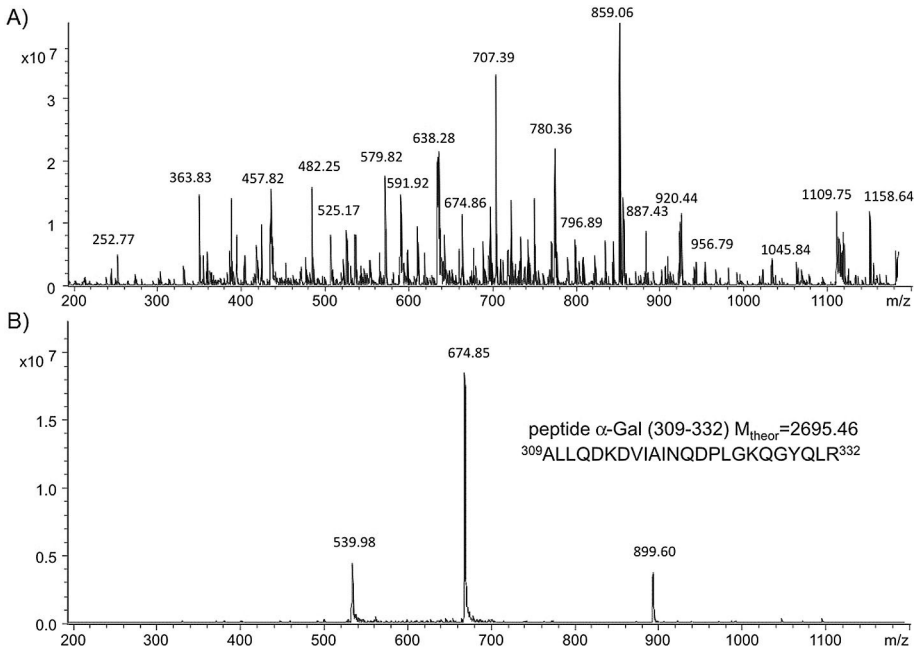

Figure 3. ESI–ion trap mass spectra of A) the supernatant fraction after αGal tryptic digestion, and B) the epitope from the affinity elution fraction after αGal tryptic digestion.

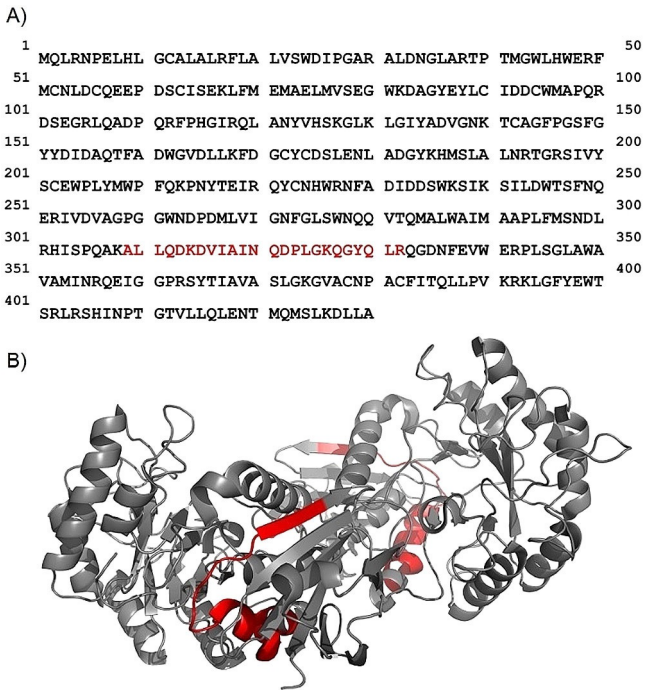

Figure 4. A) Amino acid sequence of human αGal containing a C-terminal oligohistidine tag. The (309–332) epitope is highlighted in red. B) Crystal structure (ribbon conformation; modified from Ref. [26]) of the human αGal dimer.

Affinity determination of α-galactosidase and α-galactosidase epitope peptides

Using the SPR biosensor–mass spectrometry combination, conditions were effective for determination of the affinities of the full-length αGal and their comparison to the epitope peptides of the antibody (Table 1). Dissociation constants for αGal and the synthetic peptide epitope αGal(309–332) from the human anti-αGal antibody are shown in Figure 5 A and B at concentrations of 5–20 nM and 50 nM–1 μM, respectively. Remarkably, nearly identical affinities were found with K_D values of 16 nM for the full-length enzyme, and 39 nM for the αGal(309–332) epitope. Because the peptide epitope (309–332) contains two cleavage sites for trypsin, dissociation constants were also determined for the shorter synthetic peptides. However, affinities for the peptides αGal(309–315) and αGal(316–324) were substantially lower with K_D values in the micromolar range, whereas the affinity of the C-terminal peptide αGal(325–332) was significantly higher ($K_D \approx 150$ nM; Table S3). Hence this peptide can be considered to comprise the core epitope sequence.

Table 1. Affinity determination of intact α-galactosidase, peptide epitope (309–332) and partial peptides.

	Protein/peptide	K_D [$\times 10^{-9}$ M]
Intact protein	αGal(1–429)	15.6
Epitope	αGal(309–332)	38.8
Peptide I	αGal(309–320)	15.100
Peptide II	αGal(315–326)	4.340
Peptide III	αGal(321–332)	705.2
Peptide IV	αGal(309–316)	8.160
Peptide V	αGal(317–324)	>1000
Peptide VI	αGal(325–332)	4.930

Conclusions

α-Galactosidase (αGal) is a lysosomal enzyme that hydrolyses the terminal α-galactosyl moiety from glycosphingolipids. Mu-

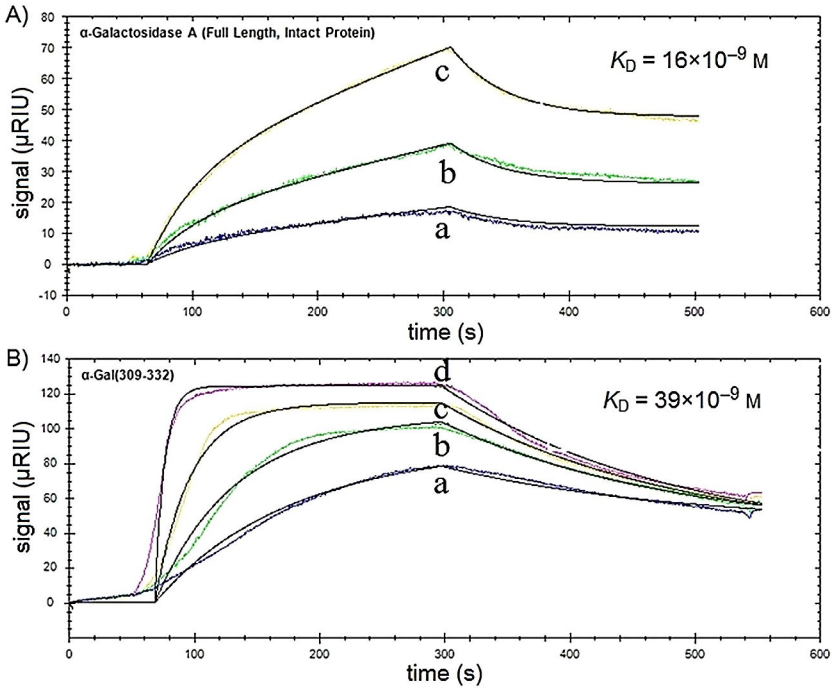

Figure 5. SPR affinity determination of A) full-length αGal and B) the epitope αGal(309–332).

tations in the gene encoding αGal lead either to the complete loss of enzyme or to expression of inactive, misfolded enzyme, resulting in accumulation of GL-3 and related glycosphingolipids in blood vessels, skin, kidney, heart, brain, with subsequent organ dysfunction and reduced life span. Most males affected with FD are negative for CRIM due to frameshift, missplicing, stop codon or unstable missense mutations. Therefore, exposure to infused αGal A is expected to result in antibody production. Defects in the αGal gene product, caused mostly by single amino acid substitutions, lead to its rapid degradation within the endoplasmic reticulum[3] and prohibit intracellular trafficking of the enzyme to its destination, the lysosome. This explains the high antibody production and binding rate, although predominantly, patients synthesize proteins with exchanged amino acids, not mutations such as in stop codons that lead to a lack of protein expression, as found for the β-glucocerebrosidase defect in Gaucher's disease.[5] In a study, three of the 14 patients who received αGal developed low IgG antibody titers (approximately 1:10), and no patient developed IgE, IgA, or IgM antibodies. However, nine patients were positive, with titers of approximately 1:2. Low-titer antibodies appeared to have no clinically significant effect on the safety and efficacy of ERT, and antibody titers decreased over time. The majority of seroconverted patients showed decreased antibody titers in a 30 month longitudinal study. However, approximately 90% of 58 patients receiving ERT with 1 mg kg^{-1} αGal over 20 weeks developed IgG antibodies. Overall, the rate of antibody formation in patients treated with αGal varied between 15% and 90%.[1–4]

In this study, we identified the epitope of human αGal to a monoclonal human anti-αGal antibody. Because the full-length enzyme and the epitope showed similar binding affinities, this provides the basis for reversing the immunogenicity, using 1) pretreatment of patients with epitope peptides to neutralizing antibodies, or 2) removal of antibodies by apheresis. Both approaches are expected to significantly improve the response to ERT. The synthesis and affinity characterization of the single 24-amino-acid peptide sequence suggested defined conformational properties, which are currently being investigated in detail.

The synthetic peptide epitope αGal(309–332) contains two shielded (uncleaved) lysine residues (Figure 4) and exhibits high nanomolar affinity similar to that of the full-length protein, whereas partial sequences showed substantially lower affinities (Table S2). Thus, the epitope peptide αGal(309–332) might be suitable for developing an effective clinical application for depleting antibodies formed during ERT, such as by apheresis, and provides numerous possibilities for optimization of affinity and stability in physiological conditions. In summary, the identification, chemical synthesis, and biochemical evaluation of the antibody epitope αGal(309–332) affords new possibilities for reversing the immunogenicity and restoring the therapeutic efficacy of αGal ERT of FD.

Experimental Section

α-Galactosidase characterization

Recombinant human α-galactosidase A was obtained from Shire Ltd (Lexington, MA), and Sino Biological Inc. (Beijing, China). The enzyme was produced in human cells and thus comprised an amino acid sequence identical to that of the wild-type human enzyme; in addition, the protein contained a C-terminal tag se-

quence of seven histidine residues, as well as the glycosylation profile of the native human enzyme.[2,3] The molecular mass of the enzyme was characterized by MALDI-TOF/TOF mass spectrometry, which showed a single molecular ion mass of *m/z* 45.305 Da (Supporting Information).

Anti-α-galactosidase antibody characterization

Monoclonal human anti-α-galactosidase A antibody was obtained from Sino Biological Inc. (Beijing, China; produced in rabbit). The molecular masses of the heavy and light chains and the N-terminal F_v sequence of the antibody were characterized by MALDI-TOF mass spectrometry, and by N-terminal Edman sequencing (Applied Biosystems Procise-494 protein sequencer), as described in Ref. [27].

Proteolytic digestion

A stock solution (100 μL) containing the galactosidase (100 μg), was mixed with NH_4HCO_3 solution (100 μL, 20 mM, pH 8.5, containing 1 $\mu g\,\mu L^{-1}$ DTT). Trypsin was added to yield an enzyme/substrate ratio of 1:20 and the mixture was incubated at 37 °C for 4 h. Additional trypsin was then added to increase the enzyme/substrate ratio to 1:10, and the mixture was further incubated for a total of 8 h. Aliquots (40 μL) of the peptide mixture, containing the equivalent of 20 μg enzyme, were frozen and stored at −20 °C until use.

Epitope identification

Epitope identification was performed by proteolytic excision/extraction MS, using proteolytic extraction affinity mass spectrometry and online SPR–MS.[15,19] The newly developed biosensor–MS system uses an SPR biosensor coupled through a microfluidic interface to an ESI mass spectrometer. Detection of the kinetic interaction between affinity pairs was obtained by SPR, whereas ESI-MS analysis provided identification of the interaction epitope. The anti-αGal antibody (≈10 μg) was immobilized on a microcolumn of an approximately 50-fold amount of activated Sepharose with incubation for 2 h at 37 °C. Then, a proteolytic peptide mixture resulting from tryptic digestion (8 h, 37 °C; as described above) was loaded onto the affinity microcolumn using the SPR autosampler/injector at a flow rate of 25 $\mu L\,min^{-1}$. After incubation for 30 min, the unbound supernatant peptides were washed away for 20 min using phosphate-buffered saline (PBS) buffer, and the remaining bound epitope peptides were eluted for 30 min with a 0.1% TFA solution, using the autosampler (flow rate, 25 $\mu L\,min^{-1}$). The eluted epitope fraction was on-line desalted for 4 min using a C_{18} microguard column, and analyzed by ESI-MS on an Esquire 3000+ ion trap MS (Bruker Daltonics, Bremen, Germany).

Affinity determination of α-galactosidase to the αGal antibody

Affinity analysis was performed with an Ametek-2CH-7500 SPR system (Ametek Reichert, Buffalo, NY, USA), consisting of an autosampler, an SPR pump and a SPR detector. Human monoclonal anti-α-galactosidase A antibody (35 $\mu g\,mL^{-1}$) was immobilized on a dextran SPR chip on which dextran carboxyl groups were activated with a mixture of *N*-(3-dimethylaminopropyl)-*N*-ethyl-carbodiimide (200 mM), and *N*-hydroxysuccinimide (50 mM), and followed by injection of the antibody (300 nM) in sodium acetate buffer (250 μL, 10 mM, pH 5.5). Remaining *N*-hydroxysuccinimide groups were then blocked with ethanolamine (1 M, pH 8.5). Determination of dissociation constants was performed after covalent immobilization of the antibody using the human α-galactosidase A solution (250 μL) at different concentrations (5–20 nM) and a flow rate of 25 $\mu L\,min^{-1}$. All affinity determinations were performed in PBS buffer (10 mM, pH 7.5) at 20 °C, followed by regeneration with glycine buffer (10 mM, pH 2.0). Final K_D values were determined by fitting to a one-to-one binding model.

Synthesis and characterization of peptide epitopes

The 24-amino-acid αGal peptide epitope (309–332), three 12-amino-acid overlapping peptide epitopes—αGal(309–320), αGal(315–326), and αGal(321–332)—and the three 8-amino-acid sequential peptides—αGal(309–316), αGal(317–324), and αGal(325–332)—were synthesized using microwave-assisted SPPS. Protected amino acids, Fmoc-Ala-OH, Fmoc-Arg(Pbf)-OH, Fmoc-Asp(*t*Bu)-OH, Fmoc-Asn(Trt)-OH, Fmoc-Glu(*t*Bu)-OH, Fmoc-Gln(Trt)-OH, Fmoc-Gly-OH, Fmoc-His(Trt)-OH, Fmoc-Ile-OH, Fmoc-Leu-OH, Fmoc-Lys(Boc)-OH, Fmoc-Met-OH, Fmoc-Phe-OH, Fmoc-Pro-OH, Fmoc-Ser(*t*Bu)-OH, Fmoc-Thr(*t*Bu)-OH, Fmoc-Trp(Boc)-OH, Fmoc-Tyr(*t*Bu)-OH, and Fmoc-Val-OH were obtained from Carbosynth Ltd. (Compton, UK). Fmoc-Arg(Pbf)-Wang, Fmoc-Asn(Trt)-Wang, Fmoc-Lys(Boc)-Wang, Fmoc-Val-Wang, and Fmoc-Leu-Wang resins were obtained from Matrix Innovation (Quebec City, Canada). Microwave-assisted syntheses were performed on a Liberty Blue Microwave Automated Peptide Synthesizer with additional Discover module (CEM Corporation, Matthews, NC), that combines microwave energy with SPPS using the Fmoc/*tert*-butyl strategy.

Fmoc deprotection was performed in two stages with an initial deprotection of 15 s at 155 W and 75 °C followed by 30 s at 30 W and 90 °C. The resin was then washed four times with DMF (4 mL each) before coupling of each amino acid. Coupling reactions of standard amino acids were performed at 5-fold excess in two stages at 90 °C: 1) 15 s at 170 W and 2) 110 s at 30 W. Arginine required a double coupling in two stages: 1) 1500 s at 25 °C without MWs and 2) 300 s at 30 W and 75 °C. Histidine coupling was performed in two stages: 1) 120 s at 25 °C without MWs and 2) 140 s, 35 W and 50 °C (Table S2, Supporting Information). After Fmoc deprotection of the last amino acid the resin was washed with CH_2Cl_2 (10 mL).

Peptide cleavage (3 h at 20 °C) from the resin and deprotection of the amino acid side chains were performed with a TFA/H_2O/TIS (95:2.5:2.5 *v/v/v*) solution. The resin was then washed with TFA and the filtrate partially evaporated. The crude product was precipitated with diethyl ether, collected by centrifugation, dissolved in water and lyophilized.

Lyophilized crude peptides were initially treated by solid-phase extraction with a RP-18 LiChroprep silica column from Merck (Darmstadt, Germany) using H_2O/CH_3CN as eluent, yielding a partially purified product. The final purification of the partially pure peptides was performed by semi-preparative RP-HPLC on a Sepax Bio-C_{18} (5 μm, 200 Å, 2500 mm × 10 mm) column at 25 °C using a Waters instrument (separation module 2695, detector diode array 2996) working at a flow rate of 4 $mL\,min^{-1}$. The solvent systems used were: A (0.1% TFA in H_2O, *v/v*) and B (0.1% TFA in 84% CH_3CN in A, *v/v*). Final purity of all peptides was ≥95%. Peptides were characterized by RP-HPLC ESI-MS (Table S3, Supporting Information). The analytical HPLC system was an Alliance Chromatograph (Waters) with a Phenomenex Jupiter C_{18} column (5 μm, 300 Å, 250 mm × 4.6 mm) working at a flow rate of 0.6 $mL\,min^{-1}$, with UV

detection at 215 nm, coupled to a single quadrupole ESI-MS (Waters 3100). The solvent systems used were: A (0.1% TFA in H_2O, *v/v*) and B (0.1% TFA in 84% CH_3CN in A, *v/v*).

Affinity determination of peptide epitopes

Affinity analyses of peptide epitopes were performed with the Ametek-2CH-7500 SPR biosensor (Ametek Reichert) on dextran SPR chips with immobilized human monoclonal anti-αGal antibody. The immobilization procedure was identical to that used for the affinity determination of intact αGal. Determination of dissociation constants was performed using an epitope peptide solution (250 μL) at different concentrations (5–200 nM) at a flow rate of 25 μL min^{-1}. All affinity determinations were performed in PBS buffer (pH 7.5) followed by regeneration with glycine buffer (10 mM, pH 2.0) at 20 °C.

Acknowledgements

We gratefully acknowledge the valuable help and advice of Dr. Elisa Peroni, Université de Cergy-Pontoise, and Stephan Rawer, Thermofisher AG Darmstadt, in the affinity characterization of peptide epitopes. This work was partially supported by the EU Marie Curie IRSES Research staff exchange programme "MS-Life". Moreover, this work was supported by the "Chaire d'Excellence" of the Agence Nationale de la Recherche (France) to A.M.P. (ANR-09-CEXC-013-01) and by the Fondazione Ente Cassa di Risparmio di Firenze (Italy) to PeptLab of the University of Florence.

Conflict of interest

The authors declare no conflict of interest.

Keywords: affinity mass spectrometry · α-galactosidase A · enzyme replacement therapy · epitope identification · Fabry disease

[1] B. W. Bigger, M. Saif, G. E. Linthorst, *Best Pract. Res. Clin. Endocrinol. Metab.* **2015**, *29*, 183–194.
[2] S. Ortolano, I. Viéitez, C. Navarro, C. Spuch, *Recent Pat. Endocr. Metab. Immune Drug Discovery* **2014**, *8*, 9–25.
[3] G. E. Linthorst, C. E. M. Hollak, W. E. Donker-Koopman, A. Strijland, J. F. M. Aerts, *Kidney Int.* **2004**, *66*, 1589–1595.
[4] R. J. Desnick, *Expert Opin. Biol. Ther.* **2004**, *4*, 1167–1176.
[5] S. N. Banugaria, S. N. Prater, Y. K. Ng, J. A. Kobori, R. S. Finkel, R. L. Ladda, Y. T. Chen, A. S. Rosenberg, P. S. Kishani, *Genet. Med.* **2011**, *13*, 729–736.
[6] S. G. Banugaria, T. T. Patel, J. Mackey, S. Das, A. Amalfitano, A. S. Rosenberg, J. Charrow, Y. T. Chen, P. S. Kishnani, *Mol. Genet. Metab.* **2012**, *105*, 677–680.
[7] V. Valayannopoulos, F. A. Wijburg, *Rheumatology* **2011**, *50*, v49–v59.
[8] J. B. Hennermann, S. Gökce, A. Solyom, E. Mengel, E. H. Schuchman, C. M. Simonaro, *J. Inherited Metab. Dis.* **2016**, *39*, 831–837.
[9] E. J. Langereis, N. van Vlies, H. J. Church, R. B. Geskus, C. E. Hollak, S. A. Jones, W. Kulik, H. van Lenthe, J. Mercer, L. Schreider, K. L. Tylee, T. Wagemans, F. A. Wijburg, B. W. Bigger, *Mol. Genet. Metab.* **2015**, *114*, 129–137.
[10] J. Muenzer, M. Cucsavas-Calikoglu, S. E. McCandless, T. J. Schuetz, A. Kimura, *Mol. Genet. Metab.* **2007**, *90*, 329–337.
[11] S. L. Gerstenbruch, C. L. Brooks, P. Kosma, L. Brade, C. R. Mackenzie, S. V. Evans, H. Brade, S. Müller-Loennies, *Glycobiology* **2010**, *20*, 461–472.
[12] B. E. Bolívar, J. E. Welch, *ChemBioChem* **2017**, *10*, 931–940.
[13] S. Dey, A. Nandy, S. C. Basak, P. Nandy, S. Das, *Comput. Biol. Chem.* **2017**, *68*, 143–152.
[14] D. Sánchez, P. Gregor, K. Čurila, I. Hoffmanová, V. Hábová, L. Tučková, H. Tlaskalová-Hogenová, *Autoimmunity* **2016**, *49*, 554–562.
[15] R. Stefanescu, R. E. Iacob, E. N. Damoc, A. Marquardt, E. Amstalden, M. Manea, I. Perdivara, M. Maftei, G. Paraschiv, M. Przybylski, *Eur. J. Mass Spectrom.* **2007**, *13*, 69–75.
[16] J. R. Engen, T. E. Wales, *Annu. Rev. Anal. Chem.* **2015**, *8*, 127–148.
[17] J. Chen, D. L. Rempel, B. C. Gau, M. Gross, *J. Am. Chem. Soc.* **2012**, *134*, 18724–18731.
[18] B. Gau, J. Chen, M. L. Gross, *Biochim. Biophys. Acta Proteins Proteomics* **2013**, *1834*, 1230–1238.
[19] M. Przybylski, L. Lupu, H. Rusche, Z. Kukacka, Y. Baschung, M. Murphy, S. Maeser, *Anal. Bioanal. Chem.* **2018**, in press.
[20] M.-I. Iurașcu, O. Marroquin Belaunzanar, C. Cozma, U. Petrausch, C. Renner, M. Przybylski, *J. Am. Soc. Mass Spectrom.* **2016**, *27*, 1105–1112.
[21] P. Juszczyk, G. Paraschiv, A. Szymanska, A. S. Kolodziejczyk, S. Rodziewicz-Motowidlo, Z. Grzonka, M. Przybylski, *J. Med. Chem.* **2009**, *52*, 2420–2428.
[22] B. A. Petre, M. Ulrich, M. Stumbaum, B. Bernevic, A. Moise, G. Döring, M. Przybylski, *J. Am. Soc. Mass Spectrom.* **2012**, *23*, 1831–1840.
[23] A. Moise, S. André, F. Eggers, M. Krzeminski, M. Przybylski, H. J. Gabius, *J. Am. Chem. Soc.* **2011**, *133*, 14844–14847.
[24] J. McLaurin, R. Cecal, M. E. Kierstead, X. Tian, A. L. Phinney, M. Manea, J. E. French, M. L. H. Lambermon, A. A. Darabie, M. E. Brown, C. Janus, M. A. Chishti, P. Horne, D. Westaway, P. E. Fraser, M. T. J. Mount, M. Przybylski, P. St. -George-Hyslop, *Nat. Med.* **2002**, *8*, 1263–1269.
[25] A. Moise, S. Maeser, S. Rawer, F. Eggers, M. Murphy, J. Bornheim, M. Przybylski, *J. Am. Soc. Mass Spectrom.* **2016**, *27*, 1071–1078.
[26] Y. Yu, T. Mena-Barragán, K. Higaki, J. L. Johnson, J. E. Drury, R. L. Lieberman, N. Nakasone, H. Ninomiya, T. Tsukimura, H. Sakuraba, Y. Suzuki, E. Nanba, C. O. Mellet, J. M. Garcia Fernández, K. Ohno, *ACS Chem. Biol.* **2014**, *9*, 1460–1469.
[27] M. Iurascu, PhD dissertation, **2015**, University of Konstanz (Germany).
[28] S. C. Garman, D. N. Garboczi, *J. Mol. Biol.* **2004**, *337*, 319–335.

Manuscript received: February 13, 2018
Accepted manuscript online: February 23, 2018
Version of record online: April 12, 2018

CHEMMEDCHEM
Chemistry & Drug Discovery

Supporting Information

Antibody Epitope of Human α-Galactosidase A Revealed by Affinity Mass Spectrometry: A Basis for Reversing Immunoreactivity in Enzyme Replacement Therapy of Fabry Disease

Zdenek Kukacka,[a, b] Marius Iurascu,[a, b] Loredana Lupu,[a, b] Hendrik Rusche,[a, b] Mary Murphy,[c] Lorenzo Altamore,[d, e, f] Fabio Borri,[d, e, f] Stefan Maeser,[a, b] Anna Maria Papini,[d, e, f] Julia Hennermann,[g] and Michael Przybylski*[a, b]

cmdc_201800094_sm_miscellaneous_information.pdf

Primary structure characterization of human αGalactosidase by MALDI-MS

The primary structure of the recombinant human alpha-Galactosidase was characterized by (i), MALDI-TOF analysis of the intact enzyme, and by (ii), MALDI-TOF and ESI-IonTrap analysis of tryptic digestion mixture. Identification by using MASCOT data base revealed the MALDI-MS analysis of the tryptic digested peptides provided almost the complete expected peptides except for a small repetitive sequences such as the RK sequence (391-393), with 95 % sequence coverage, however the ESI-MS analysis of the tryptic peptides reached up to 98% sequence coverage (Table S1). The tryptic peptides (302-308), (309-314), and (315-326), comprising the epitope sequence (309-332) and protected cleavage sites of the antibody binding, were found in the free enzyme and are included in Table S1. In the analysis of the tryptic peptide mixture, the 3 glycosylated peptide fragments comprising the N-glycosylation sites N-138, N-192, and N-408 were also detected, albeit with low abundances. The MALDI-MS and ESI-MS peptide mapping in solution was fully ascertained by in gel digestion of the full length protein band, however peptide recoveries upon in gel digestion were lower than upon digestion in solution.

Table S1: List of of α−Gal tryptic peptides identified by ESI-IonTrap MS

Peptide	Mass	Charge	Sequence
[1-17]	664.6925	3	.MQLRNPELHLGCALALR.f [1xCarbamidomethyl]
[1-17]	670.0241	3	.MQLRNPELHLGCALALR.f [1xCarbamidomethyl; 1xOxidation]
[5-30]	963.8567	3	r.NPELHLGCALALRFLALVSWDIPGAR.a [1xCarbamidomethyl]
[18-30]	482.2698	3	r.FLALVSWDIPGAR.a
[31-38]	277.1557	3	r.ALDNGLAR.t
[31-49]	742.0409	3	r.ALDNGLARTPTMGWLHWER.f
[39-49]	707.3402	2	r.TPTMGWLHWER.f
[39-49]	715.3377	2	r.TPTMGWLHWER.f [1xOxidation]
[50-67]	1045.8432	2	r.FMCNLDCQEEPDSCISEK.l [3xCarbamidomethyl]
[68-82]	900.9221	2	k.LFMEMAELMVSEGWK.d
[68-82]	908.9196	2	k.LFMEMAELMVSEGWK.d [1xOxidation]
[83-100]	754.9799	3	k.DAGYEYLCIDDCWMAPQR.d [2xCarbamidomethyl]
[83-105]	936.3880	3	k.DAGYEYLCIDDCWMAPQRDSEGR.l [2xCarbamidomethyl]
[101-112]	457.8919	3	r.DSEGRLQADPQR.f
[106-127]	859.1262	3	r.LQADPQRFPHGIRQLANYVHSK.g
[113-118]	363.7059	2	r.FPHGIR.q
[119-140]	796.8927	3	r.QLANYVHSKGLKLGIYADVGNK.t [1xHexNAc]
[131-140]	525.2849	2	k.LGIYADVGNK.t
[141-168]	1038.8112	3	k.TCAGFPGSFGYYDIDAQTFADWGVDLLK.f [1xCarbamidomethyl]
[169-185]	638.2768	3	k.FDGCYCDSLENLADGYK.h [2xCarbamidomethyl]
[169-185]	956.7915	2	k.FDGCYCDSLENLADGYK.h [2xCarbamidomethyl]
[186-193]	382.1975	3	k.HMSLALNR.t [1xHexNAc]
[197-213]	745.3532	3	r.SIVYSCEWPLYMWPFQK.p [1xCarbamidomethyl]
[214-220]	892.4523	1	k.PNYTEIR.q
[221-227]	532.2300	2	r.QYCNHWR.n [1xCarbamidomethyl]
[221-237]	752.3290	3	r.QYCNHWRNFADIDDSWK.s [1xCarbamidomethyl]
[228-237]	605.7724	2	r.NFADIDDSWK.s
[241-252]	499.2440	3	k.SILDWTSFNQER.i
[253-301]	1072.7298	5	r.IVDVAGPGGWNDPDMLVIGNFGLSWNQQVTQMALWAIMAAPLFMSNDLR.h
[302-308]	780.4363	1	r.HISPQAK.a
[309-314]	687.4036	1	k.ALLQDK.d
[309-332]	674.8658	4	k.ALLQDKDVIAINQDPLGKQGYQLR.q
[315-326]	641.8537	2	k.DVIAINQDPLGK.q
[333-356]	920.4623	3	r.QGDNFEVWERPLSGLAWAVAMINR.q
[357-363]	252.8048	3	r.QEIGGPR.s
[364-374]	1109.6201	1	r.SYTIAVASLGK.g
[375-391]	591.9188	3	k.GVACNPACFITQLLPVK.r [2xCarbamidomethyl]
[394-402]	579.7826	2	k.LGFYEWTSR.l
[394-402]	1158.5578	1	k.LGFYEWTSR.l
[405-429]	1000.5191	3	r.SHINPTGTVLLQLENTMQMSLKDLL.d [1xHexNAc]

Synthesis and characterization of peptide epitopes

All epitope peptides (24aa αGal peptide epitope (309-332), the three 12aa overlapping peptide epitopes αGal(309-320), αGal(315-326), αGal(321-332), αGal(309-316), αGal(317-324) and αGal(325-332)) were synthesized using microwave-assisted solid-phase synthesis. The characterization of the microwave cycles was done with two deprotection steps: the first for 15 s, 155W and 75°C; the second one for 30 s, 30W and 90°C. Different cycles based on the amino acid were used for coupling reactions. Deprotection steps were performed with 4 ml 20% piperidine in DMF, and washed 4 times with DMF (4 ml each). After each coupling step the resin was washed with DMF (4 mL) and following the last reaction the resin was washed with CH_2Cl_2 (10 mL). Peptide cleavage (3 hrs at 20 0C) from the resin and deprotection of the amino-acid side chains were carried out with TFA/H_2O/TIS solution (95:2.5:2.5 v/v/v).

Two purification steps were performed using the SPE strategy with a C18 silica column as stationary phase and an eluent composed by H_2O/CH_3CN with different gradients, depending on the length and hydrophobicity of the peptides, using solvents A (0.1% TFA in H_2O) and B (0.1% TFA in CH_3CN), as mobile phase. The final products were characterized by analytical RP-HPLC on a C18 column at 1 mL/min. The purity of the peptide products was checked by ESI-MS and found to exceed 95%.

Table S2. Microwave cycles used during automatic Microwave- SPPS.

Step	Temp (°C)	MW Power (w)	Time (sec)
1st deprotection	75	155	15
2nd deprotection	90	30	30
Standard coupling	90	170	15
	90	30	110
Double Arg coupling	25	0	1500
	75	30	300
50°C His coupling	25	0	120
	50	35	140

Table S 3. Purification and mass spectrometric characterization of synthetic peptide epitopes.

Number	Peptide	HPLC gradient	Retention time (min)	Monoisotopic mass (m/z) ESI-MS	Amount purified (mg)	Isolated Yield (%)	Purity (%)
I	αGal(309-332)	20%-40% B in 7 min	4.51	675.4 $[M+4H]^{4+}$=674.9	43.05	16%	>95%
II	αGal(309-320)	20%-100% B in 7 min	2.65	656.9 $[M+2H]^{2+}$=656.8	78.16	59	>95%
III	αGal(315-326)	20%-100% B in 7 min	2.47	642.2 $[M+2H]^{2+}$=641.8	36.74	29	>95%
IV	αGal(321-332)	20%-100% B in 7 min	1.30	702.1 $[M+2H]^{2+}$=701.8	60.60	44	>95%
V	αGal(309-316)	20%-100% B in 7 min	1.32	451.5 $[M+2H]^{2+}$=451.2	33.52	37	>95%
VI	αGal(317-324)	20%-100% B in 7 min	2.40	883.5 $[M+1H]^{+}$=883.4	22.37	25	>95%
VII	αGal(325-332)	20%-100% B in 7 min	0.63	475.5 $[M+2H]^{2+}$=475.2	44.05	47	>95%

ChemPubSoc Europe

DOI: 10.1002/cmdc.201900489

CHEMMEDCHEM Full Papers

Molecular Epitope Determination of Aptamer Complexes of the Multidomain Protein C-Met by Proteolytic Affinity-Mass Spectrometry

Loredana Lupu,[a] Pascal Wiegand,[a] Nico Hüttmann,[a, b] Stephan Rawer,[a] Wolfgang Kleinekofort,[a, c] Irina Shugureva,[e, f] Anna S. Kichkailo,[f] Felix N. Tomilin,[d, e] Alexander Lazarev,[g] Maxim V. Berezovski,[b] and Michael Przybylski*[a]

C-Met protein is a glycosylated receptor tyrosine kinase of the hepatocyte growth factor (HGF), composed of an α and a β chain. Upon ligand binding, C-Met transmits intracellular signals by a unique multi-substrate docking site. C-Met can be aberrantly activated leading to tumorigenesis and other diseases, and has been recognized as a biomarker in cancer diagnosis. C-Met aptamers have been recently considered a useful tool for detection of cancer biomarkers. Herein we report a molecular interaction study of human C-Met expressed in kidney cells with two DNA aptamers of 60 and 64 bases (CLN0003 and CLN0004), obtained using the SELEX (**S**ystematic **E**volution of **L**igands by **Ex**ponential Enrichment) procedure. Epitope peptides of aptamer-C-Met complexes were identified by proteolytic affinity-mass spectrometry in combination with SPR biosensor analysis (PROTEX-SPR-MS), using high-pressure proteolysis for efficient digestion. High affinities (K_D, 80–510 nM) were determined for aptamer-C-Met complexes, with two-step binding suggested by kinetic analysis. A linear epitope, C-Met (381–393) was identified for CLN0004, while the CLN0003 aptamer revealed an assembled epitope comprised of two peptide sequences, C-Met (524–543) and C-Met (557–568). Structure modeling of C-Met-aptamers were consistent with the identified epitopes. Specificities and affinities were ascertained by SPR analysis of the synthetic epitope peptides. The high affinities of aptamers to C-Met, and the specific epitopes revealed render them of high interest for cellular diagnostic studies.

Introduction

Structure-function studies of membrane receptor proteins play a key role in approaches to understand the physiological basis for the development of targeted drugs for different diseases, but their molecular mechanisms of interaction are poorly understood. As an example, the characterization of molecular interaction sites of the C-Met protein has received high interest in the study of receptors as possible targets for cancer treatment. C-Met and its corresponding ligand, the hepatocyte growth factor protein (HGF) have been intensively studied as targets for anticancer drugs, and their abnormal activities have been implicated in tumorigenesis.[1–4] C-Met is a glycosylated tyrosine kinase receptor of HGF[5] that consists of a disulfide-linked α/β heterodimer formed by proteolytic processing of a precursor protein in the post-Golgi compartment.[6] The structure of C-Met is comprising two domains, an extracellular α-region (Figure 1) and a transmembrane β-region linked by disulfide bridges. The α-region has three major domains: A Semaphorin (Sema) domain; a plexin-Semaphorin-integrin (PSI) domain; and four immunoglobulin-plexin transcription (IPT) domains.[7] The N-terminal Sema domain encompasses approximately 500 residues and shares sequence homology with domains of the semaphorin and plexin families. The PSI domain of ca. 50 residues is connected to a transmembrane helix via four IPT domains. The extracellular region is responsible for binding to HGF and is composed of the Sema domain, a cysteine-rich Met-related sequence (MRS), and four immunoglo-

[a] L. Lupu, P. Wiegand, N. Hüttmann, S. Rawer, Prof. Dr. W. Kleinekofort, Prof. Dr. M. Przybylski
Steinbeis Centre for Biopolymer Analysis and Biomedical Mass Spectrometry
Marktstraße 29
65428 Rüsselsheim am Main (Germany)
E-mail: michael.przybylski@stw.de
[b] N. Hüttmann, Prof. Dr. M. V. Berezovski
Department of Chemistry and Biomolecular Sciences
University of Ottawa
Ottawa, ON, K1N 6N5 (Canada)
[c] Prof. Dr. W. Kleinekofort
Dept. of Engineering Sciences
Rhein Main University
65428 Rüsselsheim am Main (Germany)
[d] F. N. Tomilin
Kirensky Institute of Physics
Russian Academy of Sciences Siberian Branch
Krasnoyarsk 660036 (Russia)
[e] I. Shugureva, F. N. Tomilin
Siberian Federal University
Krasnoyarsk 66041 (Russia)
[f] I. Shugureva, Dr. A. S. Kichkailo
Federal Research Center "Krasnoyarsk Science Center of the Siberian Branch of the Russian Academy of Science"
Laboratory for Digital Controlled Drugs and Theranostics
Krasnoyarsk 660036 (Russia)
[g] Dr. A. Lazarev
Pressure Biosciences Inc.
14 Norfolk Ave.
South Easton, MA 02375 (USA)

Supporting information for this article is available on the WWW under https://doi.org/10.1002/cmdc.201900489

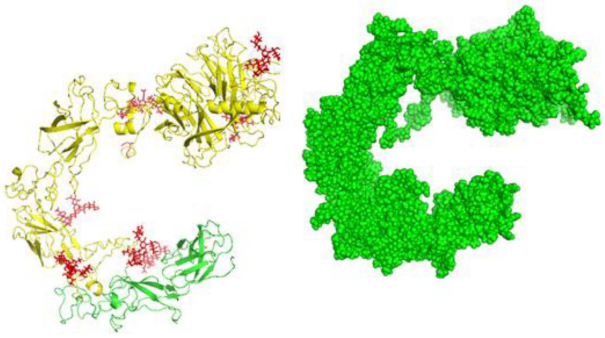

Figure 1. Structure model of the recombinant human C-Met/Fc Chimera protein according to I-TASSER.[36] Highlighted in yellow is the extracellular domain of human c-Met precursor[1–932] and in green the C-terminal polyhistidine-tagged Fc region of human IgG 1 used.

bulin-like structures (IgG domains).[8] The β-region contains a juxtamembrane segment, carboxy-terminal sequences and a tyrosine kinase domain.[3,4,8]

Upon ligand binding and autophosphorylation by a specific multi-substrate docking site, C-Met transmits intercellular signals that are essential for tissue repair, embryonic development, and liver regeneration.[3,4] Conversely, aberrant activation of C-Met can lead to tumorigenesis, schizophrenia and cardiomyocytes.[3] The interaction between C-Met and HGF triggers phosphorylation of two tyrosine residues within the catalytic loop (Tyr-1234; Tyr-1235).[1] Aberrant overexpression of C-Met by interaction with its ligand HGF causes tumor progression.[4,5] Recent studies suggest that within tumor cells, aberrant activation of C-Met by HGF occurs by an autocrine loop. Interaction studies of the signaling pathway of C-Met to HGF are currently ongoing,[1,6] but no molecular mechanism has been hitherto identified.

Several antibodies have been evaluated in the development of inhibitors of the C-Met signaling pathway.[8–10] C-Met inhibiting antibodies have been tested in first clinical trials; some were found to delay tumor progression[9] and have been recently approved by the U.S. Food and Drug Administration for treatment of several types of tumors. First studies to elucidate binding sites of C-Met with inhibiting monoclonal antibodies have been reported.[11] Cao et al.[10] showed simultaneous inhibition of C-Met with 3 monoclonal antibodies; however, despite the established antibody-based inhibition of C-Met, the detailed mechanism of affinity interaction and interaction sites of antibodies with corresponding target proteins have not yet been elucidated.

The discovery of aptamers that specifically bind to rat CD4 receptor but not to human CD4 proteins[12,13] initiated high interest in exploring aptamers as therapeutic agents. Aptamers are single stranded DNA or RNA oligonucleotides[14–16] that exert pronounced selectivity as inhibitors of signaling pathways. In contrast to antibodies, aptamers are obtained by *in vitro* selection and optimization procedures (SELEX: "**S**ystematic **E**volution of **L**igands by **EX**ponential Enrichment");[15,16] they are chemically synthesized and show a number of unique features in the development of bioassays, drug development, and targeted therapy.[15] As "chemical antibodies", aptamers are non-immunogenic and do not interfere with cell viabilities, since they specifically bind and release cells,[13] suggesting high potential for the evaluation of biomarkers. Thus, aptamers may reveal a number of advantages compared to antibodies, such as fast and easy production, high stabilities and high binding strength.[17–19]

In the present study we have pursued a new approach to elucidate the inhibiting mechanism(s) of C-Met by identifying the molecular binding sites between C-Met protein and aptamers, with the rationale to explore their binding properties and possible similarities with antibodies. Here, we report the identification of the interaction epitopes of C-Met with two DNA aptamers (CLN0003 and CLN0004) that bind to C-Met with high affinity and specificity (Figure 1; s. Table 1). Corresponding aptamers (CLN0003 and CLN0004 and analogous oligonucleotide sequences) have shown high affinity binding to C-Met and have recently gained high interest in their development for cancer therapy.[20–24] For the identification of aptamer epitopes of C-Met and determination of binding affinities, selective proteolytic extraction of C-Met-aptamer complexes in combination with electrospray (ESI) and MALDI mass spectrometry, and SPR (surface plasmon resonance) biosensor analysis were used as principal tools (PROTEX-SPR-MS)[25,26] (Supplementary Figure S1). The PROTEX-SPR-MS method has been successfully applied in a number of recent studies for epitope identifications of protein-antibody complexes, protein-peptide interactions, and carbohydrate-protein complexes.[26–32] SPR determinations of the C-Met-aptamer complexes revealed high affinities, consistent with the suitability of aptamers as specific inhibitors of C-Met. PROTEX-MS using immobilized aptamer affinity-matrices revealed specific epitopes on C-Met, with a linear epitope peptide identified for the CLN0004 aptamer, and a discontinuous epitope comprising two specific peptides for the CLN0003 aptamer. Structure modeling of the two aptamers was found to be consistent with the identified epitopes. Binding curves obtained in affinity studies suggested a conformational change following a first binding event of the aptamers, resulting in a discrete second high affinity binding step. These results show that aptamers bind to C-Met with high affinities exerting specific epitopes that may be promising biomarker candidates for cellular diagnostics.

Table 1. Sequences of the DNA aptamers CLN0003 and CLN0004.

DNA Aptamer	Sequence
CLN0003	5′-/5AmMC12/GGA GGG AAA AGT TAT CAG GCT GGA TGG TAG CTC GGT CGG GGT GGG TGG GTT GGC AAG TCT-3′
CLN0004	5′-/5AmMC12/GAG TGC CTA ATG GTA CGA TTT GGG AAG TGG CTT GGG GTG GGA TTA GTT GAG TAC TCG CTC-3′

Results and Discussion

Affinity analysis of C-Met-aptamer complexes reveals discrete interaction steps

Affinity determinations of the aptamer complexes with the C-Met protein were carried out by SPR analysis on self-assembled monolayer (SAM) gold chips, by immobilization of both the aptamers and recombinant C-Met protein (s. Experimental Section) on the chip surface using standard SAM technology (Figures S2A, B). Binding constants K_D were determined using dilution series of aptamers and the protein, respectively. The reference channel of the dual-channel detector was used to subtract unspecific interactions in the data analysis. SPR analyses of the C-Met interaction with both aptamers were performed by immobilization of aptamers and binding of a dilution series of the protein, as illustrated in Figure 2 by the interaction of CLN0004 with C-Met. Affinity determinations using the kinetic method revealed a K_D of 0.223 μM for the CLN0003 aptamer and a K_D of 0.535 μM for the CLN00004 aptamer (Table 2).

A second series of SPR determinations was performed by immobilization of the C-Met protein and provided additional information compared to the aptamer immobilization. When C-Met was immobilized on the chip surface and the analysis carried out with a dilution series of the aptamers, two discrete interaction steps were observed, suggesting different possible binding sites. Due to the imperfect shape of the curve after subtraction of the reference channel, the analyses were performed using the affinity/EC50 method, providing a K_D of 56.34 nM for the CLN0003 interaction, and 92.71 nM for CLN0004 (Figures S3 and S4). The interaction of CLN0003 with C-Met was analyzed with three different approaches: (i), determination of K_D using a one to one kinetic model of interaction sites; (ii), analysis of the sensorgram using the same kinetic measurement with a one to two interaction model; and (iii), affinity analysis and separate determination of K_D for the second binding step. The second binding event was observed after approximately one minute and the reference channel subtracted here as well. The same procedure was used for the CLN0004 aptamer and provided similar results. These results (summarized in Table S1) suggested that upon a first interaction step of the aptamer, the aptamer-protein complex undergoes a conformational modification that allows a second interaction step to occur. According to this analysis, the CLN0003 aptamer undergoes a first interaction event for about one minute, followed by a second stronger interaction. These determinations provided K_Ds of 2.0 μM (K_D1) and 0.04 μM (K_D2) for CLN0003, and 0.1 μM (K_D1) and 0.05 μM (K_D2) for the CLN0004 aptamer (Table S1).

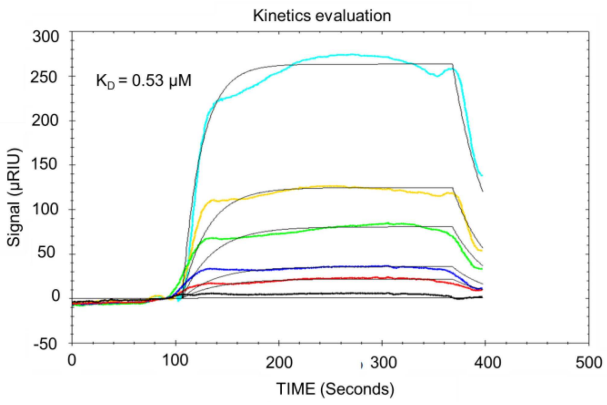

Figure 2. SPR Sensorgram for the CLN0004 – C-Met interaction complex, at a one-to-one evaluation of the complex with the aptamer immobilized and the C-Met ligand. The K_D determination yielded 0.535 μM.

Table 2. K_D determinations of CLN0003 and CLN0004 complexes with C-Met protein.

DNA Aptamer immobilized on SAM coated chip	Calculated K_D (M) from C-Met dilution series
CLN0003	2.23e-7
CLN0004	5.35e-7

Specific epitope peptides identified for C-Met-aptamer complexes

In order to obtain molecular epitope identifications, proteolytic epitope extraction mass spectrometry (PROTEX-MS) was performed as illustrated in Figure S1.[31,32] Prior to digestion, the protein was subjected to reduction of disulfide bonds and subsequent alkylation with iodoacetamide as described in the Experimental Section, followed by digestion with trypsin, and proteolytic fragment mixtures were characterized by mass spectrometric peptide mapping.

MALDI-MS analyses of C-Met with trypsin at conventional conditions (18 h; 37 °C) and at high pressure (approx. 30 kpsi; 50 min) are compared in Figure 3. In both cases digestion yields >90% were obtained providing nearly complete sequence coverage. However, high pressure digestion was found to provide substantially faster degradation, associated with a cleaner fragmentation pattern (lower background). Moreover, improved reproducibility was found regarding the detection of low abundance fragments.

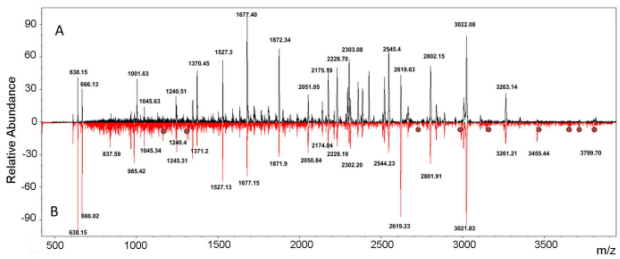

Figure 3. MALDI-MS analysis of trypsin digestion mixture of C-Met protein at standard conditions (18 h, 37 °C) (A), and high pressure using the Barocycler 2320EXT (Pressure Biosciences; 50 min, 25 °C) (B). Additional tryptic fragments identified at high pressure digestion are marked with red dots.

Epitope determinations were performed with aptamers immobilized on Sepharose microaffinity beads, using two complementary approaches as previously described[30,32] (Figure S1): (a), Proteolytic epitope extraction following aptamer immobilization on a Sepharose microaffinity column; (b), Epitope extraction and MALDI-MS following immobilization of aptamers on the SPR chip and subsequent elution. Following removal of supernatant peptides by washing with aqueous solvent, no background peptide was observed in the last washing fraction, and elution was subsequently performed with slightly acidified solvent (0.1 % TFA).

MALDI-MS analyses of the elution fractions from tryptic epitope extraction of C-Met from the CLN0004 aptamer affinity column, and elution from the aptamer-SPR chip are shown in Figures 4A, and B. Both approaches yielded identical results with most abundant singly charged epitope peptide ions, r.NSSGC(carbamidomethyl)EAR.r at m/z 881.45 (C-Met(381–388)), protonated MH^+ and Na^+ and K^+ molecular adduct ions. In the elution fraction from the affinity microcolumn, an additional smaller peptide was found at m/z 800.4 and identified as RDEYR (389–393). The identical epitope peptide sequence (381–388) was found upon elution from the SPR chip. These results provided evidence of a single linear epitope peptide, NSSGCEARRDEYR (381–393), for the CLN0004 aptamer. Additional confirmation of the epitope was obtained by CID (collision-induced-dissociation)-tandem-MALDI-MS (data not shown). Notably, the R389 residue was found uncleaved by trypsin, indicating shielding of the epitope in the aptamer interaction (s. Table 3).

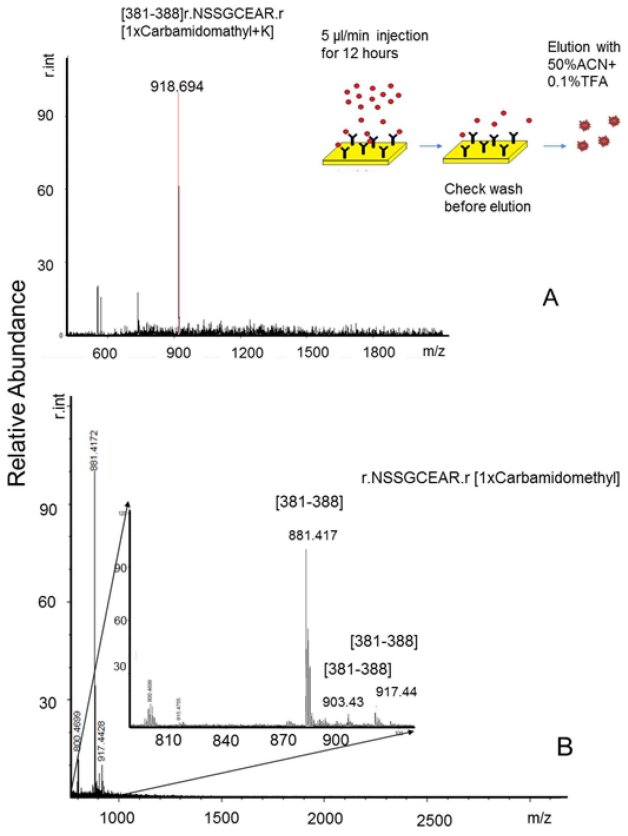

Figure 4. A) Tryptic epitope extraction-MS from immobilized CLN0004 aptamer on SAM coated SPR chip. B) Epitope extraction-MS from immobilized CLN0004 aptamer on CNBr-activated Sepharose affinity matrix.

In contrast to the CLN0004 aptamer, the epitope analysis of the C-Met complex with the CLN0003 aptamer provided two epitope peptides within adjacent structure domains, C-Met (524–543) and C-Met (568–576), (SEECLSGTWTQQICLPAIYK) and (NNKFDLKK), respectively (Table 3 and Figure S5). In this discontinuous (conformational) epitope, the residues K570 and K574 of the peptide C-Met(568–576) were found uncleaved and thus shielded from proteolytic digestion. This structural information of the binding site of the CLN0003 aptamer is of considerable interest since previous studies indicated that CLN0003 is interfering with the interaction of the growth factor HGF with C-Met,[37] suggesting the possible application of this aptamer as an inhibitor. The epitope identification was further ascertained by partial tryptic digestion in a proteolytic epitope excision experiment of the intact C-Met/aptamer complex and molecular weight filtration. The C-Met-aptamer complex was incubated with trypsin for 4 hours; the digestion solution was then passed through a 10 kDa molecular weight cutoff filter, subjected to centrifugation and washed with an excess volume of ammonium bicarbonate. MALDI-MS analysis of the epitope fraction eluted from the aptamer complex provided a major polypeptide at m/z 6139.9, C-Met (489–543), comprising the epitope peptide (524–543) (Figure S6). In the epitope peptide sequence, the residues R523 and K520 were found shielded from tryptic digestion.

Synthetic C-Met epitope peptides reveal high affinities

The tryptic epitope peptides of the aptamers CLN0003 and CLN0004 binding to the C-Met protein (NSSGCEAR; NNKFDLKK; SEECLSGTWTQQICLPAIYK) were synthesized by SPPS on a preloaded PS-PHB resin. Primary structures and homogeneities of the peptides were confirmed by mass spectrometry, and indicated >90 % purities (s. Figure S7). Affinities and binding constants of the aptamer-peptide complexes were determined on SAM-SPR chips by immobilization of aptamers, and K_D values of 30–100 µM were obtained in first affinity experiments. Affinities of the epitope peptides were found considerably lower compared to intact C-Met; however, the specificities of the epitopes were confirmed by affinity-MS experiments with proteolytic peptide mixtures of C-Met, which showed only epitope peptides in the affinity-eluate fractions.

Table 3. Epitope peptides identified for aptamer CLN0003 and CLN0004 interactions with the C-Met protein. K and R residues in the epitope peptides shielded from digestion are marked in bold.

Aptamer	C-Met epitope peptide	Sequence
CLN0003	SEECLSGTWTQQICLPAIYK	(524–543)
CLN0003	NN**K**FDL**K**K	(567–575)
CLN0004	NSSGCEAR**R**DEYR	(381–393)

Conclusions

In this study we present the molecular identification and affinity determination of specific epitope peptides of the C-Met protein binding to two high affinity aptamers, using proteolytic epitope extraction mass spectrometry, in combination with SPR biosensor analysis (PROTEX-SPRMS). The identified epitopes were found to be localized at distinct binding sites within the C-Met structure. Size and location of the epitopes and structure modeling of the C-Met complexes with the aptamer epitopes suggest that the structural requirements of epitope binding to aptamers are generally comparable to binding sites within the variable paratope regions of antibodies. Affinities of the aptamers determined by SPR were similar to those previously reported for C-Met aptamers with comparable sequences using dot blot/radioactive labeling and phosphorimaging, despite the different methodologies used.[22,23] Molecular structure modeling of the CLN0003 and CLN0004 aptamers, was performed by the Avogadro software package, using the Mfold web server for prediction of nucleic acid folding and hybridization,[38,39] and molecular docking studies of the aptamer-C-Met complexes performed using the AutoDock 4.0 software package as described in the Experimental Section (Figure 5; Figures S8, S9). The affinity determinations of the aptamers with C-Met suggest two distinct binding events, both by the observed SPR analyses and the corresponding data processing. For the CLN0003 aptamer a first interaction was found to be about 100 times weaker than the second, while for the CLN0004 aptamer the second interaction was found approximately 10 times stronger than the first interaction, consistent with a single linear epitope sequence of this aptamer.

The molecular identification of specific aptamer epitopes to C-Met, determined here for the first time by mass spectrometry, should be of considerable interest for future drug development studies with aptamers. Although C-Met antibodies have been admitted to first clinical trials, recent studies indicate considerable difficulties in the development of inhibiting antibodies with high stability and specificity.[21,22] Except for the monoclonal antibody Onortuzumab that inhibits binding to HBF, no antibody has been described inhibiting the C-Met interaction with HGF. Major problems for the development of antibodies may be encountered by difficulties in antibody delivery, and by the possible formation of immunogenic anti-drug antibodies.[22,23] These problems could be efficiently tackled with aptamers. In addition to their high stability and binding reproducibility, aptamers are shown here to bind with high affinity and specificity. Moreover, aptamers generally should have low immunogenicity.[35] Thus, the structure-based binding specificity and affinity of aptamers should render their molecular development and characterization an attractive alternative to antibodies.

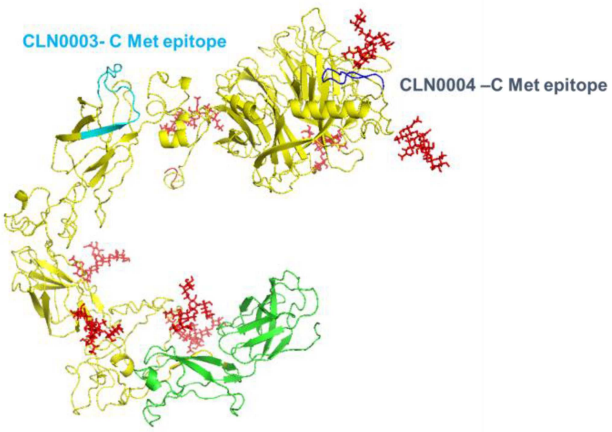

Figure 5. Structure modeling for C-Met complexes with CLN0003 (light blue) and CLN0004 aptamer epitope peptides (dark blue) at the epitope binding sites in the structures selected with the lowest docking energy the aptamer epitope ligands are shown with green balls, and the C-Met with blue balls.

Experimental Section

DNA aptamers

The C-Met specific DNA aptamer sequences CLN0003 and CLN0004 were produced by IDT Integrated DNA Technologies (Coralville, Iowa, USA) based on the published aptamers.[22] The aptamers were produced using the filter SELEX procedure with a recombinant C-Met protein, and were tested on C-Met-positive cell lines GTL-16, MKN-45, and EBC-1. The C-Met aptamers CLN0003 and CLN0004 consisting of 60 and 64 bases were synthesized with an amino group (5AmMC12) on the 5′end, respectively (s. Table 1). Affinities determined by SPR were similar to those previously reported for C-Met aptamers with comparable sequences.[23]

Preparation and characterization of C-Met

Human recombinant C-Met protein with C-terminal His and Fc Tags was obtained from Sino Biologicals (Wayne, PA; USA; Cat-No. 10692-H03H). A DNA sequence encoding the extracellular domain (Met1–Thr932) of human C-Met (NCBI Reference Sequence: NP_000236) was fused with the C-terminal polyhistidine-tagged Fc region of human IgG1 at the C-terminus. Molecular weight and sequence homogeneity of the C-Met was confirmed by MALDI-MS.

Proteolytic digestion

A stock solution of 1 mg/mL C-Met protein in MilliQ water was prepared for proteolytic digestion. Prior to digestion the C-Met protein was reduced and alkylated. For reduction of disulfide bonds four aliquots (10 μg each) of C-Met were diluted in 15 μL ammonium hydrogen carbonate (100 mM, pH 7.6) and incubated for 15 min at 25 °C with 5 μL 6 M guanidine-HCl and 1.5 μL reduction solution (10 mM DTT). Subsequent alkylation was performed by adding 5 μL of ammonium hydrogen carbonate buffer to a 10 μg aliquot of the reduced C-Met solution, and incubation of the protein with 15 μL 100 mM iodoacetamide for 1 h at subdued light.

Tryptic digestion was performed with an enzyme:substrate ratio of 1:100 (enzyme to protein). Trypsin (Serva, Heidelberg, Germany) was added to two of the aliquots and the sample incubated for 18 h at 37 °C. After digestion was complete as checked by MALDI-MS, the enzymatic activity was quenched with 0.1% trifluoroacetic acid (TFA). High pressure proteolytic digestion was performed with a Barocycler 2320EXT instrument (Pressure BioSciences; Boston/USA). The protein was dissolved in MilliQ water and aliquoted in 4

Eppendorf vials (50 μL each) at a concentration of 1 mg/mL. A aliquot of 10 μg was reduced and alkylated as described above, and 0.5 μg of Trypsin was added. The sample solution was then diluted with 30 μL 10 mM ammonium hydrogen carbonate buffer, pH 7.6. High pressure digestion was performed at 35 kpsi for 10 min (on), 1 min (off) for 5 cycles at 20 °C. A total digestion time of 50 min was used, and analysis of digest mixtures performed by MALDI-MS. MALDI-MS Analyses were performed with a Bruker Autoflex III Smartbeam-MS (Bruker Daltonics, Bremen, Germany).[31,32] All digestion mixtures were further characterized by gel electrophoresis; proteolytic peptide mixtures provided digestion yields > 95 % and were used for epitope analyses.[32]

Preparation of affinity microcolumns

Affinity microcolumns with NHS/EDC-activated Sepharose beads were prepared with 20 mg of Sepharose incubated with 0.1 M HCl for 15 min and washed with coupling buffer (0.2 M sodium hydrogen carbonate + 0.5 M NaCl, pH 8). An aliquot of 75 μg of aptamer with a 5′ amino group was added to each column and incubated with shaking for 3 hours.

The affinity column was then blocked with 0.2 M ethanolamine + 0.5 M NaCl, pH 8.3, washed three times with washing buffer (0.2 M NaOAc + 0.5 M NaCl, pH 4), and then resuspended in ammonium hydrogen carbonate buffer, pH 7.5. Affinity columns were stored at 4 °C until use.

Epitope identification

Epitope analysis was carried out by epitope-extraction mass spectrometry, as previously described.[29,30] Briefly, 10 μg of the tryptic digestion mixture was incubated with the CLN0003 aptamer affinity column. An aliquot digest mixture of 10 μg was incubated in the same manner with the CLN0004 aptamer. Identical procedures of epitope identification were used for both aptamer affinity columns. After incubating the proteolytic mixtures for 2 h, the column was washed with 5 mL ammonium bicarbonate buffer, pH 7.5, until no background signal was observed by MALDI-MS. The epitope fraction was then eluted with 100 μL 0.01 % TFA, pH 2.5, and the eluate analyzed by MALDI MS. Following MS analysis the column was resuspended in ammonium bicarbonate buffer.

Synthesis of epitope peptides

Fmoc protected amino acid derivatives were obtained from Novabiochem (Heidelberg, Germany). N,N′-dimethylformamide (DMF), N-methyl-2-pyrrolidone (NMP), dichloromethane (DCM), (2-(1H-Benzotriazol-1-yl)-1,1,3,3-tetramethyluronium-hexafluoro-phosphate (HBTU), diisopropyl-ethylamine (DIPEA) and trifluoracetic acid (TFA) were purchased from Applied Biosystems (Darmstadt (Germany); piperidine was obtained from Acros Organic and triisopropylsilane (TIS) from Alfa Caesar (Bonn, Germany). Fmoc Solid phase peptide synthesis (Fmoc-SPPS) was carried out with an automated peptide synthesizer ABI-433A from Applied Biosystems (Darmstadt, Germany). Epitope peptides (H-NSSGCEAR, H-LTICGWDFGFRR, and H-SEECLSGTWTQQICLPAIYK) were synthesized on preloaded PS-PHB resins from RAPP-Polymer (Herrenberg, Germany) with the corresponding amino acids of the C-terminus (PS-PHB-Arg(PMC)-Fmoc, capacity 0.59 mmol/g and PS-PHB-Lys (Boc)-Fmoc, capacity 0.55 mmol/g). A standard synthesis for 0.1 mmol of each peptide was performed with the Fmoc protected amino acids. Side chain protection and removal of peptides from the resin were carried out by incubating the resin for 1 h in 5 mL of 94 % TFA, 3 % TIS and 3 % MilliQ water. The peptide was then precipitated into 20 mL diethyl ether, centrifuged and the diethyl ether decanted. Purification of the crude peptides was performed by HPLC (2795 alliance HT instrument, Waters) and a C18 column (250 × 4.6 mm, Varian SN 0976069). Characterization of peptides for molecular homogeneity was carried out by ESI-MS (Waters Quattro-Ultima III; Manchester, UK).

Molecular weight cutoff filtration after epitope excision

For epitope identification in solution, 10 kDa molecular weight cutoff filters were used (Amicon; Merck Science Research, Darmstadt, Germany). The proteolytic peptide mixture resulting from trypsin digestion of intact C-Met-aptamer was added to the Amicon filter, and 300 ul ammonium hydrogen carbonate buffer (pH 8) added to remove unbound peptides. The filter was then centrifuged for 20 min at 10,000 rpm with a Heraeus Biofuge 13 (Marshall Scientific Inc., Hampton, New Hampshire, USA). The washing step was repeated 4 times to ensure that the isolated sample consisted only of the aptamer associated with the epitope. The epitope peptide was then dissociated from the aptamer by acidification by the MALDI matrix (2 mg/mL of 2.5 dihydrobenzoic acid in 50 % ACN with 0.1 % TFA), and analyzed by MALDI-MS.

Affinity determinations of C-Met-aptamer interactions

SPR Determinations were performed with an Ametek-Reichert 2Ch7500 SPR instrument (Ametek, Buffalo, N.Y., USA), using glass slides of 0.9 mm (1 × 1 cm gold chips with a 40 nm gold layer, prepared at the Institute for Microtechnologies, Rhein-Main University, Rüsselsheim am Main, Germany). Immobilization of C-Met on the SPR chips was carried out with a solution of 200 μg/mL protein in PBS. Preparation of activated SAM chips was performed with a mixture of 200 mM *N*-(3-dimethylaminopropyl)-*N*-ethylcarbodiimide (EDC) and 50 mM *N*-hydroxysuccinimide (NHS), followed by injection of 50 μg protein in 250 μL 10 mM sodium acetate buffer, pH 5.5. Remaining free NHS reagent was then blocked with 1 M ethanolamine, pH 8.5.

Affinity determinations were carried out after immobilization of the protein as described above. A repetitive sequence of seven injections of 250 μL of aptamer solution was performed at different concentrations (80 nM–1.04 μM for CLN0003; 78 nM–10 μM for CLN0004 aptamer), at a flow rate of 25 μL/min. All SPR determinations were performed in 10 mM PBST buffer, pH 7.5 at 20 °C. K_D values were determined by applying fitting models (i), to a One-To-One interaction model, (ii), a One-To-Two model, and (iii), by affinity determination using the TraceDrawer 1.7.1 software package.[36] SPR Determinations of synthetic epitope peptides were performed in the same manner, by preparation of dilution series of peptides at concentration ranges of 600 nM–3.5 μM (s. Table S1).

Molecular docking of C-Met-aptamer complexes

Secondary structure modeling was performed using the Mfold web server for nucleic acid folding and hybridization prediction.[38] The structures of the aptamers were built by the Avogadro software package,[39] and structure models optimized using the fragment molecular orbital (FMO) method at the level of two-body FMO expansion.[40,41] Docking studies of orientation and binding sites of the aptamer-C-Met complexes were performed using the AutoDock 4.0 software package (www://autodock.scripps.edu).[42] The selected structures with the lowest docking energy of the aptamer are shown in Figure 5. Ligands are presented as blue bolls, and DNA aptamer is shown as green bolls.

Acknowledgements

We gratefully acknowledge the advice and assistance of Prof. Friedemann Völklein and Oliver Müller, MSc in the preparation of chips for the SPR affinity determinations. We thank Dr. Stefan Maeser, Biogen GmbH, München, for valuable advice and critical reading of the manuscript. This work has been partially funded (Chip-MS epitope analysis) by the LOEWE-3 Funding Agency, Hessen-Agentur, Wiesbaden, Germany; Grant 696/19-16.

Conflict of Interest

The authors declare no conflict of interest.

Keywords: C-Met protein · tumor biomarkers · aptamer-C-Met complexes · aptamer epitopes · affinity-mass spectrometry · epitope peptide analysis

[1] S. L. Organ, M. S. Tsao, *Ther. Adv. Med. Oncol.* **2011**, *3*, 7–19.
[2] C. G. Huh, V. M. Factor, A. Sánchez, K. Uchida, E. A. Conner, S. S. Thorgeirsson, *Proc. Nat'l Acad. Sci. USA* **2004**, *101*, 4477–4482.
[3] J. Stamos, R. A. Lazarus, X. Yao, D. Kirchhofer, C. Wiesmann, *EMBO J.* **2004**, *23*, 2325–2335.
[4] A. Gentile, L. Trusolino, P. M. Comoglio, *Cancer Metastasis Rev.* **2008**, *27*, 85–94.
[5] N. Rahimi, E. Tremblay, L. McAdam, M. Park, R. Schwall, B. Elliott, *Cell Growth Differ.* **1996**, *7*, 263–270.
[6] N. Horiguchi, H. Takayama, M. Toyoda, T. Otsuka, T. Fukusato, G. Merlino, H. Takagi, M. Mori, *Oncogene.* **2002**, *21*, 1791–1799.
[7] P. Hyunkyu, K. Donggeon, S. Eunju, S. Sunhwa, K. S. Jason, K. Seok-Hyung, Y. Yeup, N. Do-Hyun, *Biochem. Biophys. Res. Commun.* **2017**, *494*, 409–415.
[8] N. Sharma, A. A. Adjei, *Ther. Adv. Med. Oncol.* **2011**, *3*, S37–S50.
[9] J. S. Wong, E. Warbrick, B. Vojtesek, J. Hill, D. P. Lane, *Oncotarget.* **2013**, *4(7)*,1019–1036.
[10] B. Cao, Y. Su, M. Oskarsson, P. Zhao, E. J. Kort, R. J. Fisher, L. M. Wang, G. F. Vande Woude, *Proc. Natl. Acad. Sci. USA.* **2001**, *98*, 7443–7448.
[11] H. Ki, H. Kimand, *Exp. Mol. Med.* **2017**, *49*, e308.
[12] A. Nozari, M. V. Berezovski, *Mol. Ther. Nucleic Acids* **2017**, *6*, 29–44.
[13] T. N. Zamay, G. S. Zamay, O. S. Kolovskaya, R. A. Zukov, M. M. Petrova, A. Gargaun, M. V. Berezovski, A. S. Kichkailo, *Cancers* **2017**, *9*, 155.
[14] F. Pastor, M. M. Soldevilla, H. Villanueva, D. Kolonias, S. Inoges, A. L. de Cerio, R. Kandzia, V. Klimyuk, Y. Gleba, E. Gilboa, M. Bendandi, *Mol. Ther. Nucleic Acids.* **2013**, *2*, e98.
[15] Y. Zhang, B. S. Lai, M. Juhas, *Molecules* **2019**, *24*, 941.
[16] A. S. Zamay, G. S. Zamay, O. S. Kolovskaya, T. N. Zamay, M. V. Berezovski, *Springer.* **2017**, Vol. 994.
[17] Z. Zhao, L. Xu, X. Shi, W. Tan, X. Fang, D. Shangguan, *Analyst (Lond.).* **2009**, *134*, 1808–1814.
[18] Y. Song, Z. Zhu, Y. An, W. Zhang, H. Zhang, D. Liu, C. Yu, W. Duan, C. J. Yang, *Anal. Chem.* **2013**, *85*, 4141–4149.
[19] H. W. Chen, C. D. Medley, K. Sefah, D. Shangguan, Z. Tang, L. Meng, J. E. Smith, W. Tan, *ChemMedChem.* **2008**, *3*, 991–1001.
[20] T. Kunii, S. Ogura, M. Mie, E. Kobatake, *Analyst (Lond.)* **2011**, *136*, 1310–1312.
[21] G. S. Zamay, T. I. Ivanchenko, T. N. Zamay, V. L. Grigorieva, Y. E. Glazyrin, O. S. Kolovskaya, I. V. Garanzha, A. A. Barinov, A. V. Krat, G. G. Mironov, A. Gargaun, D. V. Veprintsev, S. S. Bekuzarov, A. K. Kirichenko, R. A. Zukov, M. M. Petrova, A. A. Modestov, M. V. Berezovski, A. S. Zamay, *Mol. Ther. Nucleic Acids.* **2017**, *6*, 150–162.
[22] A. Boltz, B. Piater, L. Toleikis, R. Guenther, H. Kolmar, B. Hock, *J. Biol. Chem.* **2011**, *286*, 21896–21905.
[23] B. Piater, A. Doerner, R. Guenther, H. Kolmar, B. Hock, *PLoS One* **2015**, *10 (12)* e0142412.
[24] J. G. Bruno, *Molecules.* **2015**, *20*, 6866–6887.
[25] B. A. Petre, M. Ulrich, M. Stumbaum, B. Bernevic, A. Moise, G. Döring, M. Przybylski, *J. Am. Soc. Mass Spectrom.* **2012**, *23*, 1831–1840.
[26] A. Moise, S. André, F. Eggers, M. Krzeminski, M. Przybylski, H. J. Gabius, *J. Am. Chem. Soc.* **2011**, *133*, 14844–14847.
[27] J. McLaurin, R. Cecal, M. E. Kierstead, X. Tian, A. L. Phinney, M. Manea, J. E. French, M. L. H. Lambermon, A. A. Darabie, M. E. Brown, C. Janus, M. A. Chishti, P. Horne, D. Westaway, P. E. Fraser, M. T. J. Mount, M. Przybylski, P. St.-George-Hyslop, *Nat. Med.* **2002**, *8*, 1263–1269.
[28] R. Stefanescu, R. E. Iacob, E. N. Damoc, A. Marquardt, E. Amstalden, M. Manea, I. Perdivara, M. Maftei, G. Paraschiv, M. Przybylski, *Eur. J. Mass Spectrom.* **2007**, *13*, 69–75.
[29] P. Juszczyk, G. Paraschiv, A. Szymanska, A. S. Kolodziejczyk, S. Rodziewicz-Motowidlo, Z. Grzonka, M. Przybylski, *Simulation, J. Med. Chem.* **2009**, *52*, 2420–2428.
[30] M. I. Iurascu, O. Marroquin Belaunzanar, C. Cozma, U. Petrausch, C. Renner, M. Przybylski, *J. Am. Soc. Mass Spectrom.* **2016**, *27*, 1105–1112.
[31] A. Moise, S. Maeser, S. Rawer, F. Eggers, M Murphy, J. Bornheim, M. Przybylski, *J. Am. Soc. Mass Spectrom.* **2016**, *27*, 1071–8.
[32] Z. Kukacka, M. Iurascu, L. Lupu, H. Rusche, M. Murphy, L. Altamore, F. Borri, S. Maeser, A. M. Papini, M. Przybylski, *ChemMedChem.* **2018**, *13*, 909–915.
[33] D. Lee, E. S. Sung, J. H. Ahn, J. An, S. Huh, W. K. You, *Immunotargets Ther.* **2015**, *4*, 35–44. .
[34] Trace Drawer V. 1.7.1 ; Ridgeview Instruments AB, Vänge, Sweden.
[35] A. Lakhin, V. Tarantul, L. Gening, *Acta Naturae.* **2013**, *5*, 34–43.
[36] J. Yang, R. Yan, A. Roy, D. Xu, J. Poisson, Y. Zhang, *Nat. Methods* **2015**, *12*, 7–8.
[37] R. Ueki, S. Sando, *Chem. Commun.* **2014**, *7*, 13131–13134.
[38] M. Zuker, *Nucleic Acids Res.* **2003**, *31*, 3406–3415.
[39] M. D. Hanwell, D. E. Curtis, D. C. Lonie, T. Vandermeersch, E. Zurek, G. R. Hutchison, *J. Cheminf.* **2012**, *4*, 17.
[40] D. G. Fedorov, *Comp. Mol. Sci.* **2017**, *7*, e1322.
[41] M. Gaus, A. Goez, M. Elstner, *J. Chem. Theory Comput.* **2013**, *9*, 338–354.
[42] M. Gaus, A. Goez, M. Elstner, *J. Chem. Theory Comput.* **2013**, *9*, 338–354.

Manuscript received: August 24, 2019
Revised manuscript received: November 29, 2019
Accepted manuscript online: December 11, 2019
Version of record online: January 16, 2020

CHEMMEDCHEM

Supporting Information

Molecular Epitope Determination of Aptamer Complexes of the Multidomain Protein C-Met by Proteolytic Affinity-Mass Spectrometry

Loredana Lupu, Pascal Wiegand, Nico Hüttmann, Stephan Rawer, Wolfgang Kleinekofort, Irina Shugureva, Anna S. Kichkailo, Felix N. Tomilin, Alexander Lazarev, Maxim V. Berezovski, and Michael Przybylski*

Supplementary Figures

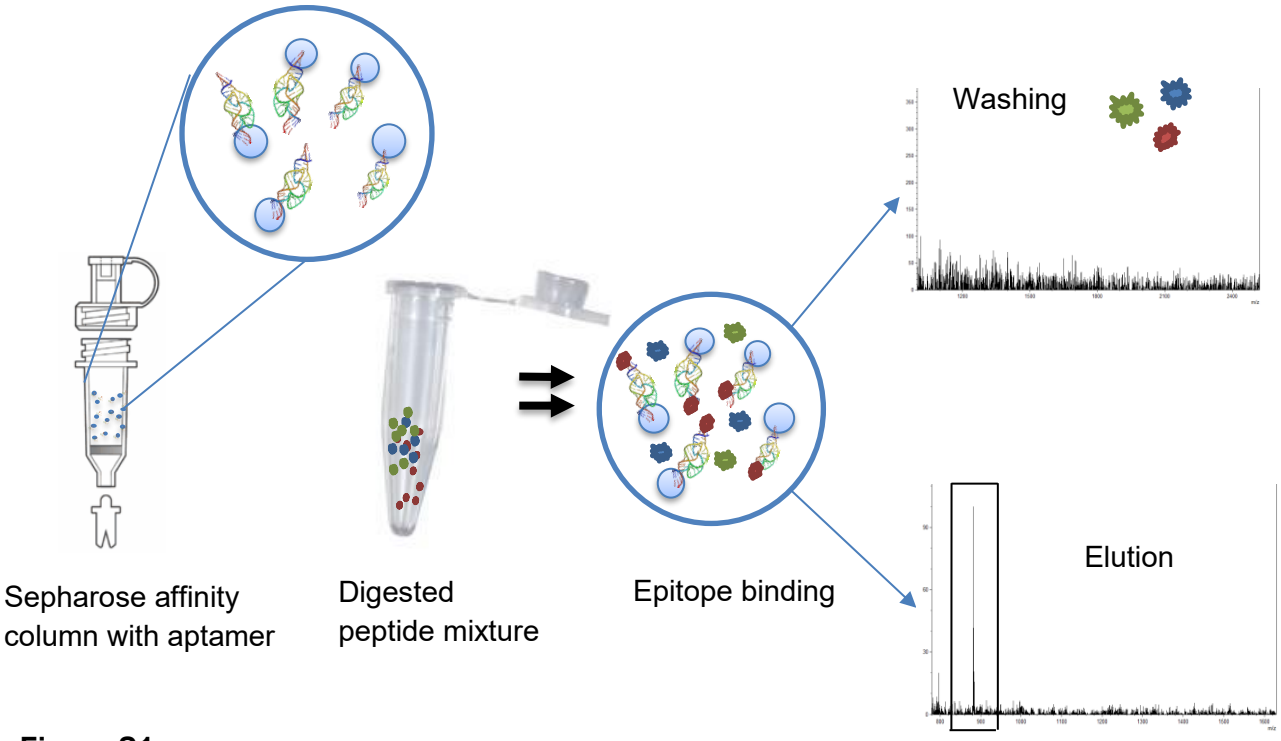

Figure S1

Epitope-Extraction MS experimental procedure. A solution of 20 mg of Sepharose beads was used to immobilize 75 µg of each aptamer incubated for 3 hrs in Coupling buffer;. Washing 4 times with washing buffer and coupling buffer; final incubation for 3 hrs with Blocking buffer.

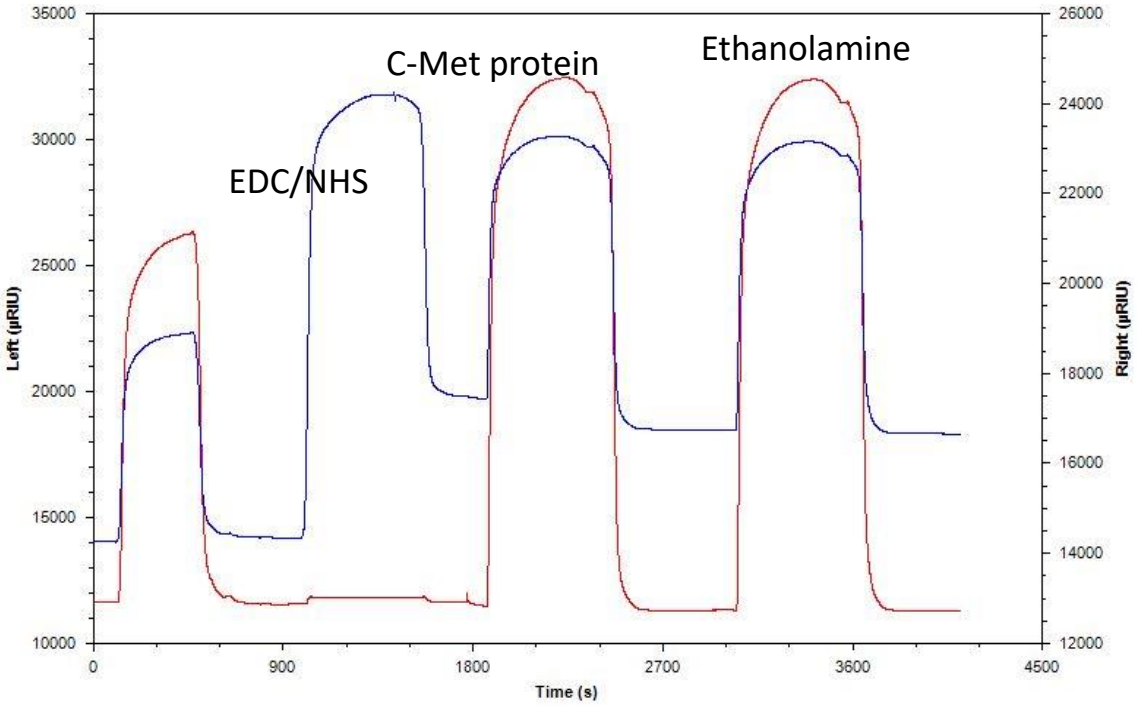

Figure S 2 A

SPR immobilization of the C-Met protein over a self assembled monolayer chip. 4:1 EDC/NHS injection for activation of the chip followed by 100ug of the protein in Sodium Acetate buffer pH5.2 and double injection of 10 mM Ethanolamine pH 8.

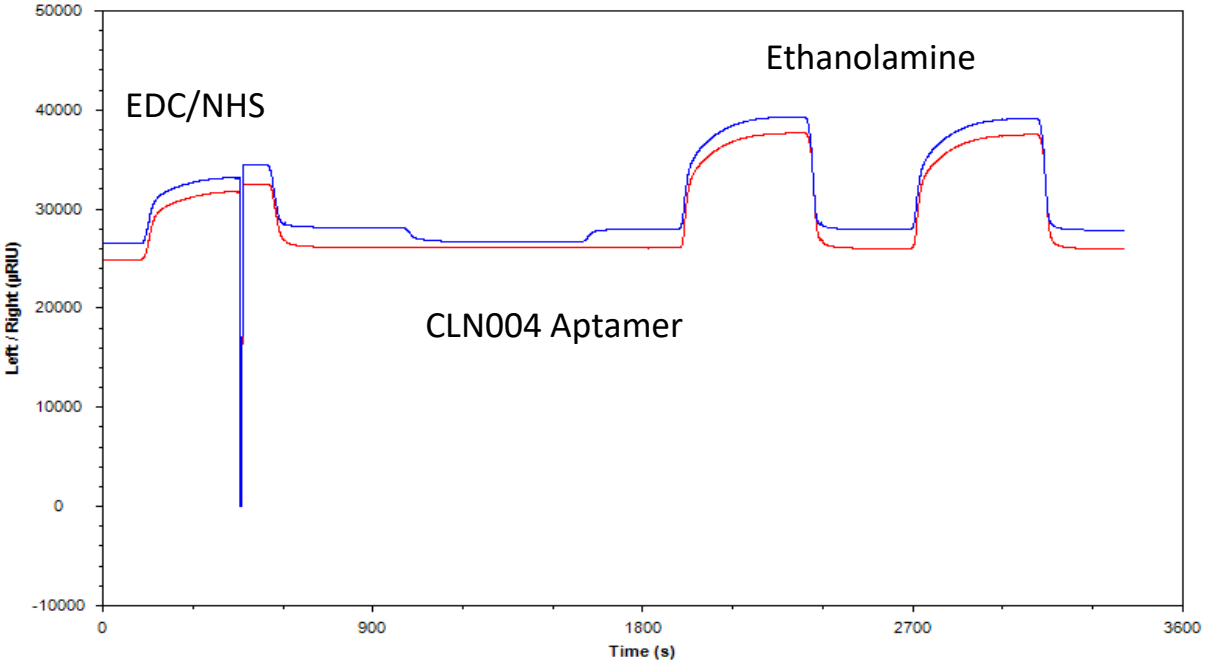

Figure S 2 B

SPR immobilization of 5ug of CLN0004 aptamer over a self assembled monolayer chip. 4:1 EDC/NHS injection for activation of the chip followed by 100ug of the protein in Sodium Acetate buffer pH5.2 and double injection of 10mM Ethanolamine pH 8.

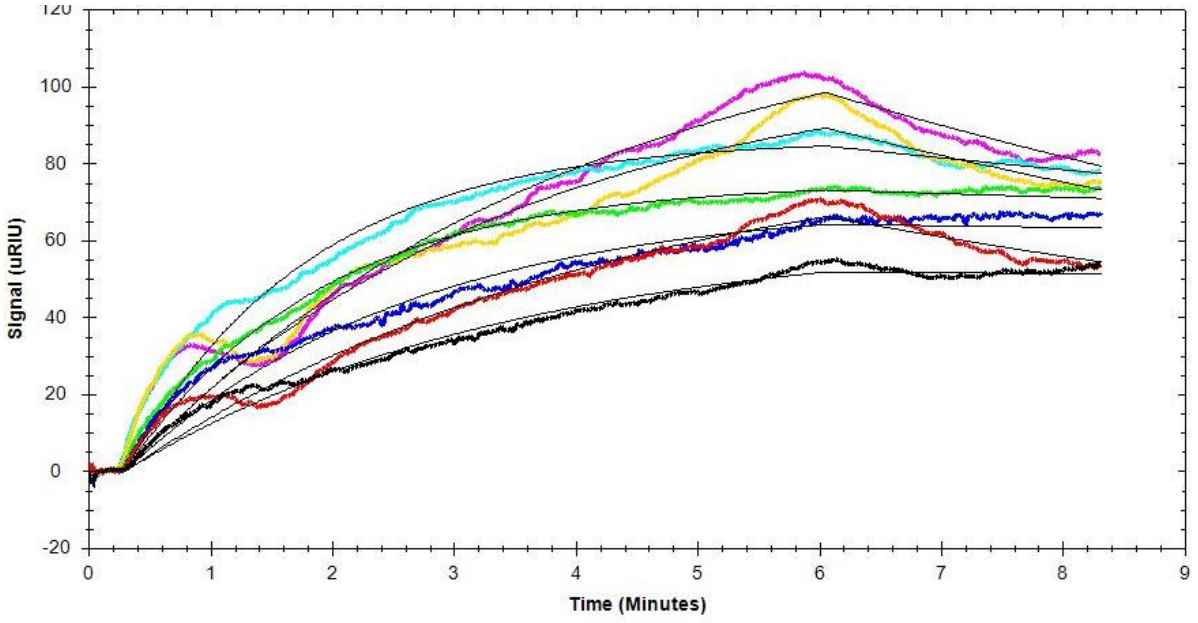

Figure S3 A

Kinetic evaluation of dilution series of CLN0003 aptamer interacting with immobilized C-Met protein.

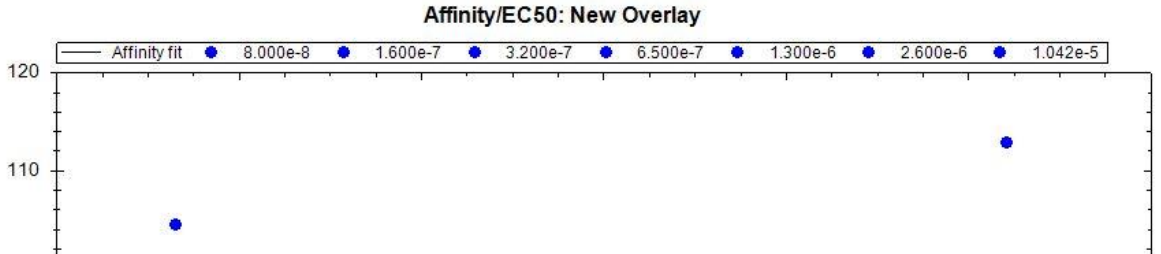

Figure S 3:

Affinity determination of a dilution series of C-Met protein interacting with immobilized CLN0003 aptamer.

Figure S3 B

Affinity plot determination of dilution series of CLN0003 aptamer interacting with immobilized C-Met protein.

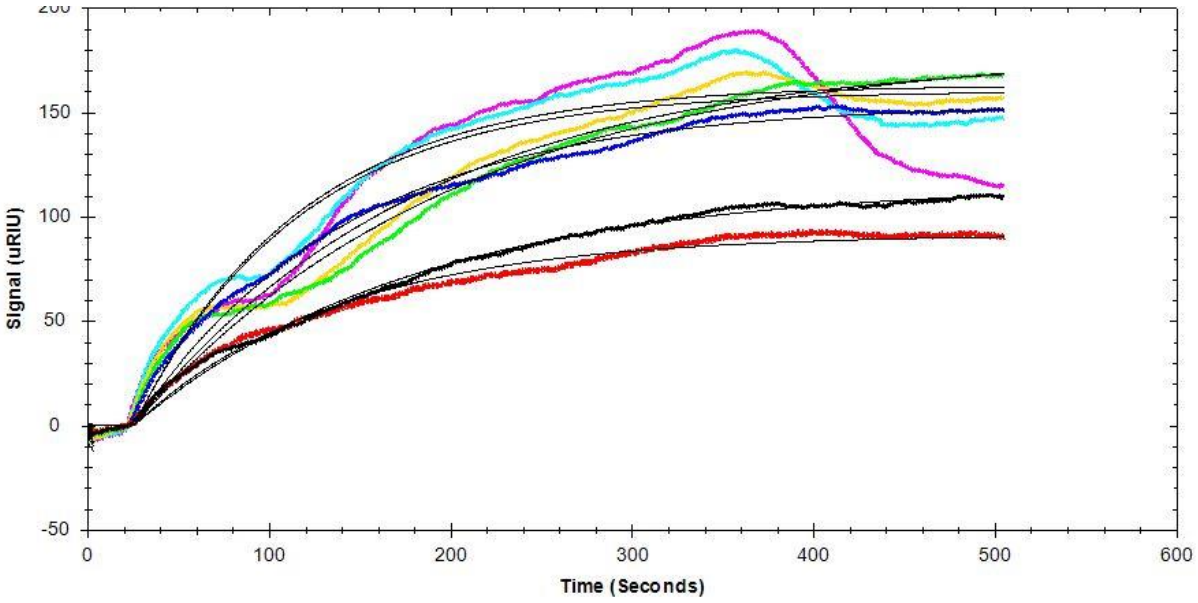

Figure S 4 A

Kinetic evaluation of dilution series of CLN0004 aptamer interacting with immobilized C-Met protein.

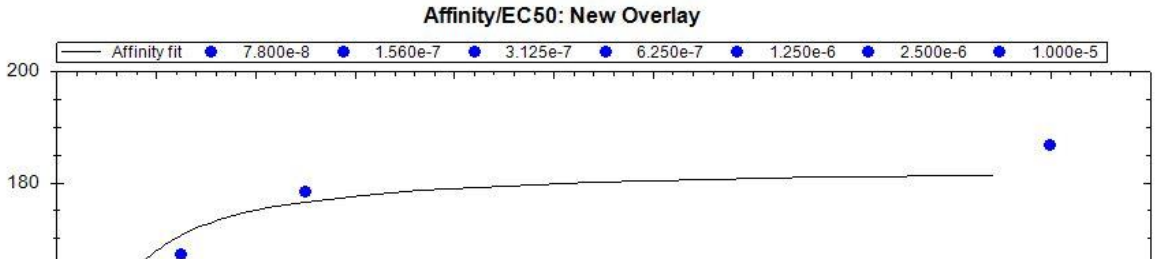

Figure S 4 B

Affinity plot determination of a dilution series of C-Met protein interacting with immobilized CLN0004 aptamer.

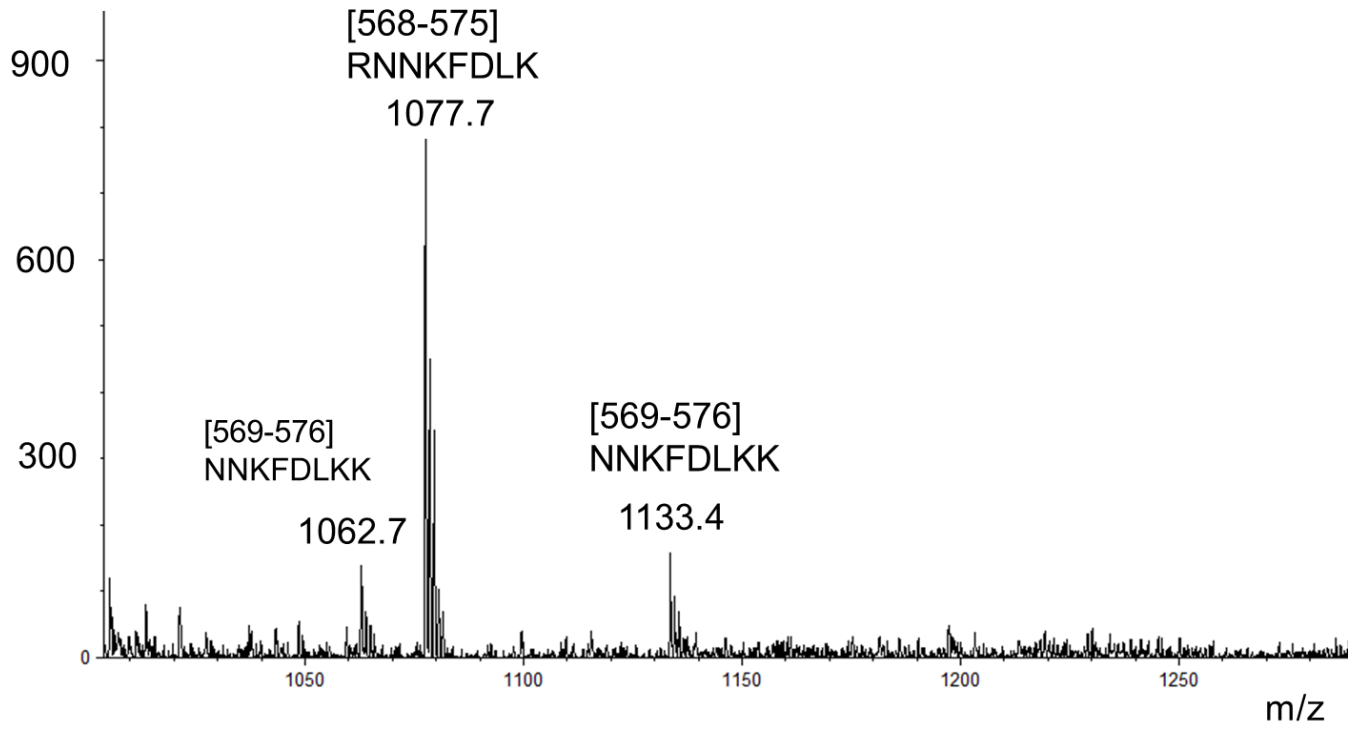

Figure S 5

Tryptic epitope extraction-MS from immobilized CLN0003 aptamer on CNBr-activated sepharose affinity matrix. The elution was preformed from the CLN0003 immobilized affinity column.

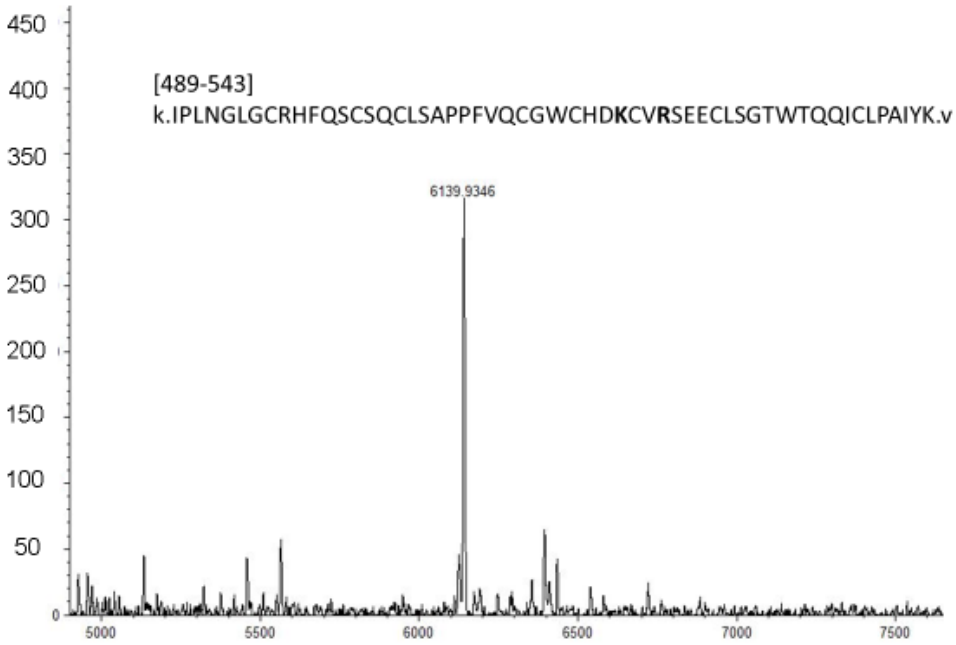

Figure S 6

MALDI-MS identification of CLN0003-C-Met epitope polypeptide fragment obtained by epitope- excision- MS. A 10 kDa molecular weight cutoff filter (Amicon; Merck Science Research, Darmstadt, Germany). was used. The proteolytic peptide mixture resulting from trypsin digestion of intact C-Met-aptamer was added to the Amicon filter, and 300 ul ammonium hydrogen carbonate buffer (pH 8) added to remove unbound peptides.

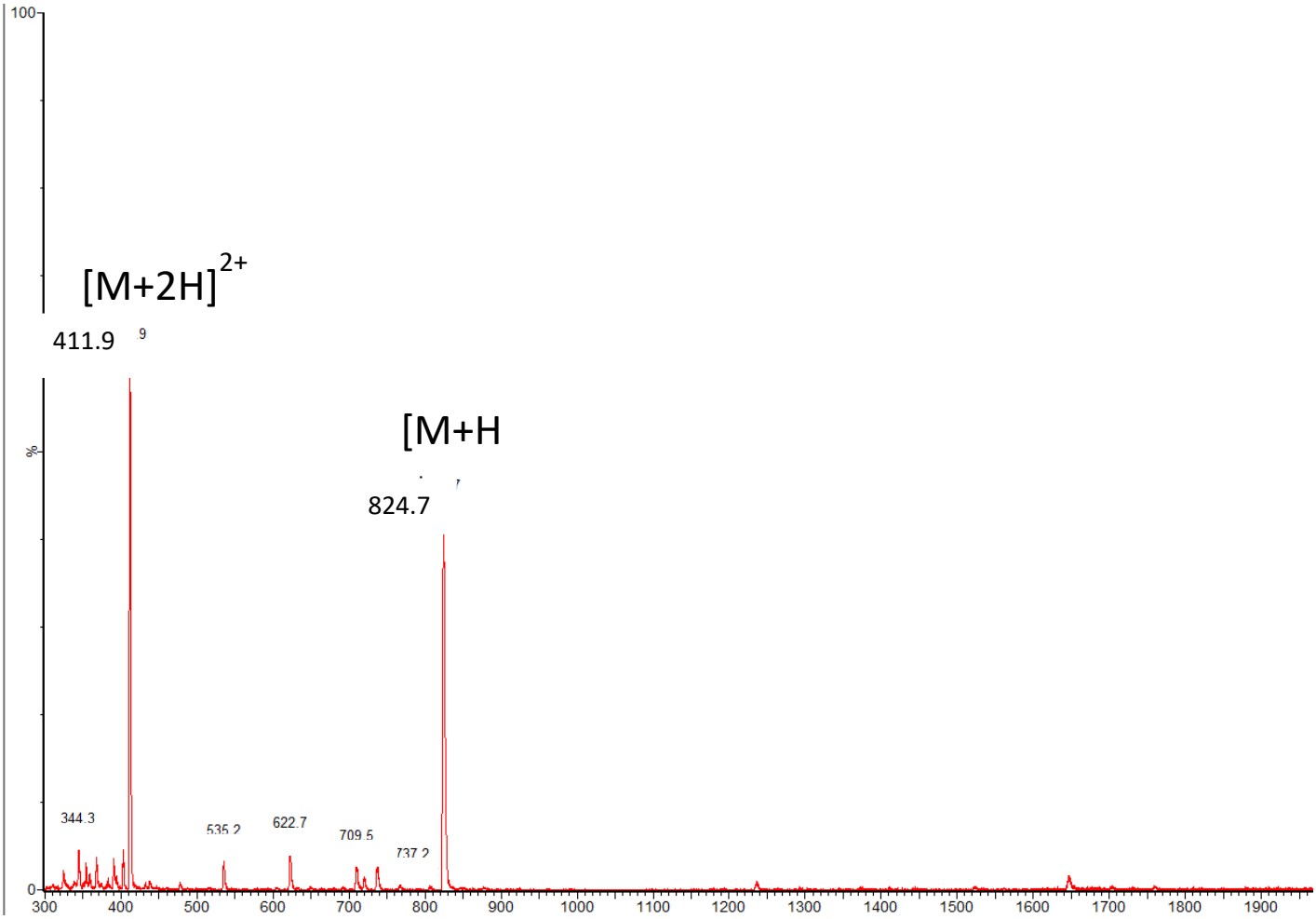

Figure S 7

ESI-MS of synthetic CLN0004 epitope peptide [381-388] r.NSSGCEAR.r

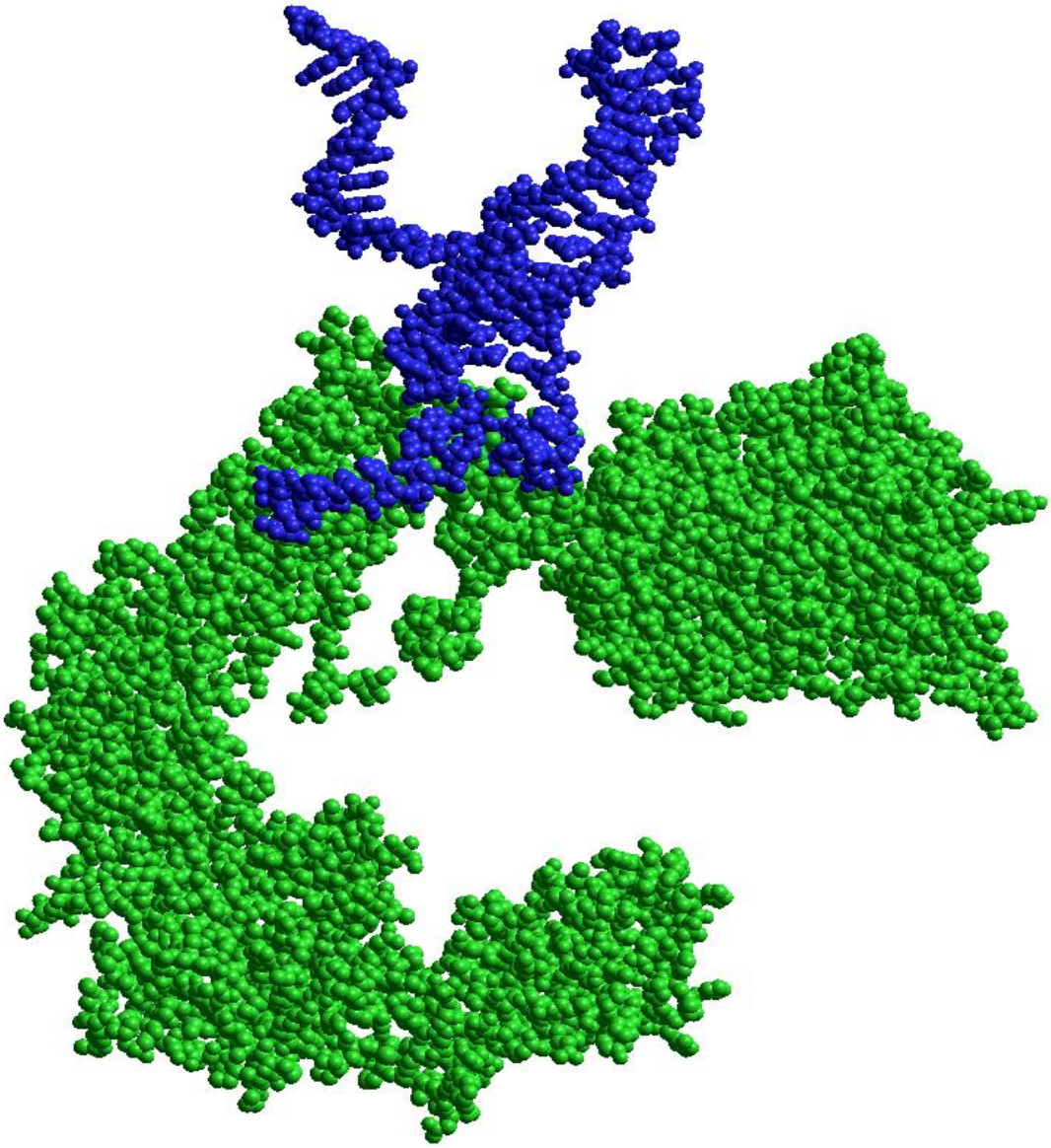

Figure S 8

Molecular modelling of CLN0003 aptamer (blue) by docking to corresponding C-Met peptides, SEECLSGTWTQQICLPAIYK and LTICGWDFGFRR.

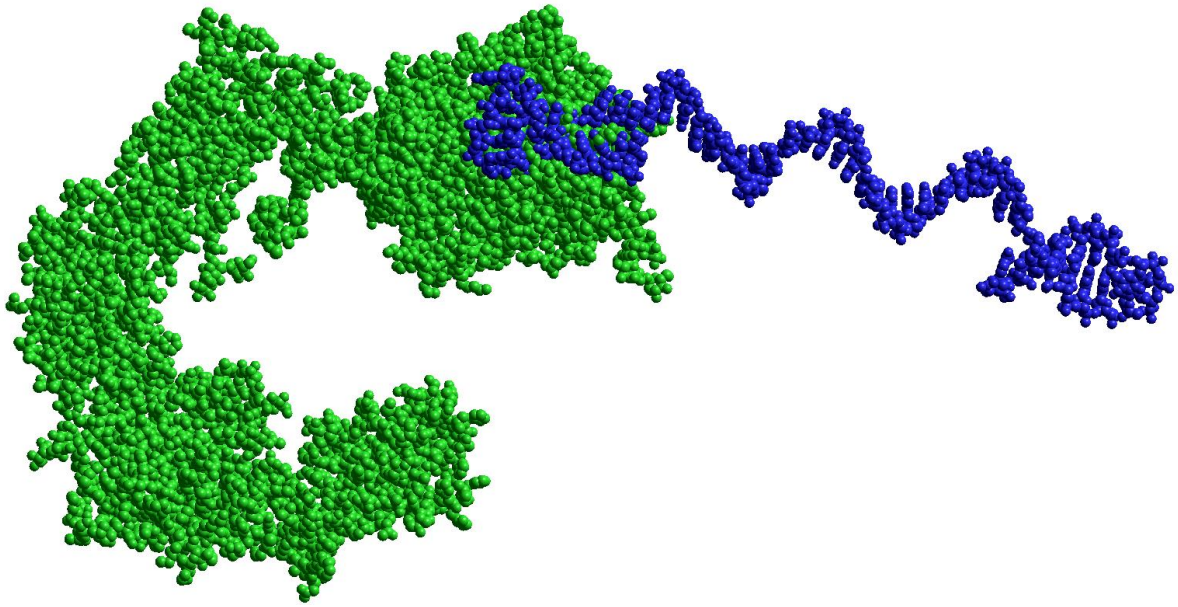

Figure S 9

Molecular modelling of CLN-0004 aptamer epitope (blue) by docking to corresponding c-Met peptides (green), NSSGCEARRDEYR .

Table S1

Kinetic analysis for the Aptamer-C-Met complexes from SPR biosensor. C-Met protein was immobilized on a SAM coated chip and a dilution series of the aptamers injected. The analysis was carried out using three different methods: Kinetic analysis Method One to One; Kinetic analysis Method One to two; and Affinity method.

CLN0003	Kinetic analysis Method		Affinity Method
	One to one-K_D (Molar)	One to Two - K_0s (Molar)	K_D (Molar)
Interaction 1	2.18-6±4.78e-7	3.83e-6 ±1.75e-6	x
Interaction 2	x	3.75e-8 ±3.41e-9	5.64e-8 ±2.63e-8
CLN0004	Kinetic analysis		Affinity
	One to one-K_D (Molar)	One to Two - K_0s (Molar)	K_D (Molar)
Interaction 1	1.05e-7±3.36e-8	5.12e-7 ±6.9e-8	x
Interaction 2	x	8.04e-8 ±3.44e-9	9.27e-8 ±7.46e-9